INFORMATION TO USERS

This manuscript has been reproduced from the microfilm master. UMI films the text directly from the original or copy submitted. Thus, some thesis and dissertation copies are in typewriter face, while others may be from any type of computer printer.

The quality of this reproduction is dependent upon the quality of the copy submitted. Broken or indistinct print, colored or poor quality illustrations and photographs, print bleedthrough, substandard margins, and improper alignment can adversely affect reproduction.

In the unlikely event that the author did not send UMI a complete manuscript and there are missing pages, these will be noted. Also, if unauthorized copyright material had to be removed, a note will indicate the deletion.

Oversize materials (e.g., maps, drawings, charts) are reproduced by sectioning the original, beginning at the upper left-hand corner and continuing from left to right in equal sections with small overlaps. Each original is also photographed in one exposure and is included in reduced form at the back of the book.

Photographs included in the original manuscript have been reproduced xerographically in this copy. Higher quality 6" x 9" black and white photographic prints are available for any photographs or illustrations appearing in this copy for an additional charge. Contact UMI directly to order.

UMI

A Bell & Howell Information Company
300 North Zeeb Road, Ann Arbor MI 48106-1346 USA
313/761-4700 800/521-0600

A Cre/loxP Binary Genetic Approach to Study Murine Spinal Cord and Limb Development

by

Xue Li

A dissertation submitted to the Graduate Faculty in Biomedical Sciences in partial fulfillment of the requirements for the degree of Doctor of Philosophy the City University of New York.

1998

to Liping and Katherine

This manuscript has been read and accepted for the Graduate Faculty in Biomedical Sciences in satisfaction of the dissertation requirement for the degree of Doctor of Philosophy.

1.9.1998
Date

Francesco Ramirez, Ph. D
Chair of Examining Committee

1/12/98
Date

Terry A. Krulwich, Ph. D
Executive Officer

Thomas Lufkin, Ph. D

Andras Nagy, Ph. D

Mitchell Goldfarb, Ph. D

Heide Stuhlmann, Ph. D
Supervisory Committee

The City University of New York

Abstract

A Cre/loxP Binary Genetic Approach to Study Murine Spinal Cord and Limb Development

by Xue Li

Advisor: **Thomas Lufkin, Ph.D.**

The Cre/loxP site-specific recombination system was designed to conditionally express a battery of dorsal neural tube specific genes in the ventral neural tube to investigate their function in neural tube patterning. Two different types of transgenic mice, E3Cre and E3loxP, were generated using the same promoter which has specific activities in the floor plate and notochord between embryonic day 8.0-14.5. The E3Cre transgene encodes *Cre* and the alkaline phosphatase reporter gene, while the E3loxP transgene encodes a STOP sequence flanked by loxP sites, which prevents translation of 3' cDNAs. Double transgenic embryos harboring both E3Cre and E3loxP transgenes display specific excision of the STOP sequence demonstrating that Cre-mediated recombination occurs efficiently *in vivo*. However, expression of downstream cDNAs is not detected. Unexpectedly, elevated levels of specific cell death in the floor plate and notochord is apparent and is independent of the 3' cDNAs included in the E3loxP transgene expression cassette.

In concert with the discovery that Cre-mediated recombination leads to chromosome deletion in transgenic mice, molecular studies in the double transgenic embryos suggest that the Cre-mediated recombination directly causes apoptosis of specific cells. Molecular and immunohistochemical analyses demonstrate that the floor plate and notochord play important roles for differentiation of the motor neurons, and for correct projection patterning of commissural axons. Strikingly, forelimbs fail to develop normally in the double transgenic embryos. This morphological defect is apparent at E9.5, at the time when

forelimb buds normally appear from the flanking regions. Molecular analyses demonstrate that the earliest known limb inducing molecules, including fibroblast growth factors 8 and 10, are not expressed in the defective forelimbs, suggesting that the defect is due to a failure of limb initiation. In view of these findings, we propose that putative limb inducing signals are present transiently in axial structures, the node, notochord or floor plate. The inducing signals are then propagated through paraxial, intermediate, lateral plate mesoderm and finally to the surface ectoderm to form the limb bud. Once the limb bud is formed, its outgrowth and patterning continue in a self-organizing fashion.

Acknowledgments

I would like to thank Dr. Thomas Lufkin, for his professional guidance and support. I will always be grateful to him for sharing his knowledge and ideas with me during past four years in graduate school. I would also like to thank all the members of Dr. Lufkin's lab, past and present, for the diversified and stimulating environment.

I thank the members of my supervisory committees, Drs. Mariann Blum, Victor Friedrich, Mitchell Goldfarb, Kevin Kelley, Andras Nagy, Francesco Ramirez, Mary Rifkin, David Sassoon, Heide Stuhlmann and all the members in Brookdale Center for their support and guidance. Very special thanks go to Drs. Robert Lazzarini, Alexander Gow, and Greg Elder for their unflagging support and encouragement, and for making my life in the United States possible.

Finally, I would like to express my deepest gratitude to my parents, my wife Liping, and my daughter Katherine, for their unconditional love, support, and encouragement, and for their complete understanding.

Table of Contents

List of Tables and Figures

I. Introduction

One of the major challenges for a developing organism is pattern formation, which dictates the spatial arrangement of differentiated tissues in a manner dependent on regulated cell proliferation, differentiation, and cell-cell communication (Gurdon, 1992; McGinnis and Krumlauf, 1992). Traditionally, this has been studied by transplantation experiments, which are powerful tools to study interactions between tissues or identify signaling centers (Jessell and Melton, 1992). For instance, when the dorsal blastopore lip tissue from an early newt gastrula is transplanted into the ventral ectoderm of another newt, it initiates gastrulation and embryogenesis in the surrounding tissue and this lead to the identification of the Spemann Organizer (Spemann and Mangold, 1924).

Over the last few decades, molecular and genetic tools have been applied successfully to study development of organisms like *Caenorhabditis elegans (C. elegans)*, *Xenopus*, and *Drosophila*. Most significantly, many important developmental genes in mammals have been identified based on the homology to their *Drosophila* counterpart, for instance, homeobox-containing transcription factors. In past decades, advances in mouse genetics enable us to pinpoint specific genes or genetic pathways involved in the patterning process, for instance, patterning of the spinal cord and the limb, in a mammalian system (Johnson and Tabin, 1997; Tanabe and Jessell, 1996). One powerful method is to generate mutant mice devoid in the function of a specific gene, loss-of-function analysis (Brandon et al., 1995). Complimentary to this approach, gain-of-function studies have been used to ectopically express genes in novel places or at novel times (Lufkin et al., 1992).

Both spinal cord and limb development have served as model systems for embryological studies using both classical transplantation and genetic approaches because of their physical accessibility and the recent identification of genes involved in these areas.

Under the scope of this thesis, I will focus the introduction on three different areas: first, dorsoventral patterning of the spinal cord; second, initiation and patterning of limbs: and finally, the mouse genetic system studying the function of genes.

1. Dorsoventral Patterning of the Spinal Cord

The development of the nervous system begins with the induction of the neural plate from undifferentiated ectoderm (Harland, 1994). The neural plate eventually folds up to form the neural tube and neural crest cells, which migrate out of the dorsal neural tube during its closure (Doniach, 1993; Jessell and Dodd, 1993). The neural tube is a hollow bilaterally symmetrical structure surrounded by surface ectoderm dorsally, axial mesoderm ventrally and paraxial mesoderm bilaterally. A cross section of the posterior neural tube reveals the dorsoventral patterning of the developing spinal cord. The roof plate and the floor plate differentiate at the midline in the dorsal and ventral region, respectively. The motor neurons differentiate ventrally adjacent to the floor plate whereas commissural neurons differentiate dorsally next to the roof plate.

Ventral neural tube patterning

Patterning along the dorsoventral axis starts during formation of the neural tube. Classical tissue transplantation assays in chick and *Xenopus* embryos, the analyses of mutant mouse and zebra fish embryos, and assays of cell differentiation in neural plate cells grown *in vitro* have shown that ventral neural tube patterning depends on inductive signals from the underling axial mesoderm, the notochord (Clarke et al., 1991; Jessell and Dodd, 1993; Smith, 1993; Tanabe and Jessell, 1996). For instance, the ventral neural tube fails to differentiate in the absence of the notochord, specifically, there is no floor plate and motor neuron differentiation without a notochord (Basler et al., 1993; Goulding et al., 1993; Yamada et al., 1991). Implantation of an additional notochord adjacent to the prospective lateral neural tube induces formation of an additional floor plate and motor neurons and suppresses dorsal neural tube development (Placzek et al., 1990; VanStraaten et al., 1989;

Yamada et al., 1993). Once the floor plate is induced, it acquires the notochord inductive activity to induce formation of the floor plate itself and the motor neurons (Hatta et al., 1991). Different genes have been identified and shown to be involved in the formation of the notochord and in patterning of the ventral neural tube, including transcription factors *Brachyury (T)* (Herrmann, 1992) and *Hepatocyte Nuclear Factor 3β (HNF3β)* (Ang and Rossant, 1994; Sasaki and Hogan, 1994); signaling molecules *Sonic Hedgehog (Shh)* (Tanabe and Jessell, 1996) and transforming growth factor *Nodal* (Conlon et al., 1994).

The notochord's inductive activity is mediated by Shh, a secreted signaling protein which is homologous to the *Drosophila* segmentation polarity gene *Hedgehog* (*Hh*) (Echelard et al., 1993). *Shh* is expressed in the floor plate and the notochord coincident with the notochord inductive activity (Echelard et al., 1993). Ectopic expression of *Shh* in the dorsal neural tube induces formation of the floor plate *in vivo* (Echelard et al., 1993). Similarly, recombinant Shh can induce formation of floor plate cells and motor neurons from cultured neural tube explants (Roelink et al., 1995). Conversely, mice knockouts of *Shh* fail to develop ventral neural tube structures and an antibody raised against Shh blocks the notochord and floor plate inductive activity *in vitro* (Chiang et al., 1996; Marti et al., 1995). The mechanism of how *Shh* executes its function is not yet fully understood, but appears to be very similar to Hh signaling in *Drosophila* in which Hh binds to the receptor complex, Patched (*Ptc*) and Smoothened (*Smo*), and transduces a signal through the protein kinase A (PKA) pathway (Chen and Struhl, 1996; Kalderon, 1995; Stone et al., 1996).

One of the early signs of Shh patterning activity is repression of the expression of transcription factor *Pax-3* and *Pax-7* at the medial neural plate (Ericson et al., 1997; Tanabe and Jessell, 1996). Both *Pax-3* and *Pax-7* are expressed in the neural plate including midline regions adjacent to the notochord (Stuart et al., 1994). However, their medial

expression domains are rapidly repressed by a *Shh*-mediated signal from the notochord (Goulding et al., 1993; Liem et al., 1995; Tanabe and Jessell, 1996). Consequently, their expression domains are restricted to the dorsal ventricular zone of the neural tube, which defines dorsal neural tube identity (Stuart et al., 1994). It is not clear whether these *Pax* genes are the direct targets of *Shh* and whether the early *Shh* repression activity is a prerequisite for ventral neural tube development. Recent report demonstrated that cells expressing *Pax-7* lose their competence to become floor plate cells and motor neurons in response to *Shh* induction (Ericson et al., 1997). Furthermore, ectopic expression of *Pax-3* at the ventral neural tube inhibits floor plate differentiation (Tremblay et al., 1996).

High concentrations of Shh induce formation of the floor plate while low concentrations of Shh induce formation of motor neurons (Ericson et al., 1997; Roelink et al., 1995). The graded action of Shh also determines the diversity of the ventral motor neurons (Ericson et al., 1997). As demonstrated *in vitro*, different neuronal progenitors, identified by differential expression of transcription factors such as *Pax-6* and *Nkx-2.2*, respond differently to Shh concentrations. The state of *Pax-6* and *Nkx-2.2* expression in the ventral progenitors determines the fate of their neuronal progeny as indicated by analyzing motor neuron distribution in the *Pax-6* mutant mice (Ericson et al., 1997). Once the ventral cell fate is determined by *Shh* inductive activity, differentiation of the floor plate requires winged-helix class transcription factors, *HNF3β*, and differentiation of motor neurons requires LIM-domain transcription factors, *Islet-1* (Tanabe and Jessell, 1996). Loss-of-function of *HNF3β* and *Islet-1* cause the loss of floor plate and motor neuron differentiation, respectively (Ang and Rossant, 1994; Pfaff et al., 1996; Weinstein et al., 1994). Conversely, ectopic expression of *HNF3β* in the dorsal neural tube induces ectopic floor plate formation (Sasaki and Hogan, 1994).

Dorsal neural tube patterning

Dorsal neural tube development, i.e. neural crest, roof plate and commissural neurons, does not depend on the notochord and floor plate inductive signals (Tanabe and Jessell, 1996). Moreover, in the absence of the floor plate and notochord, the neural tube becomes dorsalized (Basler et al., 1993; Goulding et al., 1993; Yamada et al., 1991). These observations raise several possibilities of how the dorsal fate may be determined. One hypothesis is that the dorsal fate represents a default state while the ventral fate represents an alternative fate in response to the induction from the notochord and floor plate. Alternatively, dorsal fate is acquired and the acquisition requires signals from the adjacent surface ectoderm. Recent evidence supports the latter hypothesis (Dickinson et al., 1995; Liem et al., 1997). For example, non-neural ectoderm induces formation of neural crest cells *in vitro* from the prospective lateral neural ectoderm, which is destined to become ventral interneurons (Dickinson et al., 1995; Dickinson et al., 1995; Liem et al., 1995; Moury and Jacobson, 1990).

In vitro explant culture studies also suggest that the scheme of the dorsal neural tube induction is similar to ventral neural tube induction (Dickinson et al., 1995; Liem et al., 1997). Signals originating from non-neural tissues, the surface ectoderm dorsally and the axial mesoderm ventrally, induce formation of two signaling centers within the neural tube, a dorsalizing center (the roof plate) and a ventralizing center (the floor plate). The signaling centers differentiate into specialized glial cells and acquire inductive activity. However, the molecular mechanism determining dorsal neural fate is quite different from that determining ventral neural fate. Dorsal neural tube patterning appears to involve multiple members of the *TGFβ* (Hogan, 1996; Liem et al., 1997) and possibly *Wnt* families (Parr et al., 1993), notably *BMP-4, BMP-5, Dorsalin-1, Wnt-1,* and *Wnt-3a,* and the diversity of different cell types appears to depend on the qualitative differences in the activities of different gene products (Tanabe and Jessell, 1996). In contrast, ventral neural tube patterning appears to

involve a single Shh protein, and its graded activity seems to determine the diversity of the ventral neurons (Ericson et al., 1997; Tanabe and Jessell, 1996).

Molecular definition of dorsal neural tube development is not well understood, largely due to the involvement of multiple genes and possibly functional overlaps among the members of participating gene families. However, indirect evidence suggests that a few genes may play important roles. These include some transcription factors and *Wnt* and *TGFβ* family signaling molecules.

Wnt-1: The murine *Wnt* gene family is comprised of at least 16 members that appear to encode cell-cell signaling proteins (Ikeya et al., 1997; Moon et al., 1997; Nusse and Varmus, 1992; Parr et al., 1993). *Wnt-1* is the homologue of the *Drosophila* segmentation polarity gene *wingless (wg)*. Its expression is first detected in E8.5 mouse embryos in the anterior neural plate and the lateral edges, which later become the roof plate of the neural tube (Wilkinson et al., 1987). At later stages (E10.5-E14.5), *Wnt-1* expression is restricted to the roof plate and the midbrain-hindbrain junction. Ectopic expression of *Wnt-1* induces secondary axis formation in frog embryos, suggesting a patterning activity (Nusse and Varmus, 1992; Sokol et al., 1991). Loss-of-function of *Wnt-1* leads to the complete deletion of the cerebellum (McMahon and Bradley, 1990; Thomas and Capecchi, 1990). However, there is no apparent defect in the spinal cord development although it is expressed in the roof plate. This is probably due to the functional compensation by other *Wnt* family genes, particularly *Wnt-3a* and *Wnt-4* which are expressed in the same domain (Parr et al., 1993). Loss-of-function of *Wnt-3a* reveals that it regulates paraxial mesoderm and tail bud formation (Takada et al., 1994; Thomas and Capecchi, 1990). Loss-of-function of *Wnt-4* revealed that it regulates kidney formation (Stark et al., 1994). Loss-of-function of both *Wnt-1* and *Wnt-3a* reveal that they are required for expansion of neural crest and dorsal neural progenitors (Ikeya et al., 1997).

Dorsalin-1 (Dsl-1): *Dsl-1* belongs to a *TGFβ* super family which has more then 24 members (Hogan, 1996). The biologically active forms are disulfide-linked dimers containing subunits of 110-140 amino acids. The subunits are the C-termini of the large precursors cleaved at a RXXR site. Evidence from studies of different species reveal that *TGFβ* molecules are important for normal development. For instance, the *Drosophila decapentaplegic (dpp)* gene product acts as a morphogen that sets up the dorsoventral body axis (Ferguson and Anderson, 1992). *Xenopus Vg-1, activins and BMP4* are involved in the mesoderm induction (Hemmati-Brivanlou et al., 1994; Hemmati-Brivanlou and Melton, 1994; Thomsen and Melton, 1993). Mouse *Nodal* regulates formation of the notochord. *Dsl-1* was identified from chick. Expression studies indicated that *Dsl-1* is localized to the dorsal neural tube during its closure (Basler et al., 1993). *In vitro* explant cultures demonstrated that *Dsl-1* induces neural crest cell differentiation and suppresses motor neuron differentiation (Basler et al., 1993).

Msx1: The vertebrate *Msx* family homeobox-containing transcription factors have at least three members (*Msx1, 2* and *3)* (Davidson, 1995; Holland, 1991; Wang et al., 1996). RNA *in situ* analyses demonstrate that all three members are expressed in the dorsal part of the neural tube with *Msx1* and *2* restricted to the roof plate and *Msx3* expressed dorsally next to the roof plate. The actual role of these genes in dorsal neural tube development remains to be discovered since the loss-of-function mutation of *Msx1* causes no abnormality in spinal cord development, possibly due to the functional redundancy (Satokata and Maas, 1994).

Gbx2: A homeobox-containing transcription factor expresses in the forebrain, midbrain and hindbrain junction, and the hindbrain and spinal cord in mouse embryo (Bulfone et al., 1993; Chapman and Rathjen, 1995; Matsui et al., 1993). Within the spinal cord, *Gbx2* RNA is detected in two longitudinal columns including dorsal commissural

neurons and intermediate interneurons. Loss-of-function studies demonstrate that it is involved in specification of the anterior hindbrain and establishment of a normal mid/hindbrain organizer (Wassarman et al., 1997).

CRABPI: Cellular retinoic acid binding protein I is a candidate component of the retinoic acid (RA) signaling pathway (Chambon, 1994). Over expression of *xCRABPI* causes anteroposterior defects in developing *Xenopus* embryos which resemble the effects of treating *Xenopus* gastrulae with all-trans retinoic acid (RA) (Dekker et al., 1994). Retinol and its biologically active derivative, RA, have profound effects upon vertebrate embryogenesis. These include axis duplication and limb induction (Morriss-Kay, 1992). One possible mechanism of its function is to regulate *Hox* gene expression (Krumlauf, 1994). *CRABPI* and *CRABPII* are thought to play important roles in regulating the intracellular concentration of RA. Both genes are expressed from E7.0 to adult stages, including the neural crest, roof plate, and commissural neurons (Ruberte et al., 1992).

Axonal projection pattern along the dorsoventral axis of spinal cord

Function of the nervous system depends on both the precise positioning of neurons and appropriate synaptic connections. The specificity of synaptic connections is established through pathway finding, target selection, and remodeling (Tessier-Lavigne and Goodman, 1996). Within the spinal cord along dorsoventral axis, the commissural axons extend ventrally towards the floor plate, cross the floor plate contralaterally, and then growth rostrally within the spinal cord. In contrast, motor axons project away from the floor plate, out of the spinal cord, toward their peripheral targets. *In vitro* explant studies indicate that the establishment of axonal projection patterns within the spinal cord is dependent on the floor plate axonal guidance activity (Placzek et al., 1990; Tamada et al., 1995; Tessier-Lavigne et al., 1988).

At least partially, the floor plate axon guidance activity is mediated by the secreted, extracellular matrix-like molecule *Netrin*-1, a homologue of *C. elegans UNC-6* (Goodman, 1994). UNC-6 is required for the circumferential guidance of certain pioneer axons and the migration of mesodermal cells around the inside of the worm's body wall (Hamelin et al., 1993; Hedgecock et al., 1990; Ishii et al., 1992). The striking conservation of sequence and function over 600 million years evolution strongly suggests that a common molecular mechanism is used to guide axonal projection among diverse species. Netrin-1 is synthesized by the floor plate at a time when commissural axons are growing towards the floor plate *in vivo* (Serafini et al., 1994). Recombinant Netrin-1 promotes axonal outgrowth from dorsal spinal cord explants and causes the axons to turn towards the *Netrin*-secreting cells in *in vitro* explant cultures (Colamarino and Tessier-Lavigne, 1995). *Netrin-1* loss-of-function studies reinforce the notion that this protein is important for commissural axon guidance (Serafini et al., 1996). However, the molecular mechanism underlying *Netrin-1* function is still poorly understood. A tumor suppressor gene, *Deleted in Colorectal Cancer (DCC),* has proved to be a part of the receptor component which mediates *Netrin-1* function (Fazeli et al., 1997). Like its worm homologue UNC-6, which has repulsive activity, Netrin-1 repels axons of several classes of motor neurons from the midbrain, hindbrain, and spinal cord (Dodd and Schuchardt, 1995). Recombinant Netrin-1 mimics the ability of the floor plate to repel the growth cones of trochlear motor neurons *in vitro* (Colamarino and Tessier-Lavigne, 1995). The curious bifunctional chemoattraction and chemorepulsion activity of Netrin-1 toward distinct axons may depend on which receptors are expressed in the growth cones. In this case, the commissural axons might express a "attractive" receptor while the trochlear axons might express a "repulsive" receptor.

The growth cone is the leading tip of a growing axon, which senses the guidance cues and navigates axonal outgrowth. Using an assay to measure growth cone collapse,

Jonathan Raper and his colleagues (1993) cloned the first gene, named *Collapsin*, which causes contact-dependent collapsing of the growth cone (Luo et al., 1993). Strikingly, the amino acid sequence of Collapsin is closely related to the grasshopper protein Fasciclin IV (G-Sema I), which is involved in sensory axon guidance in the peripheral nervous system (Kolodkin et al., 1992). Based on the sequence conservation between *Collapsin* and *Fasciclin IV,* many genes have been cloned from different species, forming a new family collectively called *Semaphorins* (Kolodkin et al., 1993; Luo et al., 1995; Püschel et al., 1995). The Semaphorins share a conserved "sema" domain that is approximately 500 amino acids. During spinal cord development, *Sema III* is expressed strongly in ventral gray matter but not in dorsal gray matter inside spinal cord (Luo et al., 1995; Messersmith et al., 1995; Püschel et al., 1995). The ventral expression pattern coincides with the terminus of muscle sensory afferent axons, whereas the dorsal gray matter is the target sites of the cutaneous sensory afferent axons. COS cells expressing Sema III *in vitro* deflect cutaneous afferent axons while attracting muscle afferent axons (Messersmith et al., 1995). This study suggested that Semaphorins might play important roles in segregating sensory afferent input to different regions of the spinal cord. It will be intriguing to determine whether other Semaphorins play similar roles and whether the combination of different members can fine tune the axonal wiring system.

Recently, Eph molecules, which comprise the largest known family of receptor tyrosine kinases, have been implicated directly in mediating contact-repulsion of axons and topographic mapping (Tessier-Lavigne, 1995). These receptors are characterized by the presence of a cysteine-rich region and two fibronectin-type III repeats in the extracellular domains (van der Geer et al., 1994). In an attempt to isolate the genes involved in the topographic map formation between chick retinal ganglions and the optic tectum, two groups have independently demonstrated that two ligands, ELF-1 (Eph Ligand Family 1) and RAGS (Repulsive Axon Guidance Signal), have gradients of expression in the tectum

(Cheng et al., 1995; Drescher et al., 1995). In addition, *in vitro* evidence suggests that RAGS has specific axon repelling activity (Cheng et al., 1995; Drescher et al., 1995). Both RAGS and ELF are ligands for Eph receptors. At least seven ligands have been cloned, all of which are membrane anchored either via a GPI linkage or a transmembrane domain (Davis et al., 1994; Winslow et al., 1995). The studies of RAGS and ELF raise the possibility that this large receptor-tyrosine kinase family might play a novel role in topographic mapping of nervous system.

2. Limb Initiation and Patterning

Conceptually, vertebrate limb development occurs in two steps: limb initiation, and patterning and outgrowth of the limb bud. Limb formation is evident when the limb bud is formed due to localized proliferation of lateral plate mesoderm and the overlying ectoderm. In mouse, this step takes place at E9.5 for the forelimb and at E10.5 for the hindlimb. Once the limb bud has formed, it becomes self-organized and patterning and outgrowth are coordinately controlled along all three axes: dorsoventral, proximodistal, and anteroposterior (Johnson and Tabin, 1997).

Initiation of limb bud formation

Studies on limb initiation have primarily been carried out in chick embryos using foil barrier and extirpation (Stephens and McNulty, 1981; Stephens et al., 1991). Between stages 4-9, barriers inserted lateral to Hensen's node block the wing formation. Between stages 10-11, barriers inserted lateral but not medial to the paraxial mesoderm block wing formation. At later stages between 12-15, barriers inserted lateral to intermediate mesoderm but not paraxial mesoderm will block the wing formation. Similarly, removal of intermediate mesoderm results in a defect in adjacent limb formation. One interpretation of these studies is that the limb inductive signal originates from the medial structure, possibly Hensen's node and the notochord. This signal is then propagated through paraxial

mesoderm, intermediate mesoderm, and then lateral plate mesoderm to direct formation of a limb bud. However, experiments using a foil barrier also block cell migration and the surgical manipulation also causes secondary defects unrelated to the experiment.

Fibroblast growth factor 8 (Fgf-8) was initially thought to be the endogenous limb inducing molecule because it is expressed in the mesonephros in a rostrocaudal sequence at the time when limb initiation occurs (Crossley et al., 1996; Goldfarb, 1996). In addition, it is expressed in the prospective limb ectoderm before limb bud formation. Moreover, Fgf-8-soaked beads induce ectopic limb formation at the body flanks (Crossley et al., 1996; Vogel et al., 1996). However, limb initiation and development are normal in experimental chick embryos that lack mesonephros and are deficient in *Fgf-8* expression in the intermediate mesoderm (Cohn et al., 1995; Crossley et al., 1996; Vogel et al., 1996). Therefore, Fgf-8 involvement in limb initiation remains controversial. Recently, a new member of the Fgf family, *Fgf-10*, is isolated (Ohuchi et al., 1997). Expression analyses in chick demonstrate that it is synthesized initially in the segmental plate and then becomes restricted to the prospective limb mesoderm, including intermediate mesoderm and lateral plate mesoderm, which precedes *Fgf-8* expression. Ectopic application of *Fgf-10* initiates the limb developmental machinery, including *Fgf-8* expression, resulting ectopic limb formation. Its expression persists at later stages in the developing limb bud, which coordinates the limb bud patterning process. Based upon these results, it has been speculated that *Fgf-10* is involved in determining of limb field formation, is an endogenous limb inducer, and mediates interactions between limb ectoderm and mesoderm.

Proximodistal axis formation

Once the limb bud is initialized, the rapidly dividing mesodermal cells induce its overlying ectodermal cells to differentiate into a specialized structure, apical ectodermal ridge (AER), which is responsible for maintaining the continued outgrowth of the limb bud. Surgical removal of the AER causes the distal truncation of limb (Rowe and Fallon,

1982; Summerbell, 1974). A few lines of evidence indicate that AER activity is mediated by *Fgf-8*, and possibly, other factors such as *Fgf-2* and *Fgf-4* (Johnson and Tabin, 1997). At E9.0, *Fgf-8* is expressed in the prospective forelimb ectoderm flanking the lateral plate mesoderm, which is fate mapped to become the AER (Michaud et al., 1997). At E10.0, *Fgf-8* expression is restricted to the AER and this restricted expression is maintained at later stages. Surgical removal of the AER causes distal truncation of the limb and this defect can be rescued by *Fgf-8*-expressing cells.

The initial inductive signal for AER formation derives from the underlying mesoderm, and candidate genes include *Fgf-10* as discussed above. However, the position of the AER at the distal limb bud depends on the signals coming from the ectodermal tissue along the dorsoventral axis (Johnson and Tabin, 1997). Recent evidence indicates that *radical Fringe* (r-*Fng*), a dorsal ectoderm-localized secreted signaling molecule homologous to *Drosophila fringe* (*fng*), and *Engrailed-1 (En-1),* a ventral ectoderm-localized homeodomain-containing transcription factor, play important roles for the AER positioning (Laufer et al., 1997; Panin et al., 1997; Rodriguez-Esteban et al., 1997). The interface between r-*Fng*-expressing and non-expressing cells marks the position of the AER. When this interface is disrupted experimentally, new AERs form at the created boundaries. The ventral *En*-1 suppresses r-*Fng* expression and ensures a sharp boundary between r-*Fng*-expressing and nonexpressing cells (Laufer et al., 1997; Panin et al., 1997; Rodriguez-Esteban et al., 1997).

Anteroposterior axis formation

A small group of posterior limb bud mesoderm cells, zone of polarizing activity (ZPA), is responsible for anteroposterior patterning of the limb (Saunders and Gasseling, 1968). ZPA activity is mediated by the signaling molecule Shh that is expressed in the posterior portion of the limb mesoderm (Echelard et al., 1993; Krauss et al., 1993; Riddle et al., 1993). Ectopic expression of *Shh* in the anterior limb bud induces mirror-image digit duplication, which mimics the ZPA activity (Riddle et al., 1993). The ZPA (Shh) effect is

realized at least in part by regulating expression of 5'-members of the *HoxD* cluster genes, *Hoxd-9* to *Hoxd-13* (Krumlauf, 1994). Fate mapping experiments have shown a strong correlation between the expression domains of these genes and the anlage of digits within the limb bud (Duboule, 1992). The combination of Shh and Fgfs ectopically activates *Hox* gene expression (Duboule, 1992). However, the initiation of *Hox* gene expression may not depend on *Shh* and *Fgfs* function, since in the chick *limbless* mutant nested expression of the *Hox* genes is established in the absence of detectable *Shh* (Noramly et al., 1996; Ros et al., 1996).

The mechanism to initiate *Shh* expression in the limb mesoderm is not very clear. But analyses of *Hoxb-8* ectopic expression suggest that *Hox* genes are good candidates (Charité et al., 1994). Hox proteins are known to be involved in the anteroposterior axis patterning (Krumlauf, 1994; Lufkin, 1996). In the mouse embryo, *Hoxb-8* is expressed with an anterior border at the level of the posterior portion of the forelimb bud. Anterior shifting of this expression pattern across the entire forelimb bud results in ectopic expression of *Shh* in the anterior limb bud (Charité et al., 1994). Retinoic acid may also be one of the endogenous signals that is involved in establishing the ZPA for several reasons. First, it regulates *Hox* genes, including *Hoxb-8*, and establishes the expression patterns and boundaries. Second, when retinoic acid soaked beads are applied to the anterior limb bud, they induce the expression of *Shh*, followed by a mirror-image duplication of the distal limb (Wanek et al., 1991). Therefore, interactions among retinoic acid signaling, *Hox* gene and *Shh* expression may establish pattern along the proximodistal axis.

Dorsoventral axis formation

Initial studies in chick embryos show that begining at stage 15, the limb ectoderm already has patterning activity to impose its polarity on the limb mesodermal rudiment (MacCabe et al., 1974). Thus, a 180^0 rotation of the limb bud ectoderm after stage 15

reverses limb bud patterning along the dorsoventral axis. Recently, similar experiments carried out on stage 13 chick embryos suggest that the initial determinants for dorsoventral patterning are located in the underlying mesoderm (Michaud et al., 1997). Fate-mapping studies using chick-quail chimeras demonstrate that AER maps to the wide domain of ectoderm directly above the lateral plate mesoderm (Michaud et al., 1997). Dorsal limb bud ectoderm maps to the ectoderm above the somites. And ventral limb bud ectoderm maps to the ectoderm above the lateral somatopleural mesoderm. Evidence suggests that the primary signals are synthesized in the somites and the lateral somatopleural at early stages (Michaud et al., 1997). These putative signals then induce production of the secondary signals from the overlying ectoderm. Once the secondary signals are produced, they are responsible for patterning the limb bud along the dorsoventral axis.

Although the nature of the primary signals is not known yet, a secondary dorsalizing signal, *Wnt-7a,* has been identified (Dealy et al., 1993). *Wnt-7a* is synthesized in the dorsal ectoderm and its dorsalizing activity is mediated by a LIM-domain transcription factor, *Lmx-1. Lmx-1* is expressed in the dorsal limb mesoderm (Riddle et al., 1995). Ectopic expression of either *Lmx-1* or *Wnt-7a* dorsalizes the ventral mesoderm in the distal portion of the limb bud (Riddle et al., 1995; Vogel et al., 1995). Similarly, *En-1* determines the ventral limb bud identity because loss-of-function *En-1* mutants lead to dorsalization of the ventral limb mesoderm in the distal region of the limb bud (Loomis et al., 1996). Conversely, loss-of-function of *Wnt-7a* leads to the ventralization of the distal limb bud (Parr and McMahon, 1995). Taken together, these results suggest that *Wnt-7a* dorsalizes limb bud mesoderm through activation of *Lmx-1,* while *En-1* ventralizes limb mesoderm through repression of *Wnt-7a* expression in the ventral ectoderm.

Coordination among different axes

Although the initiation of each axis seems to be independent, all three axes (dorsoventral, proximodistal, and anteroposterior) are tightly linked during later limb bud

outgrowth and patterning (Johnson and Tabin, 1997). For example, surgical removal of the AER, which is responsible for limb bud outgrowth along the proximodistal axis, results in the rapid loss of *Shh* (ZPA activity) expression, which is responsible for patterning the anteroposterior axis (Niswander et al., 1994). The signaling molecule Fgf-4, which is expressed in the posterior two thirds of AER, appears to mediate the feedback regulation between the AER and ZPA signals (Laufer et al., 1994). The feedback regulation is best illustrated in the mouse *limb deformity (ld)* mutant. The *ld* gene encodes Formin, which is expressed in the AER of normal embryos (Chan et al., 1995). In the mutant, the early initiation of both *Fgf-8* and *Shh* is normal. However, later during development, *Fgf-4* expression is attenuated and subsequently *Shh* expression is not maintained (Chan et al., 1995; Haramis et al., 1995). The integration of *Fgf-4* and *Shh* signaling is further demonstrated by the observation that both signals are required for the induction of *BMP-2* and the *HoxD* cluster genes in the posterior mesoderm (Duprez et al., 1996).

The integration of signals for the formation of the different axes is also revealed from analyses of *Wnt-7a* loss-of-function mutants (Parr and McMahon, 1995). In this mutant, the primary defect is ventralization of the distal limb. However, the limbs are also shorter and often lack the posterior-most skeletal elements, due to reduced expression of *Fgf-4* and *Shh*. Complementary to this study, Yang and Niswander (1995), demonstrated that surgical removal of the dorsal ectoderm leads to a reduction in *Shh* expression, a defect that can be rescued by grafting *Wnt*-7a-expressing cells (Yang and Niswander, 1995). Again, the *Wnt-7a* downstream gene *Lmx-1* seems to mediate *Shh* expression, since ectopic expression of *Lmx-1* induces *Shh* expression. Taken together, these results demonstrate that although the initiation of polarizing signals for different axes appears not closely linked, the maintenance of those signals and their patterning activities are highly interdependent.

3. Murine Genetic Strategies to Study Genes: Gain-of-Function

The ability to introduce foreign genes into the mouse genome to generate transgenic mice has tremendously enhanced our ability to study the function, regulation, and interaction of genes during mammalian development (Jaenisch, 1988). It has also facilitated the identification of developmentally important genes (Gossler and Zachgo, 1993). Now, transgenic mice are routinely generated by directly injecting exogenous genetic material into fertilized eggs, or alternatively, by injecting genetically engineered embryonic stem (ES) cells into mouse blastocysts (Palmiter and Brinster, 1986; Schwartzberg et al., 1989). The establishment of pluripotent ES cells with the ability to contribute to germ cells have also made it possible to disrupt specific genes, which produces loss-of-function mutations of certain genes in murine system (Capecchi, 1989; Evans and Kaufman, 1981; Martin, 1981). The loss-of-function approach has proved to be very useful to understand the biological function of many genes, especially when combined with the potential to target genes in a tissue or stage specific manner using the Cre/loxP site-specific recombination system (Lufkin et al., 1991; Jiang and Gridley, 1997).

As a complimentary approach to loss-of-function studies, gain-of-function studies offer a strong advantage when there are functional overlaps among genes, in which case, the phenotypes from a loss-of-function approach are generally less pronounced. For instance, the transcription factor *MyoD* induces muscle differentiation *in vitro* and is important for skeletal muscle formation. However, the knockout of *MyoD* does not show any defect in skeletal muscle formation unless the function of another transcription factor, *Myf 5*, is also impaired (Braun et al., 1992; Rudnicki et al., 1992; Rudnicki et al., 1993). The strategy of a gain-of-function study uses ectopic expression of a gene in novel places during development to assay its function *in vivo*. In a sense, this approach mimics classic transplantation experiments, but with the specific gene rather than tissue moved from one

place to another. The expression of the transgene largely depends on the heterologous promoter used. However, the transgene expression varies from one transgenic line to another because of position effect, a phenomenon wherein the flanking genomic sequence influences transgene expression (Palmiter and Brinster, 1986). Therefore, the ability to tightly control transgene activity in a more spatiotemporal manner would greatly facilitate the analysis of gene function (Jaenisch, 1988). A few inducible gene expression systems have been developed recently to achieve this goal. These include the steroid hormone induction system, the tetracycline system, and the Cre/loxP site-specific recombination system.

Steroid hormone inducible system

Steroid hormone receptors belong to the superfamily of nuclear receptor transcription factors, which regulate gene expression in the presence of hormone ligands (Chambon, 1994). The receptors are typically comprised of 5 to 6 domains with the ligand binding domain (LBD, region E) and DNA binding domain (DBD, region C) most highly conserved. In the absence of hormone, the receptors bind to cytoplasmic protein complexes and are maintained in the inactive state. Hormones binds to the LBD and activates the receptor by dissociating it from the complex and the liganded receptor enters the nucleus to activate/repress a variety of genes. The fusion of the LBD, particularly that of the estrogen receptor (ER), to variety of heterologous proteins results in a ligand-dependent control of their activity *in vitro* (Picard, 1994). However, due to the presence of endogenous estrogen during the mouse life cycle, the ER-LBD would not be a suitable ligand-inducible system to use in transgenic mice. An alternative to ER-LBD, the insect molting hormone ecdysone has been developed as an inducible system for use in transgenic studies (No et al., 1996).

The steroid hormone ecdysone triggers metamorphosis in *Drosophila melanogaster,* showing chromosomal puffing within minutes of hormone addition (Ashburner, 1972). A heterodimer of the ecdysone receptor (EcR) and ultraspiracle (USP) mediates this response.

This insect hormone response system was recreated in cultured mammalian cells by cotransfection of EcR, USP, an ecdysone responsive reporter, and treatment with ecdysone or the synthetic analog muristerone A (Yao et al., 1993; Yao et al., 1992). However, there was only a three-fold increase in gene expression upon hormone induction. To maximize the sensitivity of an ecdysone-inducible system, No et al. (1996), created a modified receptor, VpEcR, a combination of an N-terminal truncation of EcR attached to the VP16 activation domain (No et al., 1996). Heterodimers of this modified receptor and the retinoid X receptor (RXR), the mammalian homologue of USP, mediate more than 200-fold induction with 10uM muristerone in tissue culture.

To investigate the possibility of using this ecdysone-inducible system in transgenic mice, No et al. (1996), generated both reporter and receptor transgenic mice (No et al., 1996). The reporter transgenic mice harbor an ecdysone-inducible reporter, ESHβ. The receptor transgenic mice contain T-cell-specific expression constructs of VpEcR and RXR. Treatment of double transgenic mice harboring both reporter and receptor constructs with muristerone induced significant expression of the reporter gene controlled by the ecdysone-inducible promoter and this demonstrated the feasibility of the ecdysone-inducible system in transgenic mice. There are several advantages to using this system. First, the reporter appears to only respond to insect hormone, which is not present in mammals. Second, the insect hormone seems not to have any toxic or teratogenic activity. Third, because of the lipophilic nature of the induction compounds, they efficiently penetrate all tissues, including the brain. Fourth, The short half life of the induction agent also allows for precise and potent induction. However, this system might be of limited use because it requires generation of receptor transgenic mice, which express both RXR and VpEcR at the same time. Further more, these receptor mice have to mate with the reporter mice to generate "double" transgenic mice which essentially contain three different transgenes. Another

major concern is the potential that over expression of RXR and VpEcR might cause some undesirable effects.

Tetracycline inducible system

Another alternative to the ecdysone inducing system is the bacterial tetracycline system. This system is based on regulatory elements of the Tn10-specified tetracycline-resistance operon of *E. coli*, in which transcription of resistance-mediating genes is negatively regulated by the tetracycline repressor (tetR) (Gossen and Bujard, 1992). In the presence of the antibiotic tetracycline, tetR does not bind to its operator sequence (tetO) located at the promoter region of the operon, and therefore allows transcription. The fusion of the tetR to the VP16 transactivation domain creates a hybrid tetracycline transactivator (tTA) which stimulates transcription from minimal promoters fused to tetracycline operator sequences (tetO). In the presence of antibiotic, it binds to tTA and prevents it from interacting with tetO. Therefore, the promoter is silent. However, in the absence of antibiotics, tTA binds to tetO and activates transcription. This system has been applied to transgenic studies (Furth et al., 1994; Shockett et al., 1995; Shockett and Schatz, 1996). Two types of transgenic mice are required to use this system in transgenic studies, reporter and transactivator mice. The reporter mice, in one case, harbored the luciferase reporter under control of the tet responsive promoter which has a low basal activity (Furth et al., 1994). The transactivator mice produced tTA under the control of a CMV promoter. In double transgenic mice, the reporter gene luciferase expression was inhibited in the presence of tetracycline and observed in the absence of the antibiotic.

Although tetracycline and many of its derivatives are not toxic to eukaryotic cells at the concentration required to abolish gene expression, the continuous presence of the antibiotic is not optimal for research on transgenic animals. Moreover, the low clearance rate of antibiotics interferes with rapid and precise induction. To overcome these potential drawbacks, Gossen et al. (1995) improved the system by identifying a mutant tetracycline

repressor (rtetR). The mutant repressor revised receptor DNA binding properties such that tetracycline induces rather than abolishes its binding to the operator (Gossen et al., 1995). Combining the mutant repressor and the VP16 activation domain creates the reversed tetracycline transactivator (rtTA) which induces rather than abolishes gene expression in the presence of the antibiotic. Addition of antibiotic into the tissue culture media rapidly induces the reporter gene expression in the transfected cells. The rapid inductive property may hinder its use as a precise and efficient on-off switch in transgenic mice studies.

Cre/loxP recombination-activated gene expression system

In contrast to the inducible systems described above, where expression of genes is controlled at the transcriptional level, the Cre/loxP system is a recombination-activated gene expression (RAGE) system which controls gene expression at the DNA level (Sauer, 1993). Cre is a member of the Int family of recombinases which was isolated from bacteriophage P1 (Argos et al., 1986). It has been shown to mediate site-specific recombination at the loxP site, a 34bp DNA sequence consisting of two 13bp inverted repeats and an 8bp asymmetric core region (Sauer, 1987). Cre protein binds to the repeats and cleaves the loxP site at the core region. Strand exchange takes place after the cleavage resulting in recombination between the two loxP sites. Structural studies indicate that the recombination takes place through an intermediate structure that resembles the model of the four-way Holliday junction (Guo et al., 1997). As the result of recombination, any DNA bracketed by directly repeated loxP sites is excised as a circular DNA molecule.

One way to use the Cre/loxP site-specific recombination system is to activate gene expression in a spatiotemporal specific manner (Sauer, 1993). This strategy uses an intervening DNA STOP sequence, which consists of many translational stop condons in all three frames to prevent translation of a downstream gene. The STOP sequence is flanked by directly repeated loxP sites. In the presence of Cre protein, site-specific recombination at the loxP sites, which removes the STOP sequence, activates expression of the downstream

genes. One example of using this system was to target simian virus 40 (SV-40) large tumor antigen (tAg) expression specifically to the lens of the eye using the murine α-crystallin promoter (mαA) (Lakso et al., 1992). In this study, two types of independent transgenic mice lines were established: mαA-Stop-TAg and mαA-Cre transgenic mice. mαA-Cre transgenic mice express Cre protein specifically in the lens. All double transgenic mice harboring both transgenes developed lens tumors resulting from large T antigen expression after Cre-mediated deletion of the STOP sequence.

In principle, the Cre/loxP site-specific recombination system will allow the targeting of gene expression to any tissue at any stage during mouse development, dependent on the spaciotemporal expression of Cre. Several groups have successfully used this system to inactivate genes in a tissue-specific manner (Gu et al., 1994; Gu et al., 1993; McHugh et al., 1996; Tsien et al., 1996; Tsien et al., 1996). There is no doubt that more reports will appear soon. However, its current use is limited by the availability of well-characterized tissue- or cell type-specific promoters for making Cre-expressing transgenic mice. Therefore, an inducible *Cre* expressing transgenic mouse will greatly facilitate the ability to used Cre/loxP system. Two groups have reported the successful use of inducible *Cre* transgenic mice. One group used an interferon inducible promoter to drive expression of the *Cre* gene (Kuhn et al., 1995). Inducible deletion of the targeted gene was reported in different tissues. However, the background recombination rate was quite high, perhaps because of the endogenous production of interferon in mice. Another group has used a steroid hormone inducible system to produce chimeric Cre protein whose activity is dependent on a synthetic ligand (Feil et al., 1996). Administration of the ligand induced Cre-mediated excision of the target gene only in the tissues expressing Cre protein.

A land mark study has shown that Cre-mediated recombination can also cause deletion of the chromosome in which loxP-containing transgenes are integrated

(Lewandoski and Martin, 1997). In this study, when transgenic males carrying a loxP-containing Y-chromosome were mated with females expressing Cre protein ubiquitously at early embryonic stages, almost all progeny develop as females (either XX or XO female) because of loss of the Y-chromosome during early embryogenesis.

In view of the recent advances of murine genetics, detail analysis of the Cre/loxP system *in vivo* will undoubtedly provide insights of using this novel tool in transgenic studies. Specifically, the Cre/loxP recombination-mediated chromosome deletion may also provide an unique genetic tool to ablate certain cell lineages. To test this hypothesis, this thesis research will focus on investigating the potential to utilize the Cre/loxP recombination-mediated ablation system and studying the function of the floor plate and notochord in the spinal cord and limb development. As a result, I established and examined in detail eight different transgenic founder lines (from total 22 individual lines). The Cre/loxP system was examined both *in vitro* and *in vivo*. The role of the floor plate and notochord in the spinal cord and limb development was examined in two independent lines of double transgenic embryos harboring both E3Cre and E3loxP transgens. In the second part of the thesis, I also used the traditional gene knock-out approach to study function of two novel homeobox containing transcription factors, *Dlx5* and *Dlx6*, in murine nervous system and cartilage development.

II. Materials and Methods

In vitro expression vectors

The *Cre* gene from bacteria phage P1 was modified to generate a KOZAK sequence for eukaryatic cell expression by site-directed mutagenesis using the oligonucleotide TL203 (5' GGTCAGTAAATTGGACATGGTACACTCAGATAATGGTTTT 3'). A 3.55kb Spe fragment of pSL26 (described below), including *Cre-IRES-AP* coding sequences (internal ribosomal entry site-alkaline phosphatase), was blunt end subcloned into the Bgl II-Hind III site of p513. The resulting plasmid, pSL30, has the SV-40 promoter driving expression of both *Cre* and *IRES-AP* sequences.

A 9.8kb Hind III-Bgl II fragment from pSL56 (described below) was cloned into Hind III-Bgl II site of p513 to generate pSL84. A 760bp Pst I restricted fragment of the green fluorescent protein (GFP, Clonetech) coding region in p1220 was subcloned into the Pst I site of pSL84. The resulting plasmid, designated pSL87, has SV-40 early promoter, rabbit β-globin IVS II intron, loxP flanked STOP sequence (describe below), and followed by GFP coding region plus the SV-40 polyadenylation signal. pSL88 was derived from pSL87 in which the *lacZ* sequence was removed by *in vitro* Cre/loxP recombination using Cre recombinase (Stratagene).

E3Cre transgenes

A 0.6kb Xho I/Bam HI restricted fragment encoding the IRES sequence from pWH7A (Kim et al., 1992) was cloned into Xho I/Bgl II sites of p1064. This new plasmid, designated p1066, has human placenta alkaline phosphatase (AP), originated from p1064, fused in frame with IRES. A 2.5kb Cla I restricted fragment from p1066 encoding *IRES-AP* was then blunted with T4 DNA polymerase and subcloned into the Nru I site of p1065 (from T. Lufkin) to make pSL7. A 1.3kb Xho I/Sal I restricted fragment encoding

the *Cre* sequence from pBS39 (Clontech) was cloned into pUC21 and the resulting plasmid was used as the template for site-directed mutagenesis. Oligos TL203 (5'-GGTCAGTAAATTGGACATGGTACACTCAGATAATGGTTT-3') and TL160B (5'-ATAGCAATCATTTACTAGTTAATGGCTAATCGCC-3') were used to generate KOZAK consensus sequences around ATG for mammalian expressing system and to add a new Spe I restriction site at the 3' end of the *Cre* coding region. Site-specific mutagenesis was performed essentially as described in the Stratgene Protocol. The resulting plasmid, named pSL13, was digested with Spe I, and a 1.05kb fragment encoding *Cre* was then cloned into the Spe I site of pSL7 to make pSL26. A 1.05kb Spe I restricted fragment from pSL26 was blunt end cloned into the Sma I site of p601D. This plasmid, designated pSL29, containing the rat β-actin promoter, rabbit β-globin IVS II intron, *Cre* coding sequence and SV-40 polyadenylation signal. A 2.5kb Cla I restricted fragment from p1066 was then blunt end cloned into the Eco RI site of pSL29 to make pSL31.

E3loxP transgenes

Oligonucleotides TL143 (5'-CATAACTTCGTATAGCATACATTATACGAAGT TCTC-3') and TL144 (5'-CTAGGATAACTTCGTATAATGTCTGCTATACGAAGG TTAT-3'), which encode a loxP site, were cloned into the Kpn I-Xba I site of pUC21. This plasmid was restricted with Xho I and Kpn I enzymes and inserted by another pair of oligonucleotides, TL145 (5'-TCGAATAACTTCGTATAGCATACATTATACGAAGT TATTCTAGAGTA-3') and TL157 (5'-TCTAGAATAACTTCGTATAATGTATGCTATA CGAAGTTAT--3'), encoding another loxP site. The resulting plasmid, named pSL5, has Spe I restriction sites flanking two loxP sites facing the same direction with a unique Xba I cloning site in between the loxP sites (Spe I-loxP>Xba I-loxP>Spe I). A 4.5kb *lacZ* coding sequence and *Hoxa-1* polyadenylation signal sequence from p898, designated STOP sequence, was then cloned into the Xba I site of pSL5. Two copies of the STOP sequences were cloned into Xba I site in a head-to-tail orientation. This plasmid, designated pSL8,

was digested with Spe I and the 9.0kb fragment containing loxP flanked 2X STOP was cloned into Spe I site of p1065 which has the Enhancer III, a SV-40 basal promoter and a polyadenylation signal. The resulting plasmid is named pSL10. cDNAs *Msx1, CRABP-1, Dsl-1, Wnt-1, Gbx2* were blunt end cloned into the Nru I site of pSL10 resulting in a E3loxP transgenes pSL14, pSL16, pSL18, pSL20, and pSL45 respectively. These E3loxP transgenes were digested with Sfi I restriction enzyme and the transgene fragments were purified by gel electrophoresis and mircoinjected into male pronuclei of 0.5 day fertilized mouse embryos to make transgenic founders. The injections was performed in the transgenic core of the Brookdale Center for Molecular and Developmental Biology at Mount Sinai School of Medicine, New York.

DNA analysis

Tail tips, yolk sacs, or ES cells were digested overnight at 55^0C in 0.2M NaCl, 50mM Tris-HCl (pH7.4), 5mM EDTA, 1% SDS buffer containing 100mg/ml proteinase K. After digestion, the mixture was extracted in successive steps with equal volume of phenol:chloroform (1:1), chloroform, and then precipitated with 2 volumes of 95% ethanol. The resulting DNA pellet was washed with 70% ethanol, air dried, and resuspended in 100ul of TE (10mM Tris-HCl, pH7.5, 1mM EDTA). Ten microgram DNA was digested with the appropriate enzyme overnight and separated on 1% agarose gel in an electric field. The DNA in the gel was denatured with 0.5M NaOH and transferred onto Hybond N^+ (Amersham) nitrocellulose membrane according to the specifications of the manufacturer. Hybridization was performed at 42^0C overnight in a solution containing 50% formamide, 2X SSC, 5% dextran sulfate (800,000 MW), 1% SDS, and 50ug/ml freshly boiled sheared salmon sperm DNA. The DNA blots were washed 4x30 minutes at 60^0C in 0.2X SSC and 0.1% SDS before exposure to X-ray film. The following probes were used to screen *Dlx5* and *Dlx6* knockout ES clones and mice. Probe 1: a 2.5kb Eco RV-Xho I

fragment from pSL100, Probe 2: a 0.8kb Bgl II-Not I fragment from pDlx18+. Probes used for transgenic analyses were indicated in the text.

PCR

Stage E12.5 embryos were isolated from mating transgenic mouse lines 45-17 with 26-16s. Double transgenic mice were easily identified because of their forelimb defect. Several tissues, including defective forelimbs, hindlimbs, ventral spinal cord, and forehead were dissected from the embryos under a dissecting microscope. DNA (500ng) from each of these tissues were used for PCR reaction using the Expand™ Long Template PCR System (Boehringer Mannheim). Primers, TL573 and TL585, used in this study correspond to Enhancer III and *Gbx2* sequences respectively. TL573: 5'-GTCTTGCTGTGACTGTGAAGTCGGC-3'. TL585: 5'-AGCGAGTCTATGCTGAAGG CGGTACTAC-3'. The PCR products were separated on a 1% agarose gel for Southern analysis. Hybridization was performed using plasmid pSL45 as a probe, which has Enhancer III, *lacZ* and *Gbx2* sequences. Following hybridization, the membranes were washed and exposed to X-ray film for 20 minutes.

Transfection

pSL30, pSL87, pSL88, or pSL30+pSL87 (20ug each) were separately transfected into COS-7 cells by the calcium phosphate method as described (Sambrook et al., 1989). The cells were then treated with chloroquine at the final concentration of 100uM for 3-5 hours to increase the transfection efficiency. The results of transfection were analyzed 48 hours later by Southern blot, AP staining or visualized using fluorescence microscopy to check for green fluorescent protein (GFP) production.

β-galactosidase (β–gal) and AP staining and photography

Staining was performed essentially as described (Li et al., 1997). Embryos were dissected out and fixed for 10-30 minutes at 4^0C in phosphate-buffered saline (PBS) containing 2% formaldehyde, 0.2% glutaraldehyde, 0.02% NP-40 and 0.01% sodium deoxycholate (Sigma). Embryos were then briefly rinsed 2-3 times with PBS and stained with X-gal at 37^0C for 2-24 hours in the β-gal staining solution. The staining solution contained 5mM$K_3Fe(CN)_6$, 5mM $K_4Fe(CN)_6$, 2mM $MgCl_2$ and 100-500ug/ml X-gal in PBS. Stained embryos were washed with PBS for 2 hours and stored at 4^0C in PBS. To visualize AP, the embryos were washed with PBS and then postfixed in 4% paraformaldehyde overnight at 4^0C. After post fixation, embryos were rinsed with PBS several times and heat-treated in PBS at 70-75^0C for 30 minutes to inactivate endogenous AP activity. After heat treatment, embryos were rinsed again with PBS at room temperature and followed by 10 minutes washing with AP buffer containing 0.1M Tris-HCl (pH9.5), 0.1M NaCl and 10mM $MgCl_2$. Finally, the embryos were stained with BM-Purple AP Substrate (Boehringer Mannheim) between 4^0C and room temperature in the dark for 0.5-36 hours. After staining, embryos were washed extensively with PBS plus 0.1% tween-20 and 2mM $MgCl_2$. Embryos were then cleared with glycerol or with 2:1 benzyl alcohol: benzyl benzoate after methanol dehydration, ready for whole mount photography using a dissecting microscope under bright-field illumination. For sections, embryos were first infiltrated with 15% sucrose in PBS for 2 hours, followed by 30% sucrose overnight at 4^0C. Embryos were then embedded in OCT compound, frozen at -80^0C and sectioned on a cryostat machine. 20-30um sections were collected on Super Frost Plus glass slides (Fisher) and air-dried overnight at 40^0C on a slide warmer. The slides were then dehydrated in graded ethanol, followed by two changes of Americlear (Baxter) and coverslipped with Cytoseal (Stephens Scientific).

Immunohistochemistry

Immunoperoxidase staining for Cre was done on 30um cryostat sections. Sections were first fixed with 4% paraformaldehyde in PBS for 20 minutes at room temperature and then washed three times for 1 hour in 50mM NH_4Cl in PBS. Endogenous peroxidase activity was blocked with 1%H_2O_2 in TS-PBS (0.1% Triton X-100 and 10% fetal calf serum in PBS) for one hour. Rabbit anti-Cre antibody (Novagen) was diluted 1:1000 in TS-PBS and applied to sections overnight at 4^0C. The sections were then washed three times for 1 hour at room temperature and incubated with goat anti-rabbit IgG-horseradish peroxidase (HRP, SIGMA) diluted 150-fold in TS-PBS. HRP activity was detected with 0.05% diaminobenzidine (DAB) and 0.01% H_2O_2 in PBS after a 1 hour wash with PBS. the reaction was stopped after 4 hours with cold PBS. The sections were then dehydrated through graded ethanol, treated with Americlear, and coversliped with Cytoseal (Stephens Scientific).

For immunoflorescence staining, 30um cryostat sections were stained with the monoclonal 2H3 anti-neurofilament antibody. The 2H3 antibody developed by T. Jessell and J. Dodd is obtained from the Developmental Studies Hybridoma Bank maintained by the Department of Pharmacology and Molecular Sciences, Johns Hopkins University School of Medicine, Baltimore, MD 21205, and the Department of Biological Sciences, University of Iowa, Iowa City, IA 52242. The biotin-conjugated, species-specific secondary antibody raised against mouse IgG (Amersham) was used and visualized with rhodamine-conjugated streptavidin (Molecular Probes). The sections were then counter stained with the nuclear dye DAPI (4', 6'-diamidino-2'-phenylindole, Sigma). After staining, coverslips were mounted with buffered glycerol, which contains 2% 1,4-diazabicyclo- (2,2,2)-octane to reduce fading.

In situ hybridization on sections

This was performed essentially as described (Li et al., 1997). Embryos were fixed in 4% paraformaldehyde overnight, washed in PBS, and dehydrated through a graded series of ethanol, followed by two changes of Americlear (Fisher) and embedded in Paraplast (Fisher) overnight under vacuum. 6 um sections were cut and floated onto Super Frost Plus slides (Fisher), dried, and stored at 4^0C. Before hybridization, the sections were rehydrated, proteinase K digested, and then treated with tri-ethanolamine/acetic anhydride followed by dehydration. G-50 column purified ^{35}S-RNA probes (25,000-50,000 cpm/ul) were applied to sections and hybridized overnight at 55^0C. Following hybridization and washing, the sections were dehydrated and exposed overnight to X-ray film to determine signal strength. Autoradiography was performed by dipping the slides in Kodak NBT2 emulsion, air drying and exposing for 3-7 days, followed by developing in Kodak D19 and counter staining. The following probes were used as previously described. *Pax-1*, *Pax-5*, and *Pax-6* (Deutsch et al., 1988); *Pax-3* and *Pax-7* (Goulding et al., 1991); *Shh* (McMahon, 1993); *Dlx5* and *Dlx6* (Simeone et al., 1994); *Nkx 2.2* (Price et al., 1992); rat *Islet*-1 (Ericson et al., 1992); *Fgf-8* (Crossley and Martin, 1995); *Netrin-1* (Serafini et al., 1994); *Fgf-10* (Ohuchi et al., 1997); *Hox b8* (Charité et al., 1994).

Whole mount in situ hybridization

Whole mount *in situ* was performed essentially as described (Henrique et al., 1995). Embryos were fixed in 4% paraformaldehyde overnight at 4^0C, dehydrated in graded methanol, and stored at -20^0C. Before use, embryos were rehydrated towards PTW (PBS, 0.1% Tween-20) and digested with 10ug/ml proteinase K for 10-20 minutes. Digoxygenin labeled RNA probes were prepared according to the directions of the manufacturer (Boehringer-Mannheim). Hybridization was performed at 65^0C overnight. The hybridization solution contained 50% formamide, 1.3X SSC, 5mM EDTA, 50ug/ml yeast RNA, 0.2% Tween-20, 0.5% CHAPS, 100ug/ml Heparin, and 0.1-1ug/ml

digoxigenin (DIG)-labeled probe. After three hours PTW washing, embryos were incubated in a 1:2000 dilution of anti-DIG-AP antibody solution containing 2% Boehringer Blocking Reagent (BBR), 20% heat inactivated sheep serum, and 1x MABT (100mM Maleic acid, 150mM NaCl, pH7.5, and 0.1% Tween-20). Following four hours extensive washing, embryos were stained with BM-purple substrate manufacturer (Boehringer-Mannheim) at 4^0C. Stained embryos were photographed under a dissecting microscope.

Histological and anatomical analyses

Embryos were fixed in 4% paraformaldehyde, embedded in paraffin, and serial sections were collected on the Super frost plus slides. Sections were then stained with hematoxylin-eosin (H&E). For whole mount analysis of skeletons, new born pups were first anesthetized with chloroform, and the internal organs and skin were removed. The pups were fixed overnight in 95% ethanol and stained for cartilage in 95% ethanol, 20mM acetic acid, 15-30mg alcian blue (Sigma) for 12-48 hours. After staining, embryos were washed with 95% ethanol and treated with 2% KOH for 24 hours, followed by overnight staining in 1% KOH, 0.015% alizarin red. Embryos were then destained for about 3-7 days with 20% glycerol plus 1% KOH and stored in 50% glycerol and 50% ethanol.

TUNEL assay

Paraffin sections (6um) were rehydrated through Americlear, and serial ethanol/TBS (Tris Buffered Saline). Sections were then digested with 10ug/ml proteinase K with 2mM $CaCl_2$ in TBS for 15 minutes at 37^0C. The terminal transferase reaction was performed according to the directions of the manufacturer (Boehringer-Mannheim). After 1 hour at 37^0C, sections were rinsed with TBS and counter stained with DAPI and coversliped with buffered glycerol, which contains 2% 1,4-diazabicyclo-(2,2,2)-octane to reduce fading. Apoptotic cells were photographed using fluorescence microscopy.

Isolation and analysis of Dlx5 and Dlx6 genomic DNA

Three *Dlx5* or *Dlx6* containing genomic phage were plaque-purified from an initial screen of 400,000 plaques from a mouse 129SV genomic library (kindly provided by F. Ramirez) using a 0.4kb genomic fragment specific to the *Dlx5* gene (kindly provided by E. Boncinelli). Library screening and phage purification were performed essentially as described (Sambrook et al., 1989). Analysis of these phage clones indicated that the homeoboxes for *Dlx5* and *Dlx6* are located 11kb apart. Probes obtained from the distal ends of the two most widely separated genomic phage clones were used to rescreen the library which resulted in the isolation of three additional genomic phage from the locus. Alignment of the six genomic phage clones indicated that approximately 40kb of genomic DNA surrounding the *Dlx5* and *Dlx6* loci had been obtained. A 0.5kb Sal I/Kpn I and a 1.2kb Stu I-Bam HI genomic fragments containing the *Dlx5* and *Dlx6* homeoboxes, respectively, were subcloned into pBSK$^+$ and sequenced to confirm the screening results. Restriction mapping was performed using enzymes from Biolabs.

Chromosomal mapping

DNA from N2 animals of a [(C57BL/6J x SPRET/Ei) F1 females x SPRET/Ei males, the Jackson Laboratory] backcross were digested with Hind III and separated on a 1% agarose gel and transferred to Hybond-N+ (Amersham). The blots were probed with a 0.8kb Bgl II/Not I genomic fragment isolated from the *Dlx6* containing phage clone. This probe detects a 4.7kb specific SPRET/Ei band and a 4.2kb specific C57BL/6J band. Results of the analysis were submitted to The Jackson Laboratory Backcross DNA Panel Map Service (http://www.jax.org or http://www.jax.org/resources.documents.cmdata.). The consensus map was based on the 1994 Chromosome committee Reports obtained using the Encyclopedia of the Mouse Genome Release 3, version 1.0A13 (ftp://ftp.informatics.jax.org/pub/informatics/encyclo/data/3.0/committee.reports/) obtained from The Jackson Laboratory, Bar Harbor, Maine.

Dlx5 knockout constructs

A 13kb Not I/Bgl II genomic DNA fragment containing the *Dlx5* homeobox from a phage clone was subcloned into pBSK$^+$ Not I/Bam HI sites. A 0.5kb Sal I/Kpn I fragment isolated from this plasmid, pDlx18$^+$, was subcloned into pBSK$^+$, and used as a template to perform site-specific mutagenesis introducing a unique Xho I site in the homeobox. The resulting plasmid, called pSL48, was then reintroduced into pDlx18$^+$ to form plasmid pSL49. A 5.3kb Xho I fragment, containing *IRES-lacZ*-GT1.2-*Neo* gene from p1099, was cloned into the unique Xho I site of pSL49. This plasmid, designated pSL59, was linearized at the unique Not I site and used for ES cell electroporation. A 2.2kb Not I fragment, containing GT1.2 *TK* gene, was cloned into the Not I site of pSL59. The resulting targeting construct, designated pSL81$^+$, had both positive and negative selection markers and was linearized with Sac II for ES cell electroporation.

Dlx6 knockout constructs

An 18.3kb Not I genomic DNA fragment containing the *Dlx6* homeobox from a phage clone was subcloned into pBSK$^+$ vector. A 4.4kb Spe I/Snab I fragment isolated from this plasmid, pDlx19$^+$, was subcloned into Spe I/Sma I sites of bluescript SK vector, and used as a template to perform site-specific mutagenesis that introduced a unique Nru I site in the homeobox. The resulting plasmid, designated pSL62, was digested with Spe I/Eco RV restriction enzymes. A 4.4kb Spe I/Eco RV fragment with unique Nru I site in the *Dlx6* homeobox was subcloned into Spe I/Snab I site of pDlx19$^+$ to form pSL67. A 3.2kb Spe I fragment from pDlx19+ was then reintroduced into the Spe I site of pSL67 and the resulting plasmid is named pSL71. A 5.3kb Xho I fragment, containing *IRES-lacZ/GT1.2-Neo* gene from p1099, was cloned into the unique Nru I site of pSL71. This plasmid, designated pSL74, was linearized with Sal I and used for ES cell electroporation. pSL74 was digested with Sal I and the Sal I/Sal I fragment was then cloned into Sal I site of p572 which has the GT 1.2 promoter driving expression of the *TK* gene. Therefore, the

new targeting construct, termed pSL80, has both positive and negative selection markers. pSL80 was linearized with Sfi I for ES cell electroporation.

A 1.3kb Eco RI-Bam HI fragment containing the *PGK-Neo* expression cassette was blunt end cloned into Sal I site of p1101. A 5.3kb Xho I/Xho I fragment of the resulting plasmid, pSL96, which contains *IRES-lacZ*, the *PGA-Neo* coding sequence, and the polyadenylation signal, was then blunt end cloned into the Nru I site of pSL71. The resulting plasmid, pSL100, was linearized with Sal I for ES cell electroporation.

Dlx5 and Dlx6 double knockout construct

The oligonucleotide primer pair TL260 (5'-AGCTGGCCACTCAGGCCGGATC CGCGGCCGCTCGCGAAGATCTGGCCACTCAGGCC-3') and TL261 (5'-AATTGG CCTGAGTGGCCAGATCTTCGCGAGCGGCCGCGGATCCGGCCTGAGTGGCC-3') containing the restriction sites Sfi I-Bgl II-Nru I-Not I-Bam HI-Sfi with cohesive ends of Eco RI and Hind III was cloned into pTZ18R vector to generate pSL58. An 8.6kb Bgl II-Not I fragment from Dlx19^{+}, which is located 5' to the *Dlx5* and *Dlx6* homeoboxes, was cloned into Bam HI-Not I sites to get plasmid pSL64. A 1.2kb Nru I-Bgl II fragment from Dlx18^{+}, which is located 3' to the *Dlx5* and *Dlx6* homeoboxes, was cloned into the Nru I/Bgl II sites of pSL64 to generate pSL66. A 1.6kb Xho I/Xho I fragment containing GT1.2-*Neo* from p662 was blunt end cloned into Nru I site of pSL66. This resulting plasmid, pSL72, has a *Neo* selection gene replacing more then 13.0kb of genomic DNA containing both *Dlx5* and *Dlx6* homeoboxes. pSL72 was linearized with Sfi I for ES cell electroporation. An 11.6kb Sfi I/Sfi I fragment of pSL72 was blunt end cloned into the Xho I site of p572 (as described above). This double knockout construct, designated pSL79, has both positive and negative selection markers and was linearized with Sfi I for ES cell electroporation.

An 11.9kb Bgl II-Nru I fragment from pSL71 was cloned into the Bam HI-Nru I sites of pSL58 resulting in pSL94. A 5.8kb Eco RV-Sal I fragment from pSL96 was then blunt end cloned into the unique Nru I site of pSL94. This plasmid, designated pSL99, has an *IRES-lacZ*-PGK-*Neo*-polyadenylation signal replacing 11kb of genomic sequence between the two *Dlx5* and *Dlx6* homeoboxes with *IRES-lacZ* following *Dlx6* direction. pSL99 was linearized with Sfi I for ES cell electroporation.

ES cell growth, transfection, and selection

D3 and R1 ES cells were maintained on gelatin-coated dishes in DMEM (high glucose) containing 15% heat-inactivated fetal calf serum, 1mM sodium pyruvate, 0.1mM β-mercaptoethanol, and 1000 U/ml LIF with a feeder layer grown at 37^0C in 10% CO_2. For electroporation, 1 x 10^7 ES cells were mixed with 10ug linearized DNA in 0.5ml of DMEM containing 15% serum in a 0.4cm path length cuvette and electroporated at 400V at 125uF with a Bio-Rad Gene Pulser. The cells were then transferred to nonselective medium for 2 days and selected in either 150ug/ml G418, 150ug/ml G418 + 2uM gancyclovir, or 35ug/ml G418 for 10 days. Antibiotic resistent ES clones were picked into microwells containing a feeder layer and subsequently expanded for Southern blot analyses. Hyperselection was performed with 500ug/ml G418 for 10 days.

III. Results: Part A

1. Cre/loxP Binary Transgenic Mouse System

Introduction

There are two different results that have been reported for using the Cre/loxP system in transgenic mice. In one case, the Cre-mediated site-specific recombination was used successfully as a RAGE system to conditionally activate large T-antigen expression in transgenic mice (Lakso et al., 1993). However, in another case, it was demonstrated that the Cre/loxP recombination in the transgenic mice led to chromosome deletion (Leqandoski and Martin 1997). To further investigate the potential of utilizing this system in transgenic mice, 26 different transgenic founder mice were generated using either E3Cre or E3loxP transgenes. The E3Cre transgene encodes *Cre* and *AP* reporter gene, while the E3loxP transgene encodes a loxP flanked STOP sequence (*lacZ* gene), which prevents translation of the 3' cDNAs *(Wnt-1, Msx1, Dorsalin-1, CRABP-1,* or *Gbx2).* Double transgenic embryos harboring both E3Cre and E3loxP transgenes were examined by Southern blot and PCR for Cre-mediated DNA recombination. Conditional activation of the downstream gene expression was assessed by *in situ* hybridization, and the outcome of chromosome deletion was examined by TUNEL assay for fragmented chromatin. As a result, extensive analyses of eight different transgenic lines suggested that the Cre/loxP RAGE system needs to be further refined for efficient activation of downstream gene expression and the Cre/loxP recombination system can be used as a novel genetic tool for tissue-specific ablation in the transgenic studies.

Results

1. *Cre/loxP system acts as a molecular switch in vitro*

Cre-mediated site-specific DNA recombination was tested *in vitro* by transiently transfecting COS-7 cells with pSL30 and/or pSL87 (the plasmid is described in the materials and methods) (Figure 1A). pSL30 and pSL87 transfected cells showed strong AP and β-gal staining respectively (Figure 2A and 2B). However, cells transfected with both pSL30 and pSL87 only have AP staining indicated by the fact that there are very rare β-gal positive cells (compare Figure 2B and 2C), possibly due to the excising of *lacZ* coding sequences from pSL87 by Cre-mediated recombination. To investigate whether site-specific recombination takes place at the DNA level in the double transfected cells, genomic DNA from the transfected cells were digested with Sal I and examined by Southern blot after 48 hours transfection. The diagnostic probe using *GFP* cDNA hybridized with a 5.6kb fragment from pSL87 transfected genomic cell DNA (lane 2, Figure 1B). In the cells cotransfected with both pSL30 and pSL87, Cre-mediated site-specific recombination was apparent from the appearance of a 1.6kb band on the Southern blot which is recombination specific (compare lane 2 and 4, Figure 1B). The presence of the unrecombined 5.6kb band in the double transfected cells suggests either that not every cell was transfected with both plasmids (lane 4, Figure 1), or alternatively, that the recombination was not 100% efficient. However, these results suggest that Cre-mediated site-specific recombination takes place at the DNA level and the recombination eliminates the expression of the *lacZ* reporter gene in the *in vitro* cell culture system.

To investigate whether recombination specifically turns-on expression of downstream genes, the transfected cells were examined under a fluorescence microscope under UV illumination to detect expression of the GFP reporter gene. Cells transfected with a positive control plasmid pSL88 have a strong green fluorescence signal (Figure 2D). In contrast, cells transfected with pSL87 do not have any detectable fluorescence signal

(Figure 2E). This indicates that the STOP sequence has efficiently blocked the expression of downstream GFP expression. Non-transfected cells or those transfected with pSL30 plasmid do not have any detectable GFP expression (data not shown). However, cells transfected with both pSL30 and pSL87 show strong fluorescence signal indicating the production of GFP protein (compare Figure 2E and 2F). These results demonstrate that Cre, encoded by pSL30, has specifically enabled the expression of GFP gene by removing the upstream STOP sequence. Similar experiments were also performed using a much more sensitive reporter gene luciferase in place of the GFP reporter. Results from these studies confirm the results presented here (data not shown).

Figure 1. Analyses of Cre/loxP site-specific recombination *in vitro*. A. Schematic diagram of plasmids used for transfection assay (not to scale). The size of the plasmid after Sal I digestion is indicated below the constructs. B. Southern blot analyses of DNA from transfected COS7 cells. Red asterisk indicates the size of plasmid after recombination. A+, SV-40 polyadenylation signal; unrec, unrecombined; rec, recombined.

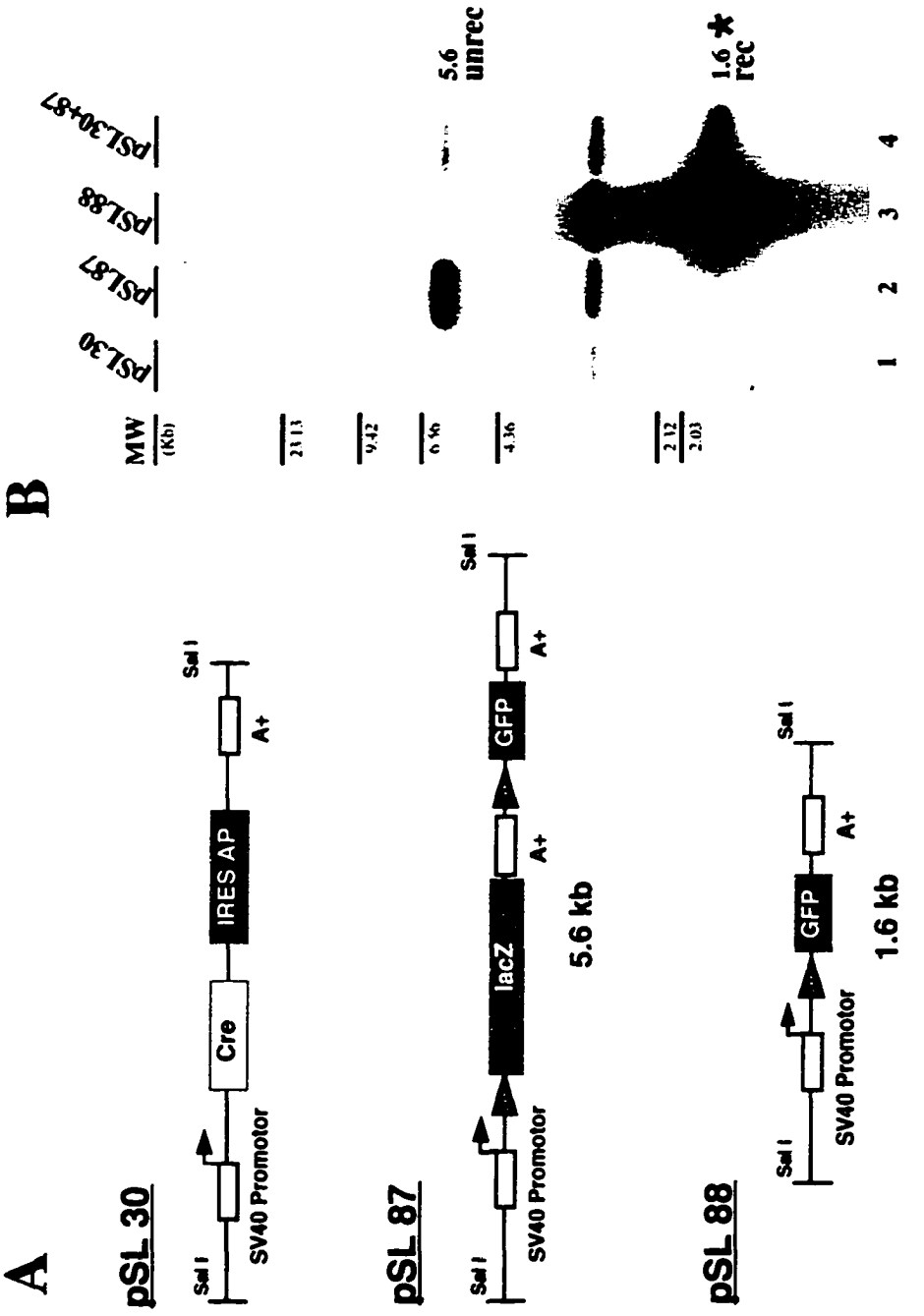

Figure 1

2. *Designing a Cre/loxP binary gain-of-function system to study dorsoventral patterning of the spinal cord*

The floor plate and notochord specific enhancer, Enhancer III, was used to express dorsal specific genes in the ventral neural tube. The Enhancer III element was isolated from the 3' end of the *Hoxa-1* gene (Frasch et al., 1995). In transgenic animals this enhancer, when linked to a basal promoter, drives expression of a reporter specifically in the floor plate and the notochord between E7.5 and E14.5. Its activity is also detectable in the gut epithelium and some ventral lateral neurons. The internal ribosome entry site (IRES) sequence used was isolated from the 5'-untranslated region of the Encephalomyocarditis virus (EMCV) (Jang et al., 1990). It enables internal binding of a ribosome that translates downstream genes in a cap-independent manner (Jang et al., 1990; Mountford and Smith, 1995). Transgenic studies indicate that it allows efficient production of two separate proteins at the same place and same time under control of a single promoter (Li et al., 1997).

Figure 2. Examination of gene activation *in vivo* after Cre recombination. A-C, double staining of transfected cells for β-gal and AP activity. The AP staining appears purple and the β-gal staining appears blue. D-F, expression of *GFP*. The constructs used for transfection are indicated at the upper right corner of each panel and shown in Figure 1A. *GFP* positive cell appears green.

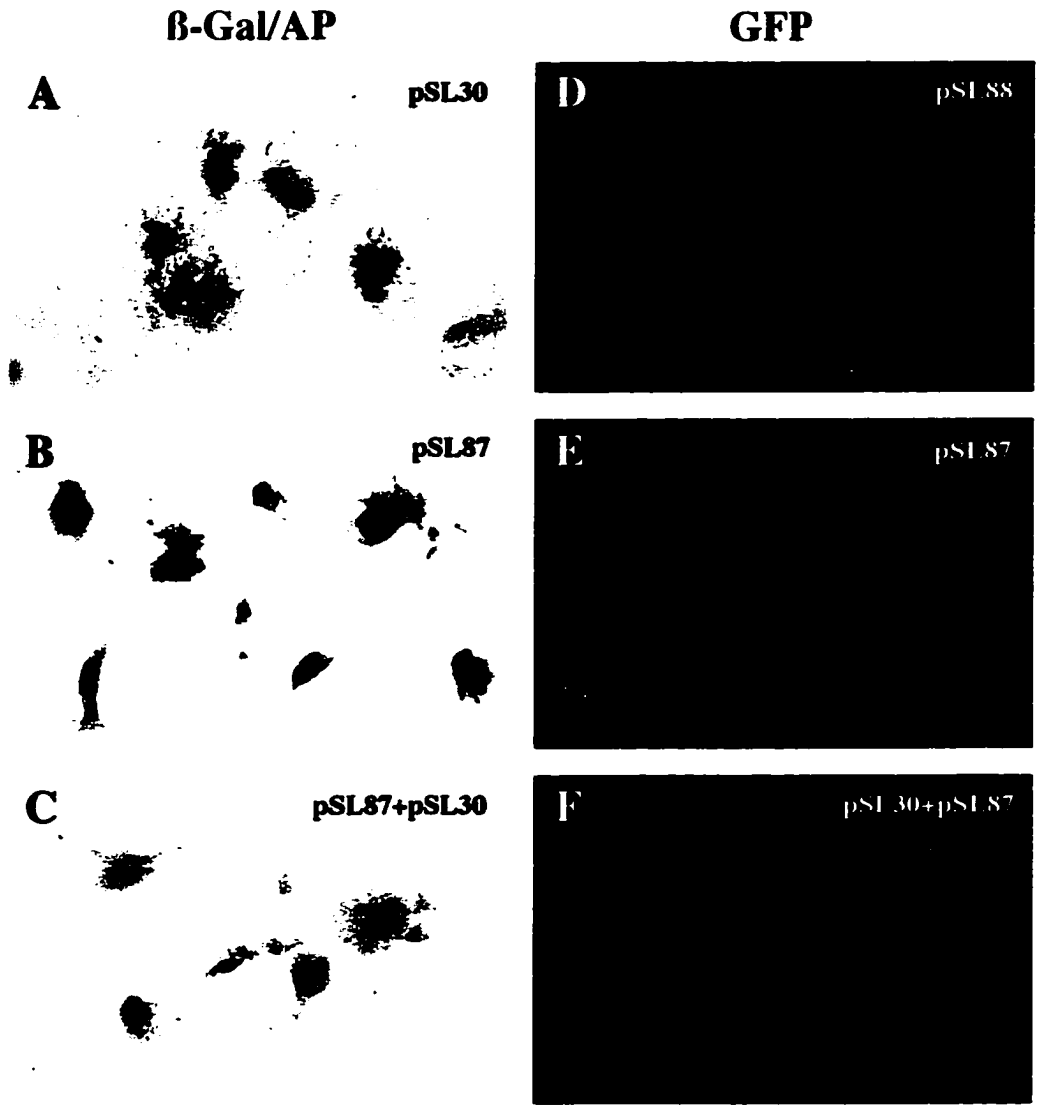

Figure 2

Two types of transgenes were designed: E3Cre and E3loxP (Figure 3). The E3Cre transgene is a dicistronic transgene with the 3' cistron encoding AP linked to the IRES sequence. The promoter of the E3Cre transgene is an 89bp basal TATA box-containing promoter from Rous Sarcoma Virus (RSV). One copy of the Enhancer III element was cloned upstream of the RSV basal promoter. A single SV-40 polyadenylation signal was placed immediately downstream of the 3' cistron. As constructed, this transgene produces a single transcript that encodes two separate proteins, Cre and AP. AP is used as a histological marker to monitor promoter activity since it can easily be detected by an enzymatic reaction (Li et al., 1997).

Table 1. Summary of Transgenic Founder Analyses

	cDNAs	FOUNDERS	SEX	EXPRESSION
E3loxP	crabp-1	14 - 9	M	no
		14 - 26	M	dead
		14 - 36	M	no
		54 - 9	**F**	**FNG**
		54 - 18	**M**	**FNG**
		54 - 26	M	no
		54 - 29	F	no
	msx-1	16 - 10	M	no
		16 - 23	F	no
		16 - 27	M	no offspring
	dsl-1	18 - 6	M	weak staining
		18 - 8	M	gut staining
	wnt-1	20 - 5	M	no
		20 - 17	F	no
		56 - 1	**M**	**FNG**
		56 - 6	**F**	**FNG**
		56 - 9	**M**	**FNG**
		56 - 17	M	no
	gbx-2	45 - 16	F	dead
		45 - 17	**F**	**FNG**
		45 - 21	M	no
E3Cre	Cre	**26-3**	**F**	**FNG**
		26-9	M	no
		26-14	M	dead
		26-16s	**N/A**	**FNG**
		26-16u	**N/A**	**U**
		26-19	F	no offspring

FNG, floor plate, notochord, and gut; U, ubiquitous

Figure 3. Schematic diagram of the transgene constructs, the predicted protein products from each transgene, and one of the predicted outcomes of the Cre/loxP recombination. Abbreviations: Enhancer III, 500bp enhancer element from 3' end of *Hoxa-1* gene; TATA, Rous sarcoma virus LTR basal promoter; IRES, internal ribosomal entry site; A+, SV-40 polyadenylation signal; CRE, Cre recombinase; AP, alkaline phosphatase; β-gal, β-galactosidase.

Transgenic Constructs

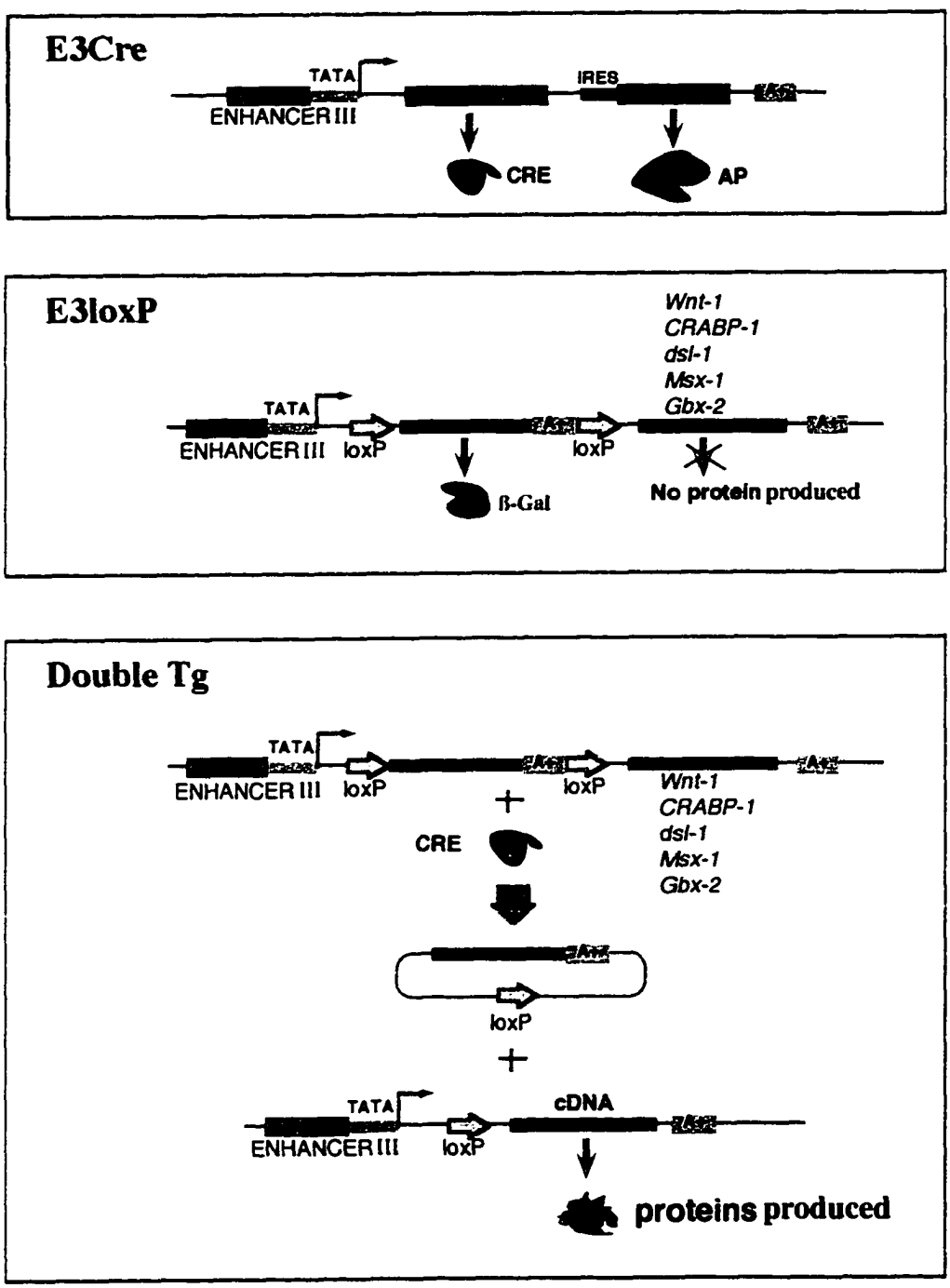

Figure 3

The E3loxP transgene includes the same promoter as used in the E3Cre transgene (Figure 3). The transgene has a loxP flanked STOP sequence, which comprises a *lacZ* coding sequence immediately followed by a polyadenylation signal. In some transgenes, two copies of the STOP sequences were positioned between the loxP sites. Only one copy is drawn in the figure for simplification. cDNA sequences (*CRABP-1, Msx-1, Dsl-1, Wnt-1,* and *Gbx-2*) were inserted 3' of loxP flanked STOP sequence. Therefore, there should be no proteins produced from these cDNAs prior to Cre-mediated recombination.

One of the predicted outcomes using the Cre/loxP system as a molecular switch is shown in Figure 3 when a mouse carries both E3Cre and E3loxP transgenes (Double Tg, Figure 3). DNA recombination occurs in the cells that express Cre. As a result, the *lacZ* coding sequence is excised to enable expression of the downstream cDNAs.

3. *Two lines of E3Cre mice express Cre in the floor plate and notochord*

The transgene expression pattern of each founder lines was analyzed by reporter gene β-gal and AP activity and the results are summarized in Table 1. E3Cre transgenic lines were initially examined at E9.5 for AP expression. Yolk sac DNA was used to genotype embryos by Southern blot. Line 26-9 founder line had no detectable AP activity. Line 26-19 did not breed. The 26-14 founder mouse died before any expression data was obtained. Both lines 26-3 and 26-16 expressed AP in the similar spaciotemporal pattern in the floor plate and notochord. The analysis of line 26-16 was chosen for the subsequent studies.

Tail DNA from the line 26-16 was digested with Bam HI and analyzed by Southern blot using a *Cre* cDNA probe. The results indicated that there were two independent integration events in this founder. One of the integration events has a 2.3kb genomic junction fragment while the other lacks this fragment (arrow head, Figure 4A). These two

integration events were subsequently segregated to two independent transgenic lines, 26-16s and 26-16u. Line 26-16u transgenic mice contain the 2.3kb genomic junction fragment. Expression analyses of these two lines of transgenic mice demonstrates that 26-16s transgenic mice have specific AP activity at the floor plate, notochord, and the gut epithelium (Figure 4C and Figure 5), while 26-16u transgenic mice display a ubiquitous AP expression pattern except for the heart and the gut region (Figure 4D).

Figure 4. Analyses of E3Cre line 26-16 reveal two independent sublines 26-16s and 26-16u. A. Southern blot analysis. Arrowhead indicates the differential genomic junction size. The 1.9kb and 0.7kb bands represent the transgene fragment. B, C, and D, E10.5 embryos stained for AP activity, which appears dark purple. The genotype is indicated on the upper right hand corner.

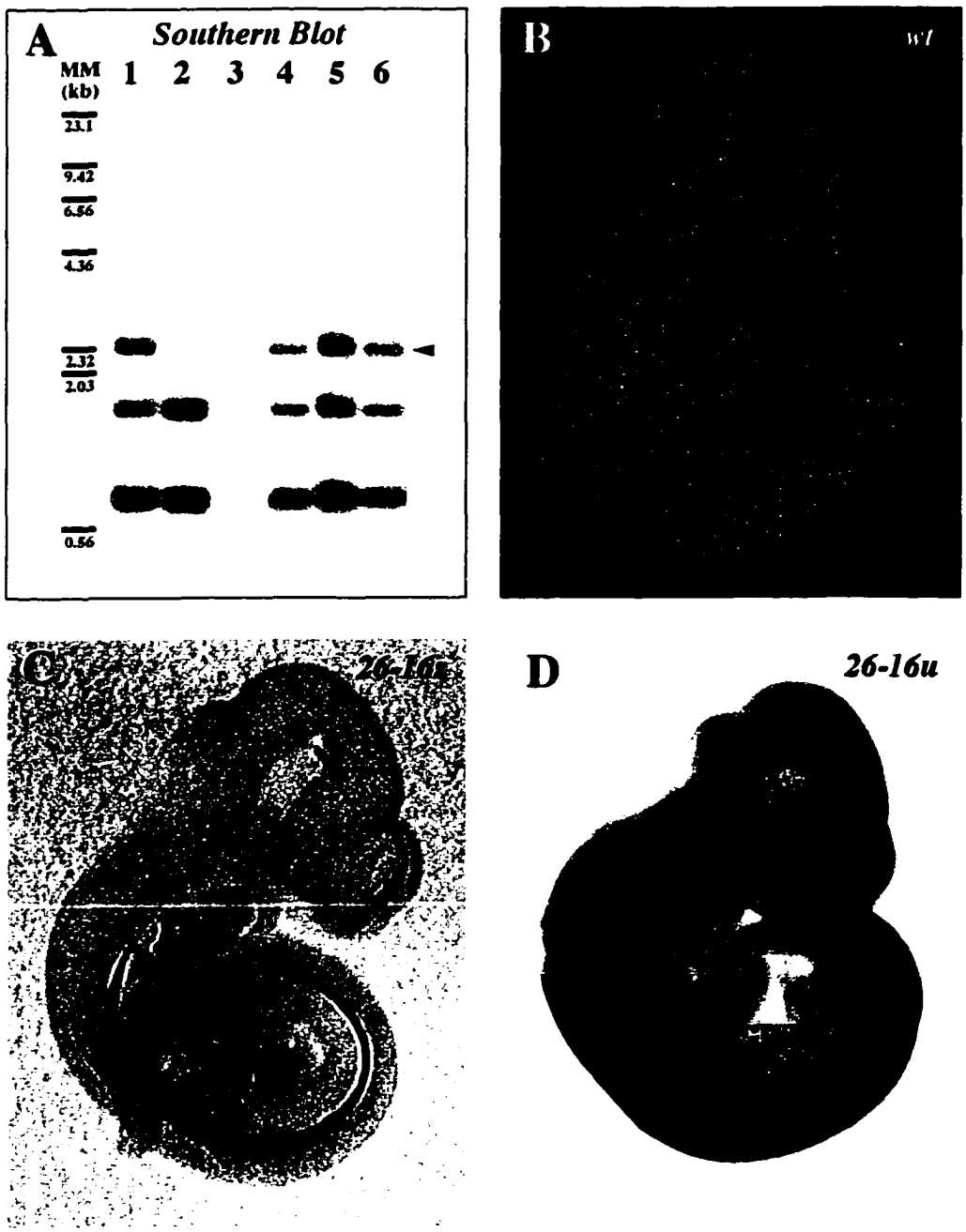

Figure 4

To further investigate the temporal expression pattern of 26-16s transgenic mice, we examined the AP reporter gene activity between E8.5-E14.5. At E8.5 (8-12 somites), AP activity is detected in the midline neuroepithelium and the notochord (Figure 5A and 5B). At E9.5, the transgene shows continued activity at the floor plate, notochord, and gut epithelium. Expression is also seen in more dorsal regions of the neural tube and in more rostral spinal cord regions. During E10.5-E14.5, the floor plate and the notochord specific expression persist as evident in whole mounts (Figure 4C and Figure 5D), and the localized expression pattern is more apparent in sections (Figure 5F). At these stages, AP activity is also detected in some motor neurons in the ventral lateral spinal cord (Figure 5F). Notably, there is no expression at the intermediate mesoderm, lateral plate mesoderm, or the limb bud. By E15.5, and later stages, the transgene activity is no longer detectable in any region of embryos (data not shown).

To investigate whether Cre protein is produced and co-localized with the expression of AP in subline 26-16s, E11.5 non-transgenic and transgenic embryos were examined for Cre and AP protein expression in adjacent serial frozen sections. Cre protein is detected in the 26-16s transgenic embryos in the floor plate and a subpopulation of motor neurons following Cre-specific antibody staining, whereas no Cre-specific signal is found in the non-transgenic embryos (compare Figure 6B and 6D). The function of Cre protein in line 26-16s transgenic mice was also examined and will be described below. Adjacent serial sections from the same embryos stained for AP activity, showing AP staining in the floor plate and motor neurons of the transgenic embryo but not in the wild type embryo (compare Figure 6A and 6C). The AP activity co-localizes with Cre protein (compare Figure 6A and 6B); therefore, we conclude that reporter AP gene activity faithfully represents Cre protein localization.

Figure 5. Developmental expression pattern of subline 26-16s. A-D, whole mount AP staining; E and F, sections after whole mount staining. Arrow head indication the position of the floor plate and the specific AP staining appears purple.

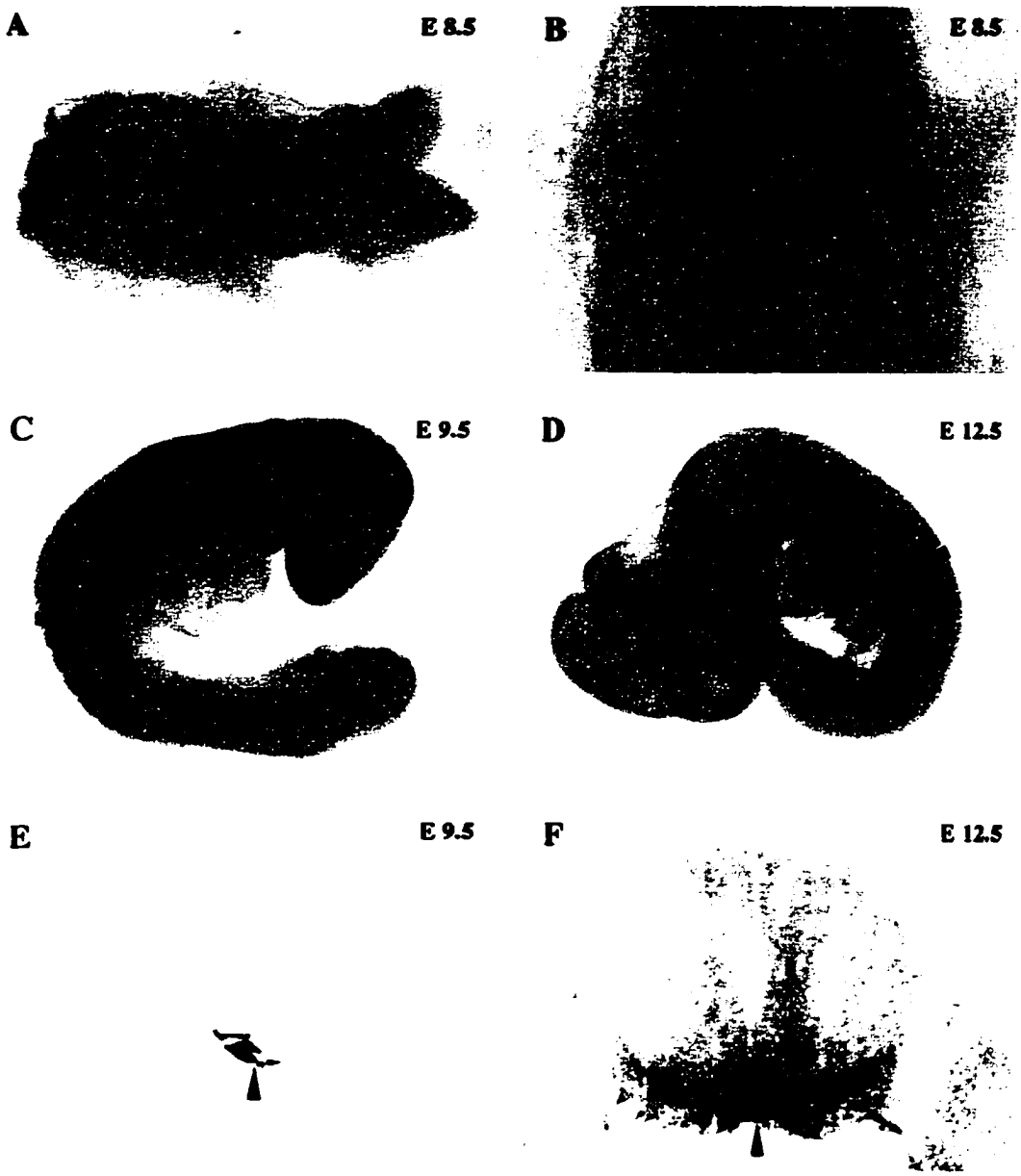

Figure 5

Figure 6. Cre antibody staining and co-localization with AP activity. E11.5 transgenic embryos (Tg) for 26-16s (A and B) and non-transgenic embryos (C and D) are stained for AP activity (A and C) and Cre protein localization (B and C). Specific AP staining appears purple and Cre-antibody staining appears brown.

Colocalization of Cre and AP proteins

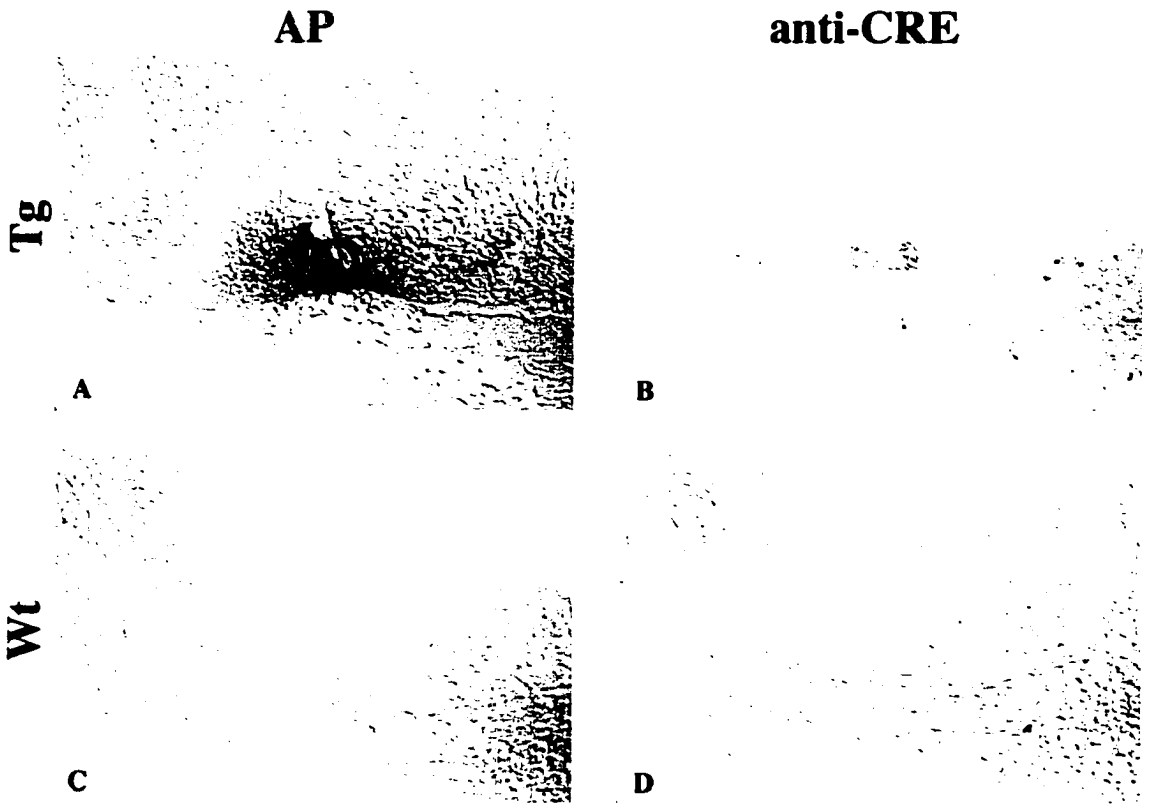

Figure 6

4. *Six lines of E3loxP mice express the lacZ gene in the floor plate and notochord*

In total, 21 independent E3loxP transgenic mice lines were established (Table 1). Embryos at E9.5 and E10.5 were harvested from individual lines and stained for β-galactosidase (β-gal) activity. The results are summarized in Table 1. Six lines show floor plate, notochord, and gut epithelium specific expression as seen in both whole mount and frozen tissue sections and four lines are shown in Figure 7 (described below), which recapitulates the Enhancer III activity (Frasch et al., 1995). The remaining transgenic mice lack specific staining or lack any staining and were not analyzed further.

Transgenic founder lines 56-1, 56-6, and 56-9 carry *Wnt*-1 cDNA-containing E3loxP transgene. Line 56-1 has predominant staining in the floor plate and notochord with very weak staining in the gut epithelium and dorsal neural tube (Figure 7A and 7B). Line 56-6 has weak expression in the floor plate, notochord and a weak ubiquitous expression pattern (data not shown). Line 59-9 has the expression pattern in the floor plate, notochord, gut, and a group of unidentified cells located at the forebrain (Figure 7E and 7F). Line 54-9 and 54-18 carry *CRABP*-1-containing E3loxP transgene. Both lines give very similar expression patterns. Strong β-gal activity is detectable in the floor plate and notochord as shown both in whole mount and frozen tissue sections. Also, there is some weak staining in the gut region, dorsal-anterior spinal cord, and the ventral forebrain region (Figure 7C and 7D). Another E3loxP line, 45-17, has specific β-gal activity in the floor plate and the notochord and gut region (Figure 7G and 7H). However, this transgene has two tandem copies of STOP sequence, due to cloning artifact, that are flanked by loxP sites and followed by *Gbx*2 cDNA (Figure 9A).

Figure 7. β-gal expression pattern of E3loxP transgenic founders in whole mounts and sections at E9.5. Founders are indicated at the upper right hand corners. Specific β-gal staining appears blue.

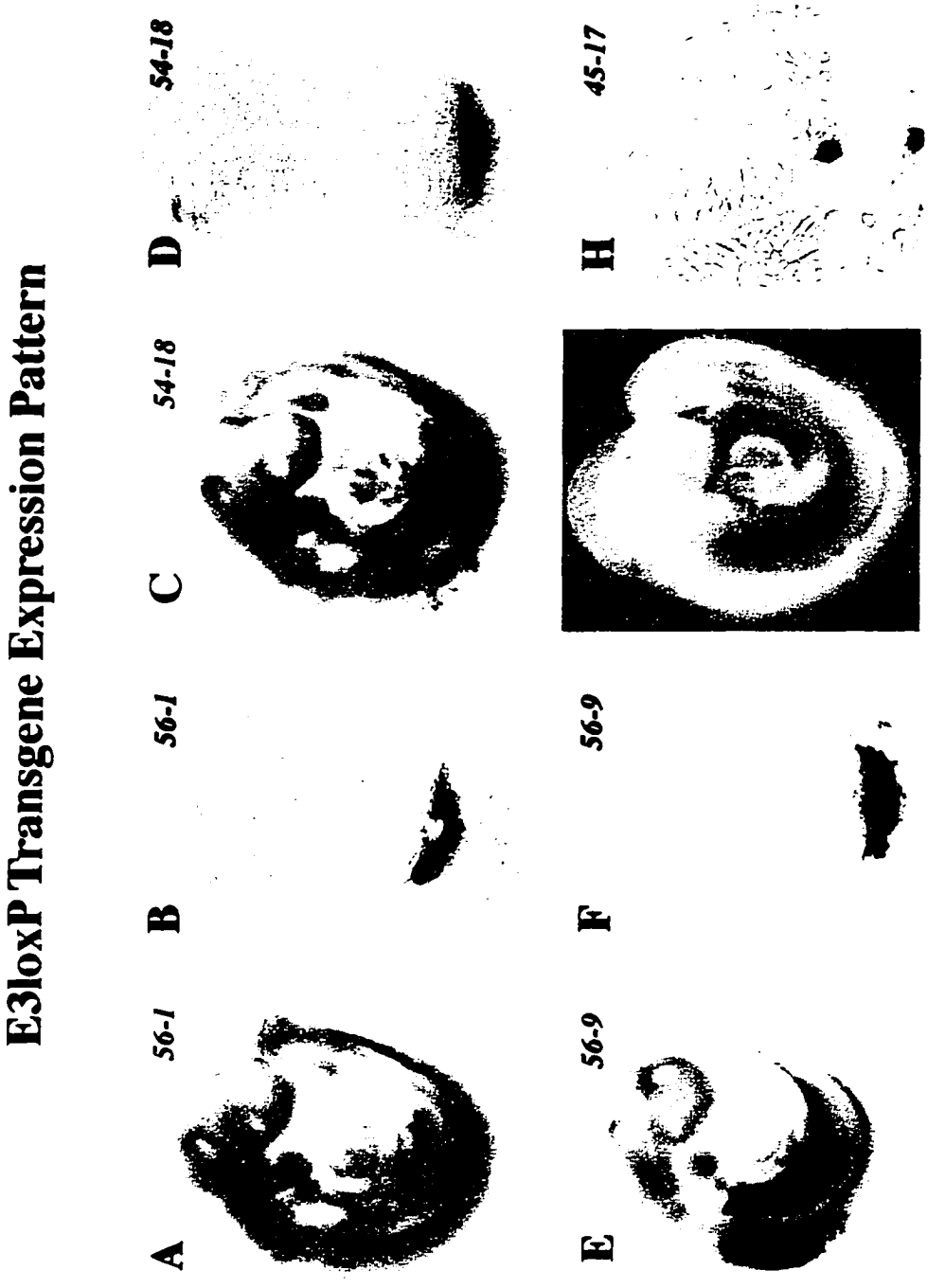

Figure 7

5. *Dicistronic transgenes and simultaneous detection of both IRES-lacZ and IRES-AP*

To explore the possibility of using both *IRES-AP* and *IRES-lacZ* simultaneously in the transgenic mice, the 26-16s transgenic mice were mated with different transgenic line harboring the *IRES-lacZ* transgene (Li et al., 1997). Stage E12.5 embryos were double stained for AP and β-gal activity. Non-transgenic embryos show no background activity following the entire staining protocol (wt, Figure 8). AP activity in the *IRES-AP* transgenic embryos appear dark purple at the floor plate and notochord (IRES-AP, Figure 8), and β-gal activity in the *IRES-lacZ* transgenic embryos appear blue at the peripheral nervous system (*IRES-lacZ*, Figure 8). Double transgenic embryos carrying both *IRES-AP* and *IRES-lacZ* display a staining pattern that is a precise superimposition of the individual β-gal and AP staining patterns (*IRES-lacZ/AP*, Figure 8). This demonstrates that *IRES-AP* and *IRES-lacZ* can be used simultaneously in transgenic embryos.

6. *Cre/loxP site-specific recombination occurs in vivo*

To investigate whether site-specific recombination can occur when the Cre protein is present in the E3loxP transgenic mice, E3loxP transgenic mice were mated with the CMV-*Cre* transgenic mice (kindly provided by A. Nagy, Mount Sinai Hospital, Toronto). The CMV-Cre transgene has a CMV promoter driving expression of *Cre* ubiquitously at early developmental stages. Therefore, the majority of tissues should undergo site-specific recombination in double transgenic mice harboring both E3loxP and CMV-*Cre* transgene. The yolk sac DNA or total embryo DNA was used for Southern blot analyses to detect site-specific recombination. The results are summarized in Table 2. In total, 8 independent E3loxP transgenic lines were examined for Cre-mediated recombination in the double transgenics between E9.5-E12.5 and the results indicated that Cre-mediated site-specific recombination occurred in all the lines examined.

One example of the Southern blot analysis is shown in Figure 9B. Double transgenic embryos for both line 45-17 and CMV-*Cre* undergo site-specific recombination as indicated by the presence of the 1.0 kb recombination-specific band (asterisk, Figure 9B, lane 1-3). Other lines of E3loxP transgenic mice were also tested for site-specific DNA recombination by Southern blot analysis and the results are summarized in Table 2. Taken together, we conclude that site-specific recombination takes place in all E3loxP lines in the presence of Cre protein.

To investigate whether the E3Cre 26-16s transgenic line produces functional Cre protein in the floor plate and the notochord, E12.5 double transgenic embryos from line 45-17 and 26-16s transgenic mice were isolated and the forelimb (FL), hindlimb (HL), floor plate (FP), and forehead (H) were dissected for analysis. DNAs were purified from these tissues and examined for Cre-mediated site-specific recombination by PCR (Figure 9C). A 0.6kb recombination specific band was detected from the positive control and the floor plate DNA, but not from the forelimb, hindlimb, and forehead DNA. These results suggest that the E3Cre transgenic line 26-16s produces functional Cre protein specifically in the floor plate region but not in the limbs and forebrain. Notably, the forelimb was defective as will be discussed later in Section V. Therefore, the limb defect is not directly related to "leaky" expression of Cre protein at the limb region.

Figure 8. β-gal and AP double staining of *IRES-AP* and *IRES-lacZ* double transgenic, single transgenic, and not-transgenic embryos. E12.5 double transgenic embryos (*IRES-lacZ/AP*), single transgenic embryos (*IRES-AP* or *IRES-lacZ*) and non-transgenic embryos (wt) are stained with X-gal first and followed by AP staining. Specific AP staining appears purple and specific β-gal staining appears blue.

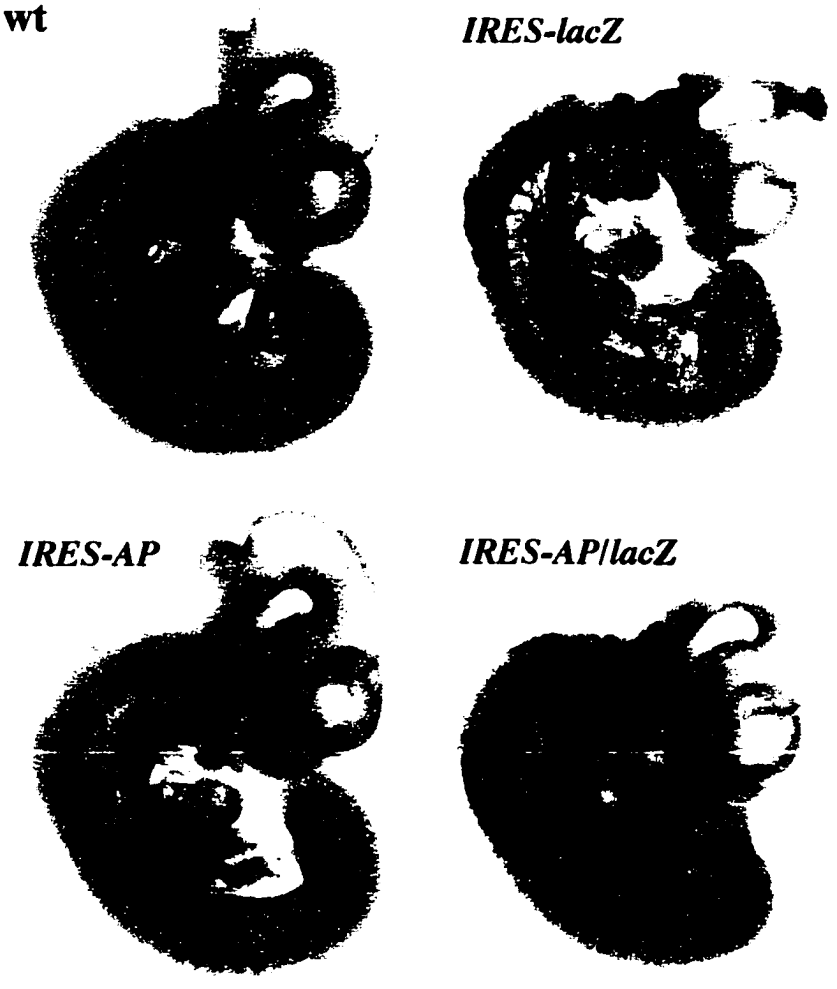

Figure 8

Figure 9. DNA analyses of Cre-mediated site-specific recombination *in vivo*. A, Schematic diagram of transgene 45-17 before and after Cre-mediated recombination (not in scale). The *Gbx2* cDNA (as indicated) is used as a probe for Southern and PCR experiments. The predicted sizes are indicated before and after recombination. B. Southern blot analysis of DNA from total E10.5 embryos from cross mating 45-17 and CMV-*Cre* mice. Each lane represents an embryo from the same litter. All four embryos are Cre-expressing transgenic mice, however only embryos 1, 2, and 3 are 45-17 transgenic mice identified by the presence of 1.75kb unrecombined band (unrec). Cre-mediated site-specific recombination is evident as the presence of the 1.0kb recombined band (rec). 4.0kb *Gbx2* represent the endogenous loci. C, PCR analysis using primers as indicated in panel A. DNAs used is indicated on top of each lane. -, negative control DNA from 45-17 single transgenic embryo; +, positive control DNA from embryo 3 in panel B; FL, forelimb; HL, hindlimb; FP, floor plate; H, head. The 0.6kb band identify the Cre recombination-specific band.

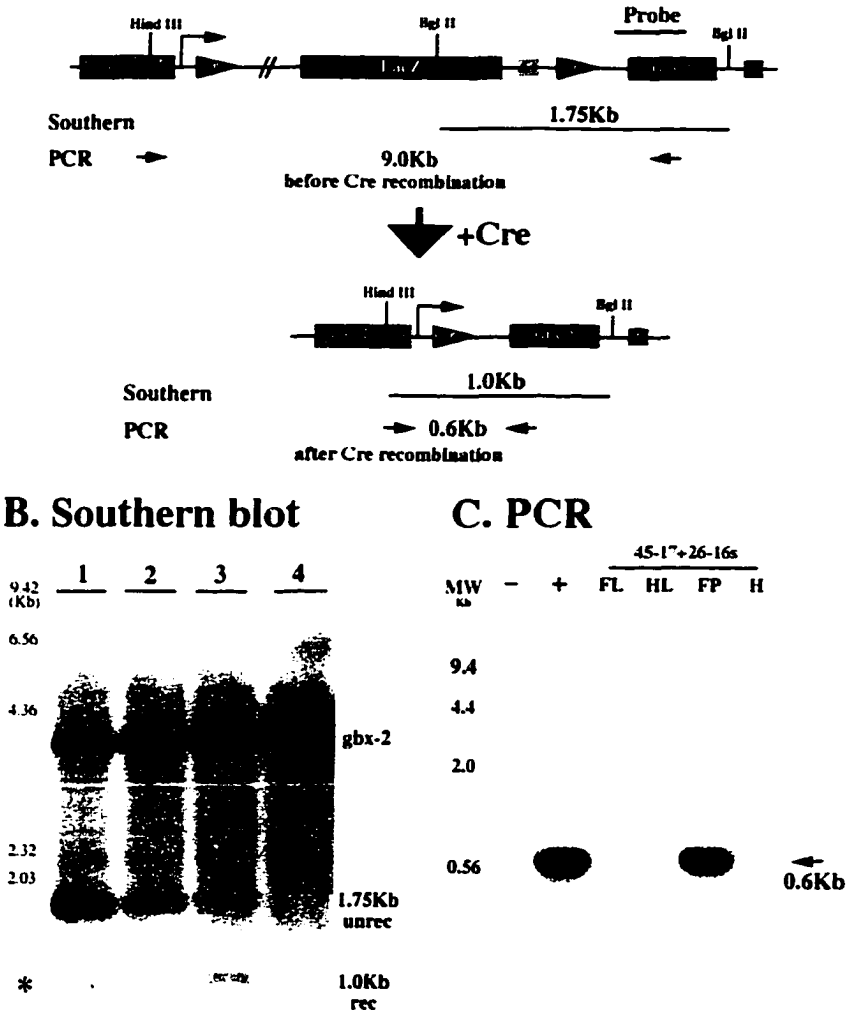

Figure 9

7. Recombination turns-off lacZ expression and causes the floor plate and forelimb defect

To investigate whether Cre-mediated site-specific recombination turns-off *lacZ* gene expression in the E3loxP lines, E10.5 embryos derived from mating E3loxP transgenic mice 45-17 with E3Cre transgenic mice 26-16s were stained for AP and β-gal reporter activities. Single E3loxP transgenic embryos express β-gal in the floor plate, notochord, and gut, as shown in Figure 10A. However, double transgenic embryos express AP in the same domain while expression of β-gal is completely turned off (compare Figure 10B and 10C). This results demonstrate that the Cre protein produced by this transgenic mouse line 26-16s has efficiently excised the *lacZ* coding sequence.

Two major phenotypes are apparent in the double transgenic embryos from mating E3Cre transgenic mice, 26-16s, and E3loxP transgenic mice, 45-17 or 54-18. All double transgenic embryos have a forelimb truncation (red arrow, Figure 10B and 10C) and the floor plate defect (Figure 10E). At E12.5 embryos, the floor plate at the thoracic region has a typical triangular shape morphology, as indicated by AP staining of the E3Cre transgenic mouse (Figure 10D). However, this morphology is completely lost in the double transgenic embryos (compare Figure 10D and 10E). A detailed analysis of these phenotypes will be presented in the next two chapters.

8. No ectopic expression after Cre/loxP recombination

To address whether Cre-mediated recombination in the floor plate specifically activates downstream gene expression which in turn causes the mutant phenotypes, double transgenic mice between E8.5 and E12.5 were examined for the presence of ectopic mRNA in the floor plate by *in situ* hybridization. The results are summarized in Table 2. Eight different transgenic lines were analyzed for ectopic expression of the specific genes after Cre-mediated site-specific recombination. At least 6 double transgenic embryos from each of the E3loxP lines at each stage were identified by Southern blot and embedded in

paraffin. Serial cross sections from 95 double transgenic embryos (out of 325 embryos analyzed) were hybridized with the appropriate ^{35}S labeled RNA probes. In all cases, *in situ* hybridization failed to detect any ectopic mRNA at the floor plate, notochord, and gut region. An example of these *in situ* analyses is shown in Figure 11. Double transgenic 45-17 and 26-16s mice between stages E8.5 and E12.5 were examined for ectopic expression of the *Gbx2* gene. At E10.5 and E12.5, endogenous *Gbx2* expression is detected in both double transgenic mice and wild type/single transgenic mice in dorsal commissural neurons and intermediate interneurons. However, no ectopic *Gbx2* is detectable in the floor plate region (compare Figure 11B and 11C; 11E and 11F). The control experiments using *lacZ* as a probe demonstrated that the promoter is active enough to produce detectable amounts of mRNA by *in situ* analysis before recombination. In double transgenic embryos, the *lacZ* mRNA is no longer detectable suggesting that Cre-mediated site-specific recombination has taken place (data not shown). Taken together, we conclude that although Cre-mediated site-specific recombination *in vivo* is efficient, downstream gene expression is **not** observed.

Table 2. Summary of Ectopic Expression Analyses

cDNAs	Founders	Cre Recom	Ectopic Exp (E9.5;10.5;12.5)
CRABP-1	54-9	yes	no
	54-18*	yes	no
Wnt-1	56-1	yes	no
	56-6	yes	no
	56-9	yes	no
Gbx-2	45-17 *	yes	no
Dorsalin-1	18-6	yes	no
	18-8	yes	no

Figure 10. Recombination *in vivo* turns-off *lacZ* expression. Staged embryos (E10.5 and E12.5) are stained with either β-gal (A and B), or AP (C, D, and E). β-gal specific staining appears blue and AP specific staining appears purple. Red arrows indicate the defective forelimbs in double transgenic embryos. D and E, 30um cryostat section after AP whole mount staining.

Recombination Turns-off *lacZ* and Causes the Forelimb and the Spinal Cord Defects

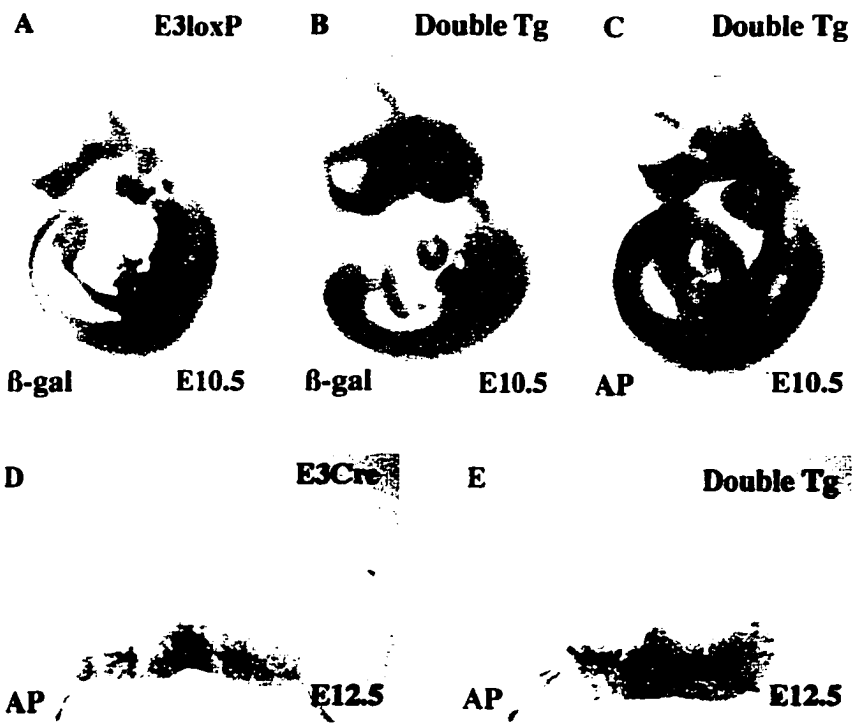

Figure 10

Figure 11. Comparison of *Gbx2* expression pattern in the wild type and double transgenic embryos. Similar level cross sections were taken at the thoracic region from both wild type and double transgenic embryos and hybridized with ^{35}S labeled *Gbx2* RNA probe. A and D, bright field from double transgenic sections. B and F, dark field of wild type sections. C and D, dark field of double transgenic sections. Top panels are E10.5 sections and bottom panels are E12.5 section. * indicates double transgenics have defects.

No Ectopic mRNA Detectable in the FP after Cre/loxP Recombination

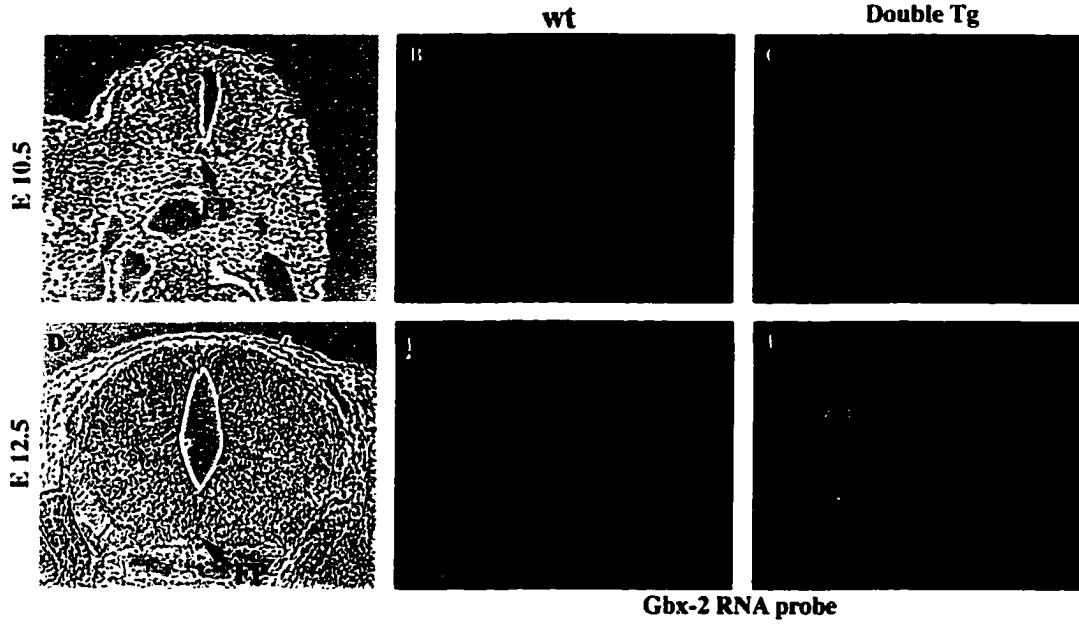

Figure 11

9. *Recombination causes cell death*

The specific phenotype at the floor plate and forelimb in several independent strains of double transgenic mice prompted us to look at whether there was specific cell death in the double transgenic mice. Serial paraffin sections from double transgenic embryos were examined for the presence of apoptotic cells using the TUNEL assay (Promega), which labels the 3' termini of fragmented chromatin DNA present in apoptotic cells with a fluorescent nucleotide. As early as E8.5 when *Cre* expression commences, increased levels of dying cells were apparent in the notochord (data not shown). At E9.5 and E10.5 in double transgenic mice, many dying cells were detected in the floor plate region (red arrowhead, Figure 12B; and data not shown). There were only a few dying cells present in the single transgenics or wild type embryos (yellow arrow, Figure 12A; and data not shown). Although there was no detectable ectopic activation of the transgenes (Figure11 and data not shown) in two independent E3loxP lines carrying different cDNAs, *Gbx2* and *CRABP*-I, these strains have identical phenotypes (Table 2). Therefore, we conclude that the cell death is independent of the E3loxP transgene expression and insertion site. The Cre-mediated recombination directly causes the cell death. At E9.5, extensive cell death was also observed in the intermediate mesoderm (red arrow, Figure 12B). Because neither AP activity nor Cre protein was detected in the intermediate mesoderm region (Figure 4C; Figure 5; and Figure 6), these results suggest that cell death in the intermediate mesoderm region is a secondary defect to the floor plate and notochord. At E12.5, there was no detectable cell death although *Cre* is expressed at this stage (Figure 12D and Figure 5F).

Figure 12. TUNEL assay of wild type and double transgenic embryos. Cells are stained with the blue dye DAPI for nuclei. Dead cells appear green. Red arrowhead indicates specific cell death at the floor plate and red arrow points to the intermediate mesoderm region. White arrows indicate non-specific cell death at the wild type embryos.

Cell Death in the Cre/loxP Double Transgenics

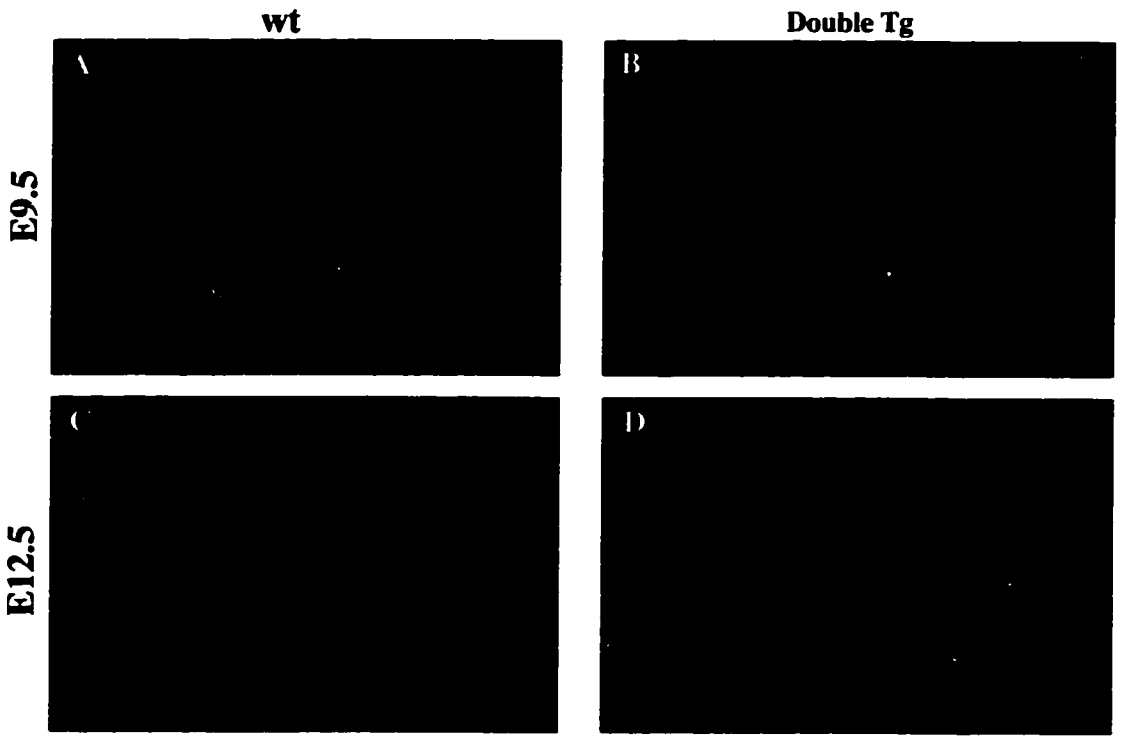

Figure 12

Discussion

1. *Cre/loxP binary transgenic gain-of-function system*

In vitro experiments clearly demonstrate that Cre-mediated recombination occurs and the system can be used as a molecular-switch to activate the expression of one gene by excising the STOP sequence, a coding region of the reporter gene, in the same construct. *In vivo* experiments, however, indicate that the system ablates the expression of β-gal but fails to activate downstream gene expression. This striking difference might reflect the problems that arise when the loxP-containing transgene is integrated into the genome. *In vitro* experiments were performed by transiently transfecting the loxP-containing transgene into COS-7 cells as circular DNA. Under these conditions, the transgene rarely integrates into the genome and each copy of the transgene is an independent unit. Therefore, the function of each unit is not altered by Cre-mediated site-specific recombination. However *in vivo*, at least 10 copies of the E3loxP transgenes are integrated into the genome at a single site as head-to-tail, head-to-head or tail-to-tail concatamers. Because each copy of the transgene has two loxP sites, the transgenic mice have multiple loxP elements potentially facing different directions. Depending on the orientation of the loxP sites, Cre-mediated recombination could either delete the internal sequence or invert the internal sequence (Sauer, 1993). Therefore, the outcome of Cre-mediated recombination *in vivo* is less predictable.

Another possible consequence of Cre-mediated recombination in the transgenic mice is shown in Figure 13. E3loxP transgenic mice have multiple copies of the transgene and previous studies have demonstrated in many instance that only a few copies are transcriptionally active (Wight and Wagner, 1994). To illustrate, five copies of the transgene are drawn at head-to-tail orientation in Figure 13 and two copies of the transgene (indicated) be transcriptionally active. The two end-copies have mutations or deletions due to integration of the transgene into the genome. After Cre-mediated recombination, the

transgene is reduced to one copy, which is the combination of the two end-copies. In this example, it is clear that the resulting transgene is not active.

The studies presented here demonstrate that the binary Cre/loxP molecular switch must be refined before the ectopic expression of transgenes can be achieved in the transgenic mice. A potential modification may be the generation of E3loxP transgenic mice that have only one copy of the transgene. This can be achieved using ES cells as an intermediate. The advantage of generating transgenic mice through ES cells is that the single copy-containing ES clones can be screened *in vitro* and the expression of the transgene can be tested rapidly through tetraploid fusion techniques (Nagy and Rossant, 1993; Nagy et al., 1993).

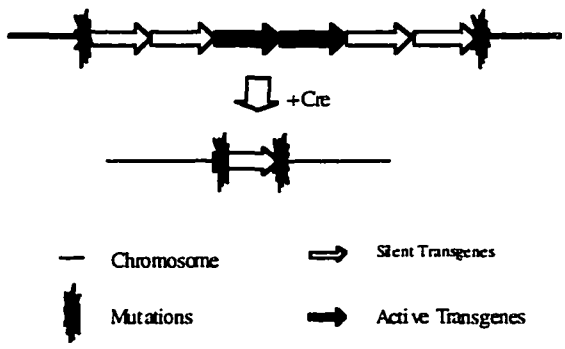

Figure 13. Cre-mediated recombination *in vivo*. Five copies of E3loxP transgenes are present before Cre-mediated recombination. Each copy of transgene is represented as an arrow with the same orientation integrated in the chromosome. At the present of Cre protein, the transgenes is reduced to one copy, the combination of two end-copies.

2. Cell specific ablation by Cre/loxP recombination

Cell death in the double transgenic embryos is unlikely a result of the ectopic expression of the cDNAs included in the transgene. First, we were unable to detect ectopic mRNA during the time when *Cre* was expressed, although we can not exclude the possibility that the expression was below the level of detection. Second, two independent lines, 45-17 and 54-18, carrying different cDNAs, *Gbx2* and *CRABP*-1 respectively, had identical phenotypes suggesting that it is not the cDNAs *per se* that are directly related to the phenotypes.

A possible explanation of the cell death phenotype is that Cre-mediated recombination causes a chromosomal rearrangement or deletion. Lewandoski and Martin (1997) have demonstrated that chromosomal deletions can occur after Cre-mediated recombination. When one of their loxP-containing transgenes was integrated into the Y-chromosome, Cre recombination led to the deletion of the Y-chromosome resulting in more than 95% of the offspring being female (either XX or XO female). When the loxP transgene was integrated into an autosome, Cre recombination led to the deletion of the autosome resulting in an early embryonic lethal phenotype. Consistent with their results, when we mated 45-17 transgenic mice with the CMV-*Cre* transgenic mice, we observed a high frequency of resorbed embryos. This is consistent with the hypothesis that Cre-mediated recombination can cause cell death. It is conceivable that mating 45-17 or 54-18 transgenic mice with different *Cre* expressing mice could specifically ablate certain cell lineages when a tissue-specific or cell type-specific promoter is used to express the *Cre* gene. Notably, cell death was not detectable in E12.5 double transgenic embryos (Figure12D), although Cre protein was highly expressed at this stage (Figure 5D and 5F). This implies that the state of Cre-expressing cells, either terminal differentiated or active dividing, influences the outcome of Cre-mediated recombination too.

3. *Influence of intermediate mesoderm by the floor plate and notochord*

It is clear that cell death occurs in the intermediate mesoderm. From both AP staining and immunostaining using anti-Cre antibody, we know that the Cre protein is only expressed in the floor plate, notochord and the gut region. There is no detectable *Cre* expression in the intermediate mesoderm (Figure 4C; Figure 5; and Figure 6). Therefore it is unlikely that cell death in the intermediate mesoderm is the direct cause of Cre-mediated recombination. The results implies that the floor plate and the notochord might secrete as yet uncharacterized factors, which are required for the development of the intermediate mesoderm. The nature of putative signals needs to be further investigated. Alternatively, the dead cells might be derived from the axial or paraxial structures.

2. Dorsoventral Patterning of the Spinal Cord

Introduction

Our understanding of ventral neural tube pattern formation has advanced dramatically in recent years by the combination of both classical surgical ablation and modern genetic approaches. Results generated from both approaches have demonstrated that ventral neural tube development depends on the inductive signal secreted from the notochord (Tanabe and Jessell, 1996). The nature of this inductive activity has been identified as the secreted signaling molecule *Shh* (Echelard et al., 1993). Mice lacking functional Shh have provided a model system to study the molecular mechanism for early neural tube patterning formation (Chiang et al., 1996). However, *Shh* mutant mice are early embryonic lethal therefore they can not be used to study the formation, function and maturation of different cell types within the neural tube at later developmental stages (Chiang et al., 1996). Available strains of mutant mice which survive to birth have proven to be very useful model system to study the neural tube development at late stages. These model systems include *T* and Danforth's short tail *(Sd)* mutant. In these mice, the posterior floor plate and notochord degenerate, and as a result, development of the caudal neural tube is affected. However, the rostral region is relatively normal in these mutants. In our double transgenic embryos, the floor plate and notochord degenerate between E8.5 and E11.5. Using tissue and cell type specific markers along the dorsoventral axis of the neural tube, the spinal cord defect in the double transgenic embryos was analyzed by *in situ* hybridization and immunohistochemistry. In contrast to the *T* or *Sd* mouse mutants, these double transgenic mice have defects only in the rostral region but not in the caudal region of the spinal cord. Therefore, they represents another mouse model system to study nervous system development.

Results

1. *Histological analysis of the floor plate defect*

H&E stained cross sections from double transgenic embryos were compared with wild type sections at a similar level along the anteroposterior axis. Between E9.5-E11.0, there is no apparent morphological difference between double transgenic mice and wild type/single transgenic mice (data not shown). At E12.5, the floor plate of wild type/single transgenic mice develops a typical triangular shape morphology consisted of a few cells with the cell bodies located at the ventricular zone and their processes extending ventrally toward the surface of the spinal cord (left panels, Figure 14). In double transgenic embryos, however, the floor plate at the thoracic region is severely disorganized and has lost its typical triangular-shaped morphology. The wall of the ventral neural tube is enlarged dramatically with lots of cells occupying the ventral midline region (compare wt and double Tg at the thoracic region, Figure 14). This morphological defect was observed only at the thoracic region of the spinal cord but not in the posterior region (compare wt and double transgenics at the lumbar region, Figure 14).

2. *Reduced expression of the floor plate-inducing molecules, Shh and HNF3β*

The defect was further analyzed for the expression of known genes that are involved in floor plate formation. Both *Shh* and *HNF3β* are expressed in the floor plate. Genetic gain-of-function and loss-of-function experiments demonstrated that the expression of these genes is required for floor plate formation and is sufficient to induce ectopic formation of the floor plate if these genes are expressed in the dorsal neural tube (Tanabe and Jessell, 1996). Both double transgenic mice and wild type/single transgenic mice were examined for the expression of *Shh* and *HNF3β* between E8.5-12.5. During E8.5 and E11.0, expression pattern and expression level of both *Shh* and *HNF3β* in double transgenic mice are similar to wild type/single transgenic mice (compare Figure 15B and 15C; and data not shown). However, at E12.5, the expression level of both *Shh* and

HNF3β is dramatically reduced (compare Figure 15E and 15F; 15H and 15I). These results indicate that the number of the floor plate cells is reduced in the double transgenic embryos (compare Figure 15F and 15I) and the putative floor plate cells are poorly differentiated (compare Figure 15E and 15H). In the lumbar region of the same double transgenic embryos, the expression of *Shh* and *HNF3β* is similar to the wild type/single transgenic mice (data not shown). These results may account for the fact that the morphology of the posterior part of the spinal cord remains relatively normal in the double transgenic embryos.

Figure 14. H&E staining of wild type and double transgenic embryos. Sections from the same double transgenic embryos (right panels) are compared with the similar level wild type sections (left panels). Arrowhead indicates the floor plate dysmorphology in the double transgenic sections at the thoracic region.

Histological Analysis of the Cre/loxP Double Transgenics

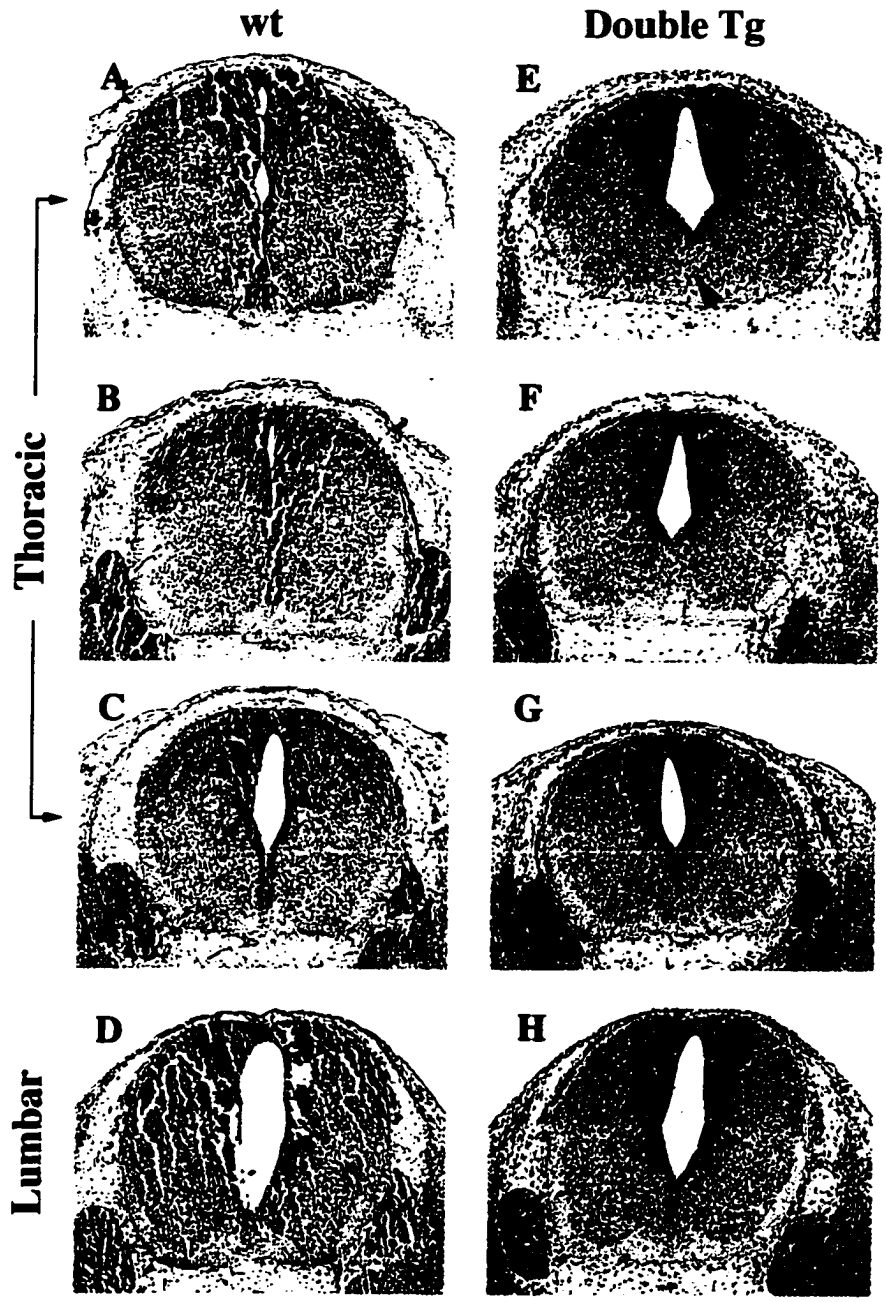

Figure 14

Figure 15. Expression of the floor plate specific markers, *Shh* and *HNF3β*. E10.5 and E12.5 sections of both wild type and double transgenic section at the similar level at hybridized with the *Shh* probe (B, C, E, and F) and *HNF3β* (C, F, and I). Left panels are bright field from double transgenic sections. FP, floor plate; RP, roof plate; DRG, dorsal root ganglia; Arrowhead, putative floor plate in the double transgenic embryo.

The Floor Plate Defect in the Cre/loxP Double Transgenics

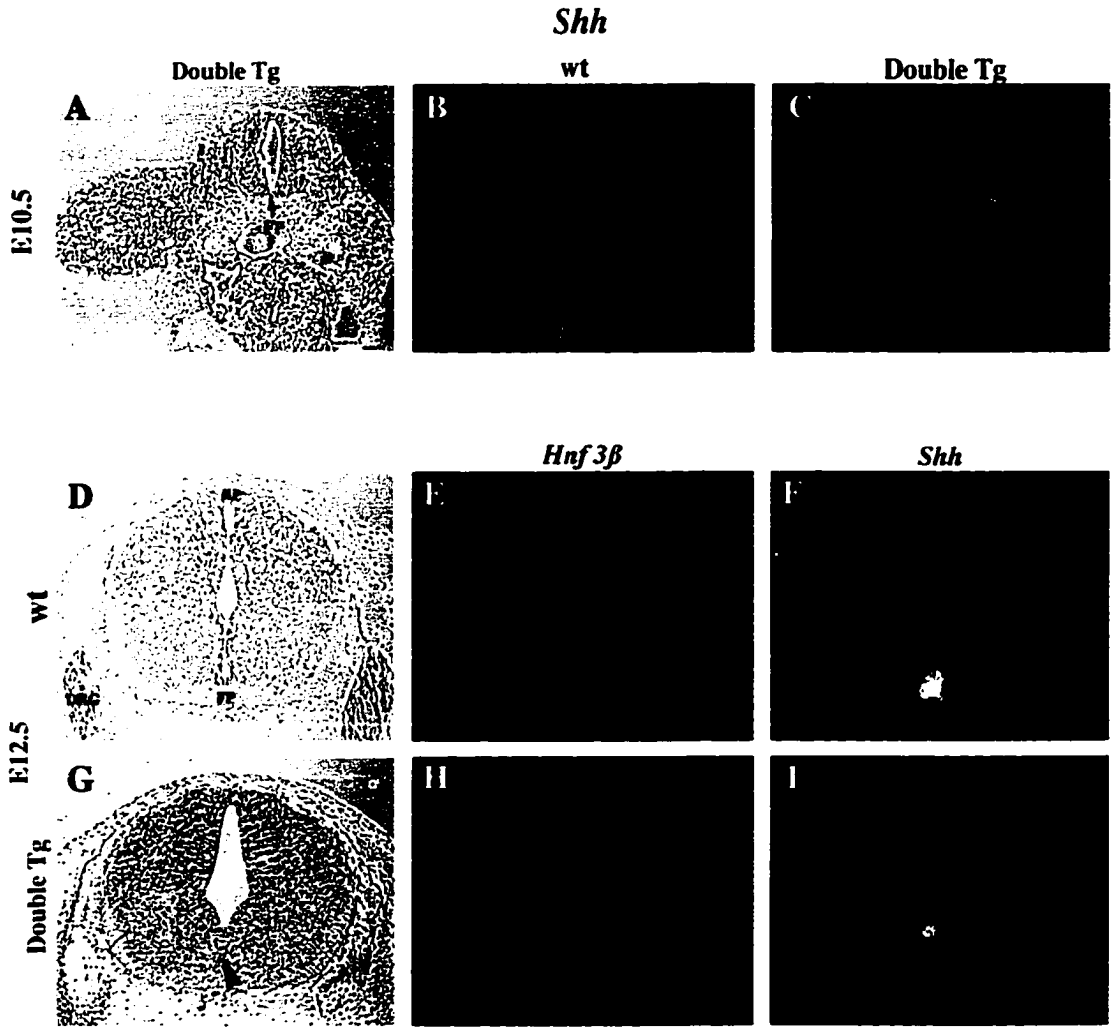

Figure 15

3. *Ventral motor columns are fused along the midline*

Previous studies have demonstrated that motor neuron development is dependent on the inductive *Shh* signal from the floor plate and notochord (Tanabe and Jessell, 1996). The observed reduction of *Shh* expression in E12.5 double transgenic embryos led us to investigate whether motor neuron development was altered in the double transgenic mice. The motor neuron specific markers, *Islet*-1 and *Nkx*-2.2, were used because they are genes that are required for motor neuron differentiation (Ericson et al., 1997; Lumsden, 1995). Between E8.5 to E11.0, the expression patterns of these two genes have no detectable alterations on wild type/single transgenic, or double transgenic mice (data not shown), consistent with the observation that the expression of *Shh* is normal before E12.5 in double transgenic mice. At E12.5, the expression of both genes is reduced in double transgenic (compare double transgenics and wild type, Figure 16) indicating reduced numbers of motor neuron and consistent with a reduction in *Shh* expression. Moreover, two ventral motor columns are fused along the ventral midline in the double transgenic mice (compare wt and double transgenics, Figure 16). The expression pattern of *Pax-6* in the ventral motor columns are also fused along the ventral midline (Figure 17F, and data not shown). These results demonstrate that fewer motor neurons terminally differentiate in the double transgenic embryos and the two motor columns are fused along the ventral midline.

Figure 16. Expression of the motor neuron specific markers, *Islet-1* and *Nkx 2.2*. E12.5 wild type (B and C) and double transgenic (E and F) sections are hybridized with *Islet-1* probe (B and E) and *Nkx 2.2* probe (C and F). Left panels are bright field from double transgenic sections. FP, floor plate; RP, roof plate; DRG, dorsal root ganglia; Arrowhead, putative floor plate in the double transgenic embryo.

The Motor Neuron Defect in the Cre/loxP Double Transgenics

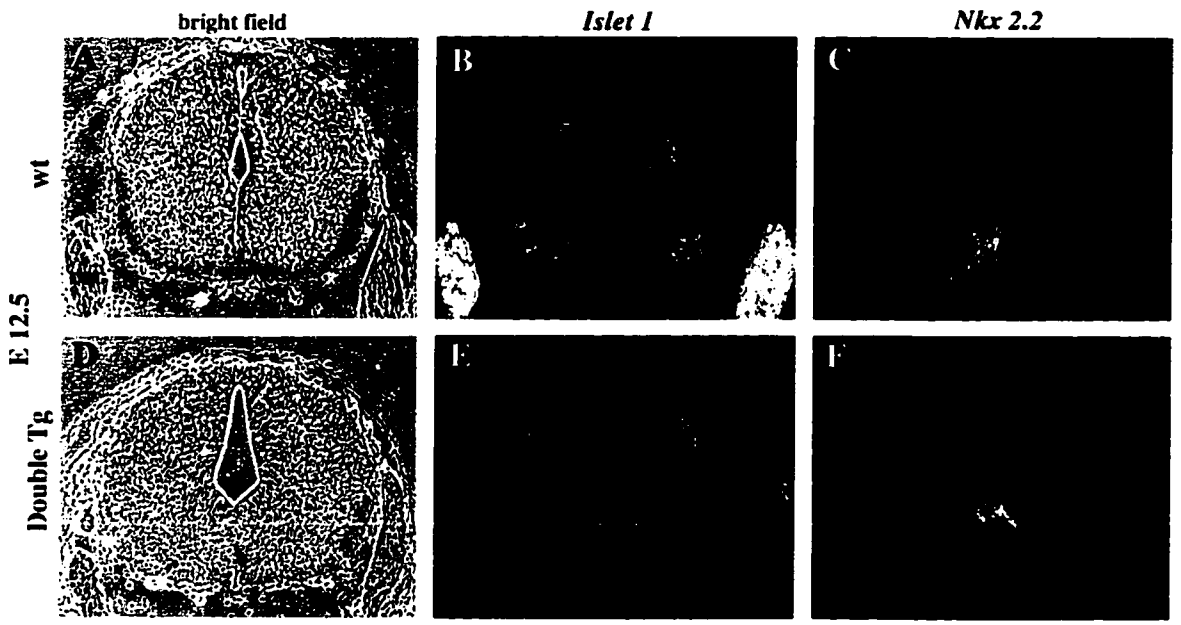

Figure 16

4. *Dorsal neural tube and paraxial mesoderm development appears normal*

To further investigate the spinal cord defect along the dorsoventral axis, we examined expression patterns of dorsal neural tube specific genes, including the signaling molecule *Wnt-1*, homeobox-containing transcription factors *Msx1* and *Msx3*, and the paired box-containing transcription factors *Pax-3*, *Pax-6*, and *Pax-7*. Both double transgenic mice and wild type/single transgenic mice were analyzed between E9.5 and E12.5. The overall expression pattern and dorsoventral boundary is normal in the double transgenic mice at all stages examined (Figure17, and data not shown). For example, both *Pax-3* and *Pax-7* are expressed in the dorsal one half of the ventricular zone in the a double transgenic mice, which is very similar to wild type/single transgenic mice (compare Figure 17B and 17E, 17C and 17F). *Pax-6* has two expression domains in the neural tube. Its expression domain in the ventral motor column is fused along the ventral midline, consistent with the *Islet-1* and *Nkx2.2* expression patterns in the double transgenic embryos (Figure 17F). However, the gradient expression domain of *Pax-6* in the dorsal part of the spinal cord appears normal in the double transgenic mice (compare Figure 17C and 17F).

Figure 17. Expression of the dorsal neural tube specific markers, *Pax-3* and *Pax-6*. E12.5 wild type (B and C) and double transgenic (E and F) sections are hybridized with *Pax-3* probe (B and E) and *Pax-6* probe (C and F). Left panels are bright field from double transgenic sections. FP, floor plate; RP, roof plate; Arrowhead, putative floor plate in the double transgenic embryo.

No Detectable Alteration in the Dorsal NT of the Cre/loxP Double Transgenics

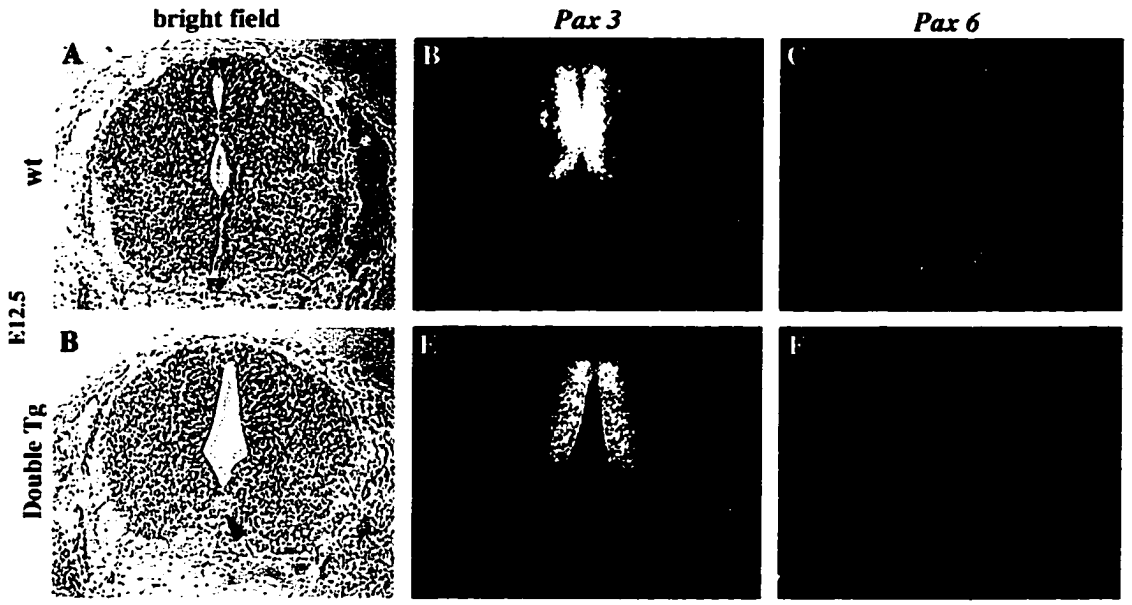

Figure 17

The expression pattern of the sclerotome specific gene, *Pax-1*, was also examined between E9.5-E12.5 to determine whether somite formation might be defective. At E10.5, *Pax-1* is highly expressed in sclerotome (Figure 18B). By E12.5, strong expression is detected in the mesenchymal condensation around the notochord, which develops into the vertebral column (Figure 18E). In double transgenic mice, this expression pattern is maintained (compare wt and double transgenics, Figure 18). To investigate whether the axial skeletons, which are derived from the paraxial mesoderm, are abnormal, neonatal double transgenic mice and wild type/single transgenic mice were stained with alizarin/alcian for skeletal elements. Gross examination failed to find any axial skeleton defect in the double transgenic pups compared with the wild type skeletons (Figure 22). Together, these results suggest the paraxial mesoderm development is normal in the double transgenic embryos.

Figure 18. Expression of the sclerotome specific marker *Pax-1*. E10.5 (top panels) and E12.5 (bottom panels) double transgenic sections (C and F) and wild type sections (B and E) are hybridized with *Pax-1* probe. Left panels are bright field from double transgenic section. FP, floor plate; S, sclerotome; V, vertebra.

Pax-1 Expression Is not Affected in the Double Transgenics

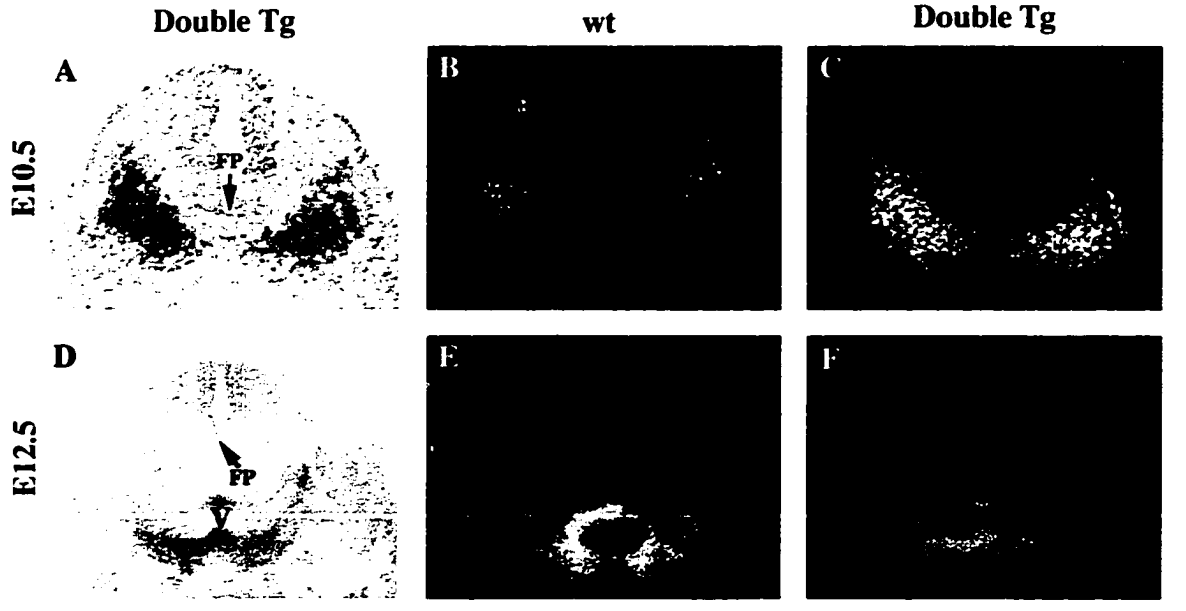

Figure 18

5. *Axonal projection defect in the double transgenic embryos*

The floor plate has guidance activity to navigate both motor axons and commissural axons (Dodd, 1993). To investigate the axonal projection pattern in the spinal cord along the dorsoventral axis, E12.5 cryostat sections were stained with the monoclonal neurofilament antibody, 2H3, which stains most axons. Two major defects were observed at the thoracic region in the double transgenic embryos compared with wild type/single transgenic mice. First, the wild type floor plate normally comprises axons that cross the midline, However, in the double transgenic mice, longitudinally migrating axons were observed in the putative floor plate in addition to these crossing axons (green arrowhead, compare Figure 19A and 19B). Second, the thickness of the spinal tracts is reduced by two to three fold in the double transgenic mice compared with wild type spinal tracts (white arrows, compare Figure 19A and 19B). This reduced thickness might simply stem from axons migrating rostrocaudally inside the putative floor plate. The defect was observed at the thoracic region of the spinal cord but not in the lumbar region (compare Figure 19B and 19D) which is consistent with the previous analysis of morphological and molecular defects (Figure 14).

It has been shown that the secreted molecule Netrin-1 is important for the floor plate axonal guidance activity (Colamarino and Tessier-Lavigne, 1995; Kennedy et al., 1994). To determine whether the axonal projection defect stems from the alteration of *Netrin-1* expression, *in situ* hybridization was performed using a *Netrin-1* specific probe. At E9.5 and E10.5, the expression pattern of *Netrin-1* in the double transgenic mice was the same as in wild type mice (compare Figure 20B and 20C). However, at E12.5, the expression level was significantly reduced at the ventral midline region in the double transgenic mice (compare Figure 20E and 20F). The altered *Netrin-1* expression pattern might explain the axonal guidance defect in the spinal cord. However, we can not rule out the possibility that this defect is simply because of the physical absence of the floor plate cells.

Figure 19. Anti-neurofilament antibody 2H3 staining of both wild type and double transgenic embryos at the thoracic and lumbar region at E12.5. 30um cryostat cross sections from a E12.5 wild type embryo (A and C) and a double transgenic embryo (B and D) are stained with 2H3 antibody. Arrow head point to the floor plate and arrows are pointing to the spinal tracts.

Axonal Projection Defects in the Cre/loxP Double Transgenics

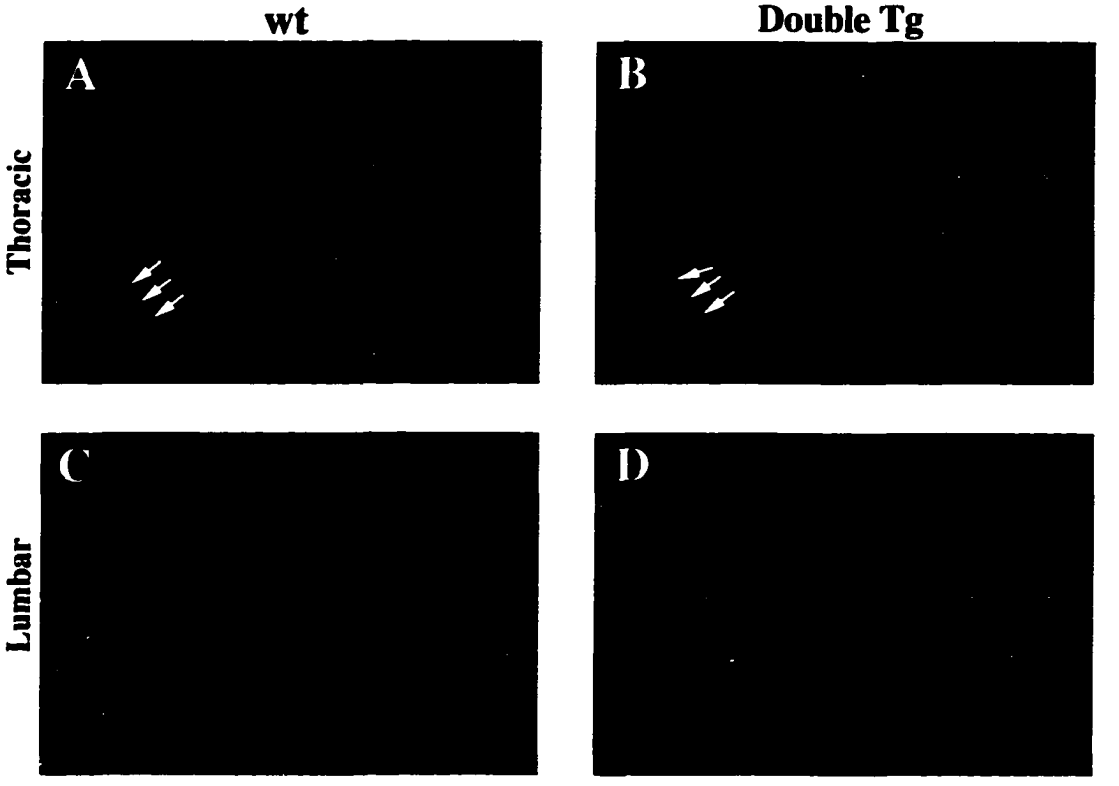

Figure 19

Figure 20. Expression of *Netrin-1* in the double transgenic and wild type embryos. E10.5 (top panels) and E12.5 (bottom panels) from wild type (B and E) and double transgenic (C and F) sections are hybridized with *Netrin-1* probe. A and D, bright field form the double transgenic sections.

Netrin-1 Expression Is Affected in the Double Transgenics

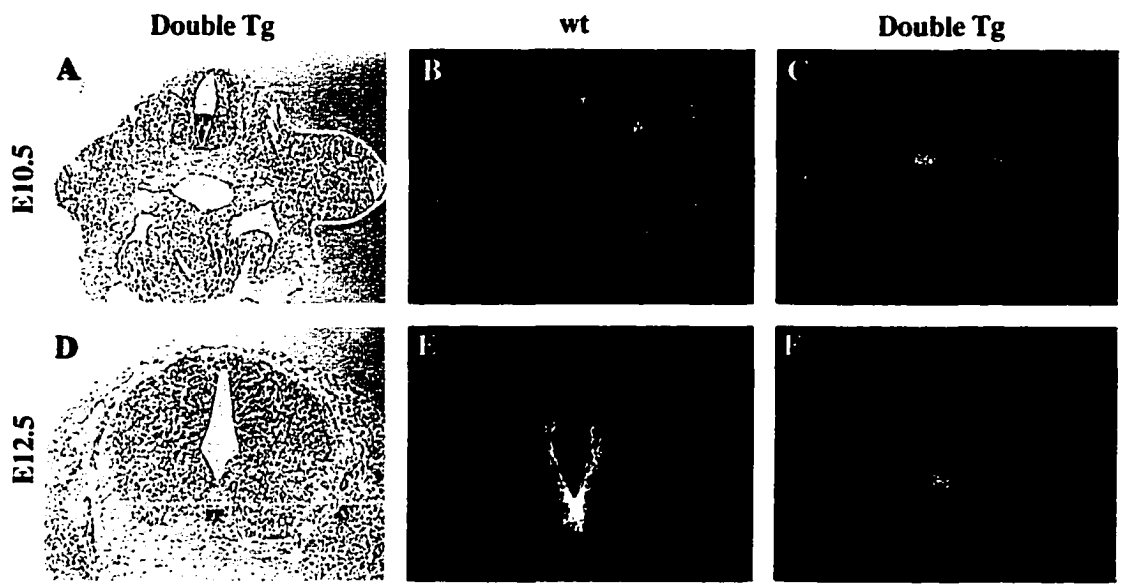

Figure 20

Discussion

The analyses presented outline the characteristics of a novel genetic ablation mechanism in which the floor plate was specifically deleted by Cre-mediated site-specific recombination. In contrast to classical tissue ablation assays, this genetic ablation does not cause physical damage to adjacent tissue, and the cells undergo apoptosis. Therefore, there is no inflammation or tissue wounding response.

The floor plate is the ventral midline tissue of the neural tube that is induced by secreted factors such as *Shh* from the underlying notochord. Once the floor plate is formed, it acquires an activity that induces adjacent neural tube cells to differentiate into the floor plate cells or motor neurons (Hatta et al., 1991). Consistent with this nature, even though we found that the floor plate cells were dying between E8.5-E11.5 in double transgenic embryos after Cre-mediated site-specific recombination, we did not detect morphological or molecular defects at these stages possibly because additional cells were induced to replenish the dead cells. However, we did detect severe phenotypes after E12.5. These results suggest that there is a critical period during neural tube induction when the neural tube cells lose their competency to respond to the floor plate and the notochord inductive signals.

Consistent with previous studies that the floor plate is important for motor neuron induction, we found that *Islet-1* positive motor neurons are reduced in numbers and two ventral motor columns are fused along the ventral midline. A simple explanation for the fused motor columns along the ventral midline is that deletion of floor plate removes the physical barrier between the two ventral-lateral motor columns. Alternatively, those motor neurons are newly induced because of the reduced *Shh* level, because *Shh* induces floor plate formation at high concentrations and motor neuron differentiation at low concentrations (Ericson et al., 1997). In double transgenic mice, low levels of *Shh* could

potentially induce ventral midline tissue to become motor neurons rather than the floor plate cells.

In contrast to the ventral neural tube development, the acquisition of dorsal neural tube fate appears to be controlled by signals from the overlying ectoderm (Dickinson et al., 1995; Liem et al., 1997). In addition, the formation of dorsal fate is suppressed by the ventralizing signal *Shh* from the floor plate and the notochord (Basler et al., 1993; Goulding et al., 1993; Yamada et al., 1991). In double transgenic mice, the *Shh* expression domain is shifted dorsally by approximately one third of the neural tube diameter (Figure 15I), which is in close proximity to the *Pax-3* and *Pax-7* expression domain (compare Figure 15I and Figure 17E). An expectation from this shifted expression is that the neural tube might be partially ventralized. However, this was not the case since dorsal neural tube specific markers, including *Pax-3* and *Pax-7,* were unaffected in the double transgenic embryos. Such a result is not totally unexpected considering that at E12.5 *Shh* expression is low in the double transgenic mice, and that at this time, *Pax-3* and *Pax-7* expressing cells might already have become unresponsive to *Shh* signaling. Similarly, we did not detect any defects in somatic patterning and skeleton formation.

At E12.5, the double transgenic embryos exhibited severe axonal projection defects as revealed by neurofilament immunostaining. Expression level of the axon guidance molecule *Netrin-1* was also reduced. This defect is similar to the *short-tail* mutant in mouse and the *cyclop* mutant in zebra fish (Bovolenta and Dodd, 1991; Hatta, 1992; Hatta et al., 1991). However, we do not know whether the defect is a direct cause of the floor plate ablation or the reduction in *Netrin-1* expression. Future studies will focus on the ectopic expression of *Netrin-1* in the floor plate of double transgenic mice in an attempt to rescue the phenotype.

3. Limb Induction

Introduction

Conceptually, vertebrate limb development occurs in two steps: initiation of the limb bud and patterning and outgrowth of the limb bud. Much has been known about the molecular regulation of limb bud outgrowth and patterning (Johnson and Tabin, 1997). However, little is known about the nature and origin of the endogenous limb inducing activity. In an attempt to address this issue, the double transgenic embryos were used as a model system since the forelimb defect occurs early during the step of limb bud initiation at E9.5. Expression of the earliest known limb inducing molecules, including *Fgf-8* and *Fgf-10*, are examined in the double transgenic embryos. Expression of genes responsible for limb bud outgrowth and pattern formation were also examined. Taken together, the results suggested that a putative limb inducer(s) is synthesized in axial structures, possibly the node, notochord or the floor plate, and that this signal is propagated through paraxial mesoderm, intermediate mesoderm, lateral plate mesoderm and finally the surface ectoderm to initiate limb bud formation.

Results

1. *Abnormal forelimb bud development in the double transgenic mice*

Forelimb bud formation becomes morphologically distinct at E 9.5. In double transgenic embryos, abnormal development of the forelimb bud is apparent at this stage compared to the wild type/single transgenic embryos (Figure 21A). However, the hindlimb bud develops normally through all stages (asterisks, Figure 21). The forelimb defect persists at later developmental stages and becomes even more obvious as shown in Figure 21. About 25% of the double transgenic embryos fail to develop forelimbs, while others have partially formed forelimbs (compare Figure 21D with 21E, arrowheads). The anterior structures of the partially defective limb buds are more severely affected than posterior

structures (Figure 21E). The early defect of limb formation at E9.5 suggests that limb initiation is altered in the double transgenic embryos.

Double transgenic mice survived to postnatal day one and died thereafter. It is not fully clear yet what causes the postnatal lethal phenotype. To examine the skeletal defects in the double transgenic mice, cartilage and bone staining were performed on the newborn double transgenic and wild type/single transgenic pups. Gross skeletal defect were absent (compare wt and Double Tg, Figure 22) besides the truncation of the limb skeletons in the double transgenic mice (Figure 22). In about 25% cases, there is a complete loss of all limb skeletal structures, including the humerus, radius, ulna, and digits. The scapula is derived from somatic tissue and its development is normal in all the double transgenic embryos analyzed (total 17 new born pups, right panel, Figure 22). This is consistent with the notion that somatic development is normal in the double transgenic embryos.

Figure 21. Morphological forelimb defect in the double transgenic embryos. Whole mount picture of the wild type and double transgenic embryos at E9.5 (A), 10.5 (B), and 12.5 (C, D, and E). Genotype of each embryos are indicated. Arrows point to the wild type forelimb and arrowheads point to the mutant forelimb. Asterisk indicates the hindlimb.

Forelimb Defects in the Cre/loxP Double Transgenics

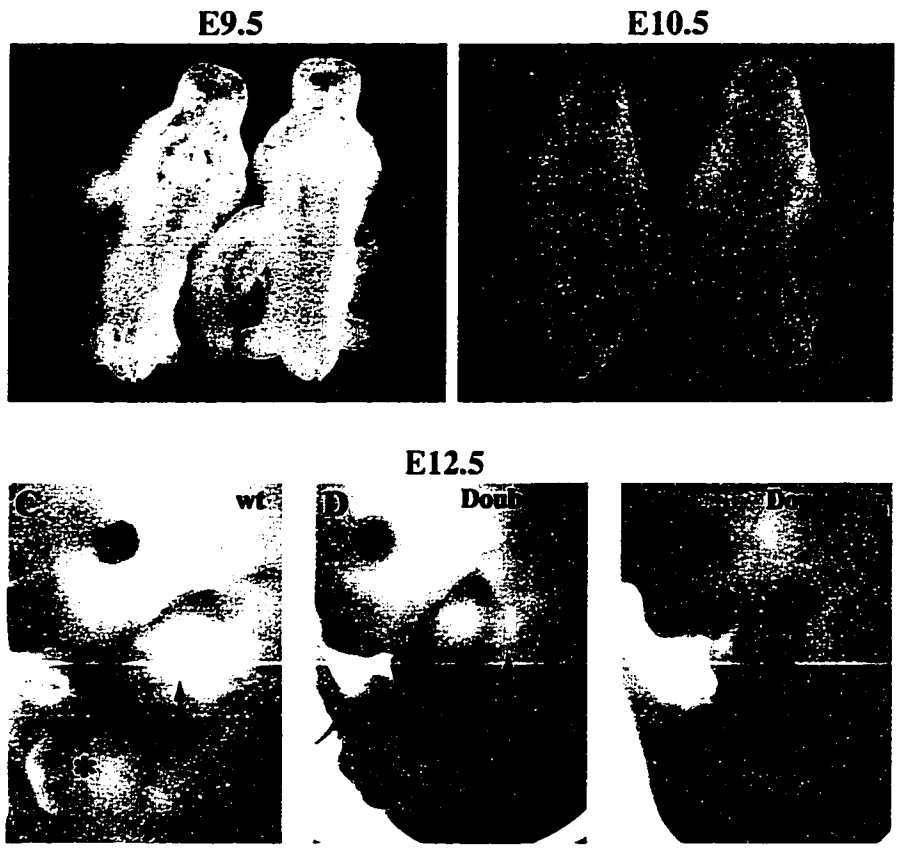

Figure 21

Figure 22. Skeletal staining of newborn pups. Right hand panel is whole mount wild type mouse and middle panel is whole mount double transgenic mouse. Right hand, top, wild type forelimb skeleton; bottom five, double transgenic forelimb skeleton. S, scapula; H, humerus; R, radius; U, ulna; and D, digits.

Forelimb Defects in the Cre/loxP Double Transgenics

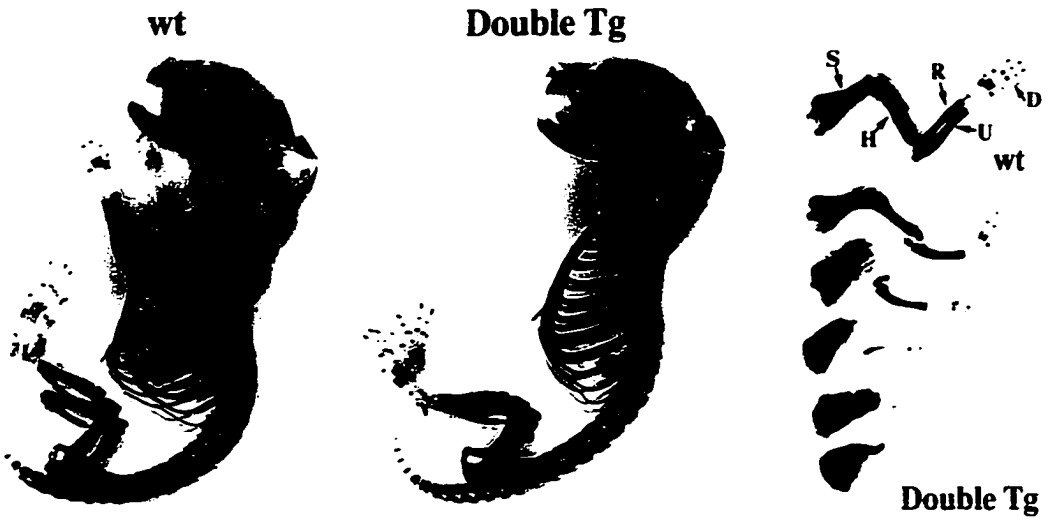

Figure 22

2. Failure of limb initiation in the double transgenic embryos

To investigate whether the forelimb malformation in the double transgenic embryos is an limb initiation defect or limb outgrowth and patterning defect, *Fgf-8* expression was analyzed by RNA *in situ* hybridization in whole mount embryos at E9.5 and E10.5. At E9.5, *Fgf-8* is expressed strongly in the forelimb bud ectoderm, which is just emerging from the body wall, and the presumptive hindlimb bud ectoderm in the wild type/single transgenic embryos (Figure 23 A). By E10.5, *Fgf-8* expression becomes restricted to the AER (Figure 23C). *Fgf-8* is also expressed in other regions like the forebrain/midbrain junction, bronchial arches, somites, and tail bud at these stages (Crossley and Martin, 1995). In double transgenic embryos at E9.5 and E10.5, *Fgf-8* expression pattern is indistinguishable from the wild type/single transgenic mice in all domains except the forelimbs (compare left and right panels, Figure 23). At E9.5, no *Fgf-8* mRNA was detected in the putative forelimb ectoderm (Figure 23B). By E10.5, when AER is already formed in wild type embryos, a malformed bud is apparent at the prospective forelimb region and it is devoid of *Fgf-8* mRNA (arrowhead, Figure 23D). In contrast, the hindlimb bud develops normally with high levels of *Fgf-8* expression at the AER (asterisks, Figure 23). In some cases, where the limb defect is less severe, local expression of *Fgf-8* and truncated formation of AER is apparent (Figure 26F, discussed later). This may explain why there is a partial limb formation in some cases.

Figure 23. *Fgf-8* whole mount *in situ* hybridization on wild type and double transgenic embryos at E9.5 and E10.5. Arrows indicate wild type forelimbs and arrowheads indicate double transgenic forelimbs. Asterisks indicate hindlimbs.

Fgf-8 Expression Is Diminished in the Forelimbs of the Cre/loxP Double Transgenics

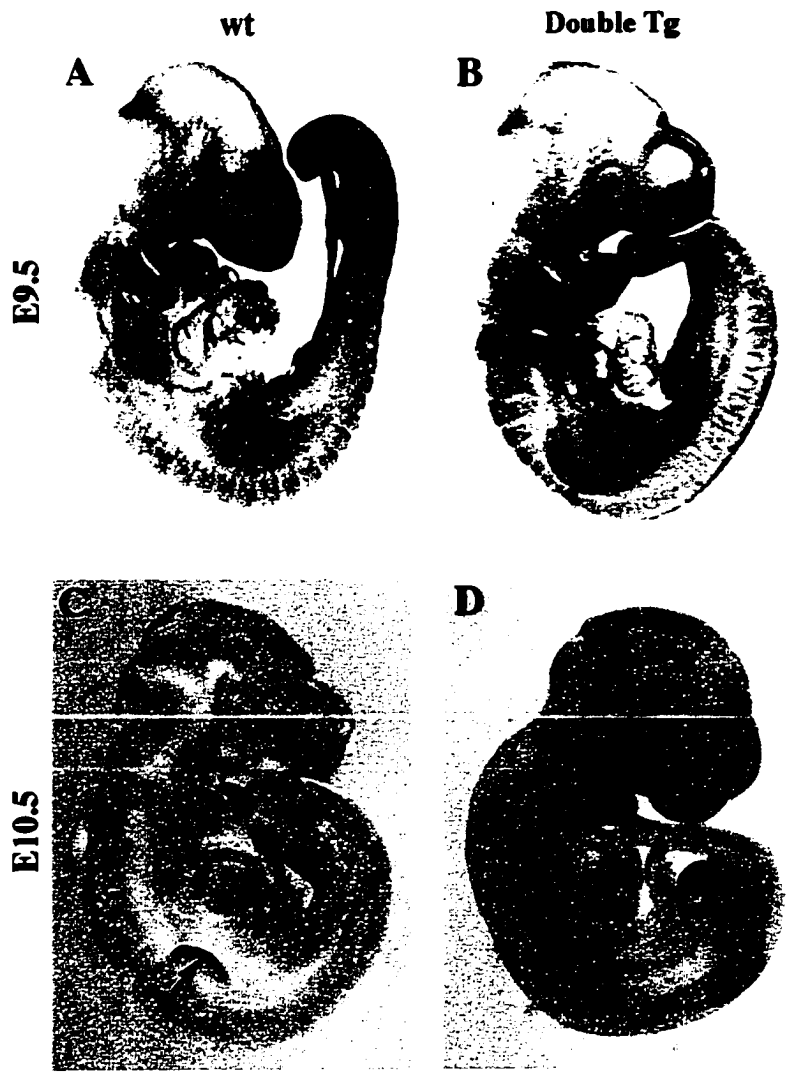

Figure 23

Figure 24. *In situ* hybridization using ^{35}S labeled *Fgf-8* probe. Wild type sections (left panel) and double transgenic sections (right panels) at E9.5 (top four panels) and E10.5 (bottom four panels) are hybridized with ^{35}S *Fgf-8* probe. NT, neural tube; IM, intermediate mesoderm; AER, apical ectodermal ridge; FL, forelimb; arrowhead indicates signal at the intermediate mesoderm in the double transgenic embryo.

Fgf-8 Expression in the Double Transgenics

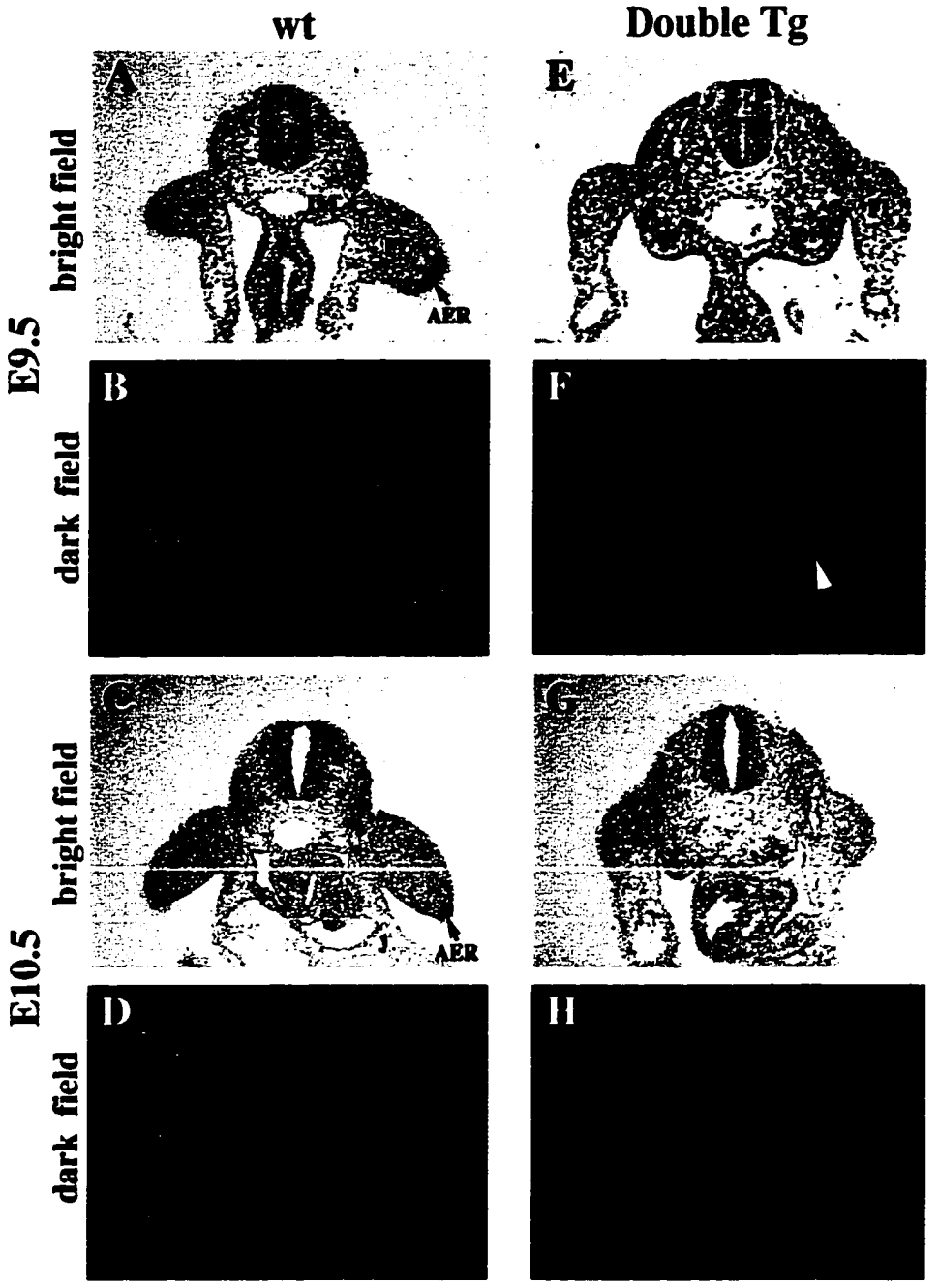

Figure 24

Previous studies have suggested that *Fgf-8* expression at the intermediate mesoderm mesonephros induces limb formation (Crossley et al., 1996). To investigate whether *Fgf-8* expression is altered at the mesonephros in double transgenic embryos, *in situ* hybridization was performed on paraffin sections at E9.5 and E10.5 embryos using a *Fgf-8* RNA probe, *Fgf-8* is expressed strongly in the forelimb AER of wild type/single transgenic embryos but not in the double transgenic embryos (Figure 24, compare panels A and B, D and E), which is consistent with the whole mount studies (Figure 23). However, *Fgf-8* mRNA was detected in the mesonephros of the double transgenic embryos (white arrowhead, Figure 24F). Considering there is no forelimb formation in the double transgenic embryos, these results indicate that the expression of *Fgf-8* in the mesonephros might not be directly involved in limb initiation. In support to this notion, Ros et al. (1997) demonstrated that limb initiation and development were normal in the absence of both *Fgf*-8 expression and the formation of the mesonephros in chicks. However, we can not role out the possibility that the expression of *Fgf-8* in the intermediate mesoderm is reduced in levels.

Fgf-10 functions upstream of *Fgf*-8 and is expressed at the segmental plate and presumptive limb bud mesoderm preceding formation of the limb bud. To determine whether the absence of *Fgf-8* expression in the limb buds of double transgenics stems from altered *Fgf-10* expression, *in situ* hybridization was performed using a rat *Fgf-10* probe At E9.5 and E10.5. *Fgf-10* is expressed in the intermediate and lateral plate mesoderm in wild type/single transgenic embryos at the limb bud level (Figure 25B and 25D). However in double transgenic embryos, these expression domains were not detected at either E9.5 or E10.5 (Figure 25F and 25H). In contrast, the hindlimb *Fgf-10* expression is normal in the same double transgenic embryo (white arrow, Figure 25H). This result supports the hypothesis that expression of *Fgf-10* induces *Fgf-8* expression at the AER and accounts for

the absence of *Fgf-8* at the surface ectoderm at E9.5 and at the AER in later stages in forelimbs of double transgenic embryos.

Presently we have been unable to ascertain the molecular basis underlying the absence of *Fgf-10* expression in the double transgenic embryos. From results discussed in Section IV and V, the primary defect in the double transgenic embryos is that the population of cells in the floor plate and notochord undergo apoptosis after Cre-mediated recombination. Secondary to that, a portion of intermediate mesoderm cells degenerates. Therefore, it is conceivable that the floor plate and notochord might express signaling molecules that are required for the initiation and/or maintenance of *Fgf-10* expression.

Figure 25. *Fgf-10* expression pattern in the double transgenic and wild type embryos at E9.5 and E10.5. NT, neural tube; FL, forelimb; HL, hindlimb; arrow indicates signal at the hindlimb mesoderm in the double transgenic embryo.

Fgf-10 Expression in the Double Transgenics

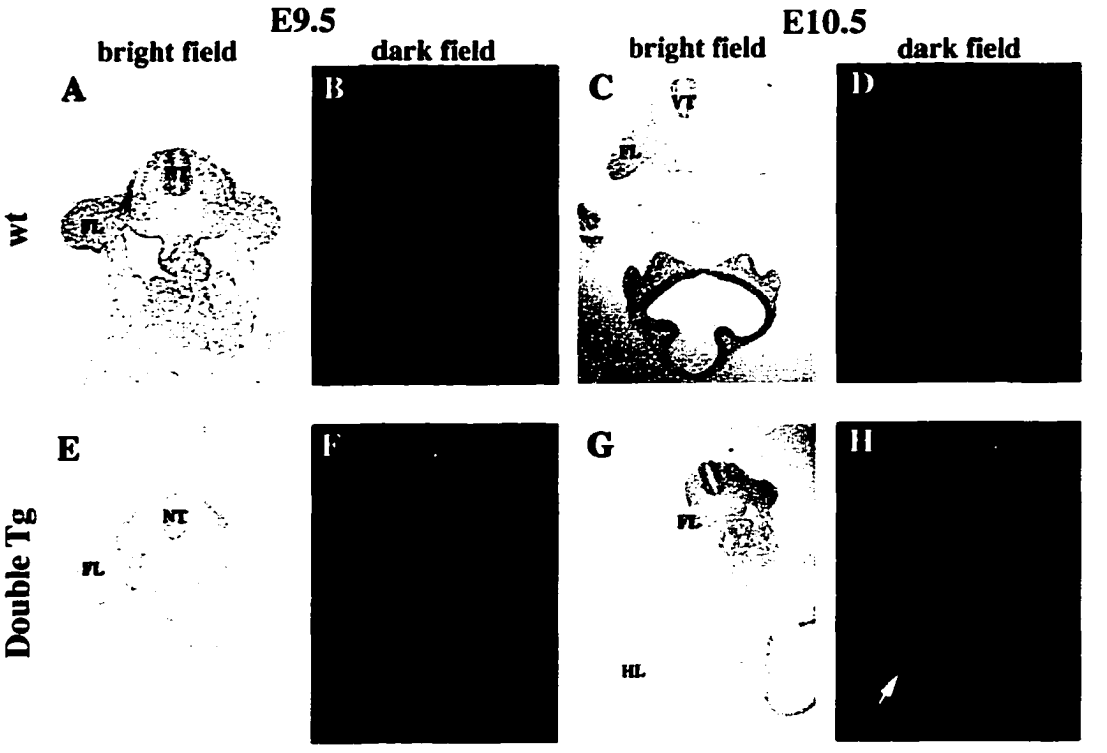

Figure 25

3. *Patterning of the forelimb is normal in double transgenic embryos*

To determine whether the limb patterning process is altered in the double transgenic mice, embryos with relatively mild phenotypes were screened for expression of *Shh, Fgf-8,* and *Wnt-7a* in the forelimbs. These genes are known to regulate anteroposterior, proximodistal, and dorsoventral axis formation, respectively. At E9.5 and E10.5, *Shh* is expressed in the ZPA of the posterior limb bud mesoderm in wild type/double transgenic embryos (Figure 26A and 2C). In those double transgenic embryos with severely affected forelimbs, *Shh* was not detectable at either E9.5 or E10.5 (Figure 26B and 26D). The absence of *Shh* expression may be a primary or secondary effect of the limb defect, because maintenance of *Shh* expression is dependent on a functional AER (Johnson and Tabin, 1997). However, *Shh* is expressed in the putative ZPA in the mildly affected limb buds and weak *Fgf-8* expression is detected at the distal most region of the limb bud ectoderm (Figure 26 E and 26F, respectively). These results suggest that the establishment of the anteroposterior axis and the competence to generate the proximodistal axis are unaffected in the double transgenic embryos.

To investigate patterning along the dorsoventral axis, double transgenic embryos were sectioned and hybridized with *Wnt-7a* probe. At E9.5, *Wnt-7a* mRNA is detected at the dorsal ectoderm of the limb bud in wild type/single transgenic embryos (Figure 27B) and is maintained at E10.5 (data not shown). In the double transgenic embryos, similar expression patterns are found at E9.5 and E10.5 (Figure 27D, and data not shown). Therefore, these data suggest that formation of the dorsoventral axis is maintained in the double transgenic mice, supporting the notions that establishment of the dorsoventral axis is independent of formation of AER and also that the initial dorsalizing signal originates in the paraxial mesoderm, a structure that is not affected in double transgenic embryos.

To further investigate pattern formation in embryos with mild limb defects, newborn pups were processed for skeletal staining. Consistent with the molecular studies that patterning molecules are not affected, formation of the humerus, radius, ulna, and digits is observed in the mild affected limbs, and the overall patterning of the proximodistal and anteroposterior axes are preserved (right panel, Figure 22). Patterning along the dorsoventral axis is also normal based on the presence of dorsal fur and ventral fat pad structures (data not shown). Therefore, we conclude that pattern formation in the forelimb is normal in the double transgenic embryos.

Figure 26. *Shh and Fgf-8* whole mount *in situ* hybridization of the double transgenic and wild type transgenic embryos at E9.5 and E10.5. FL, forelimb; AER, apical ectodermal ridge; asterisk, double transgenic forelimb; arrowhead, defect AER.

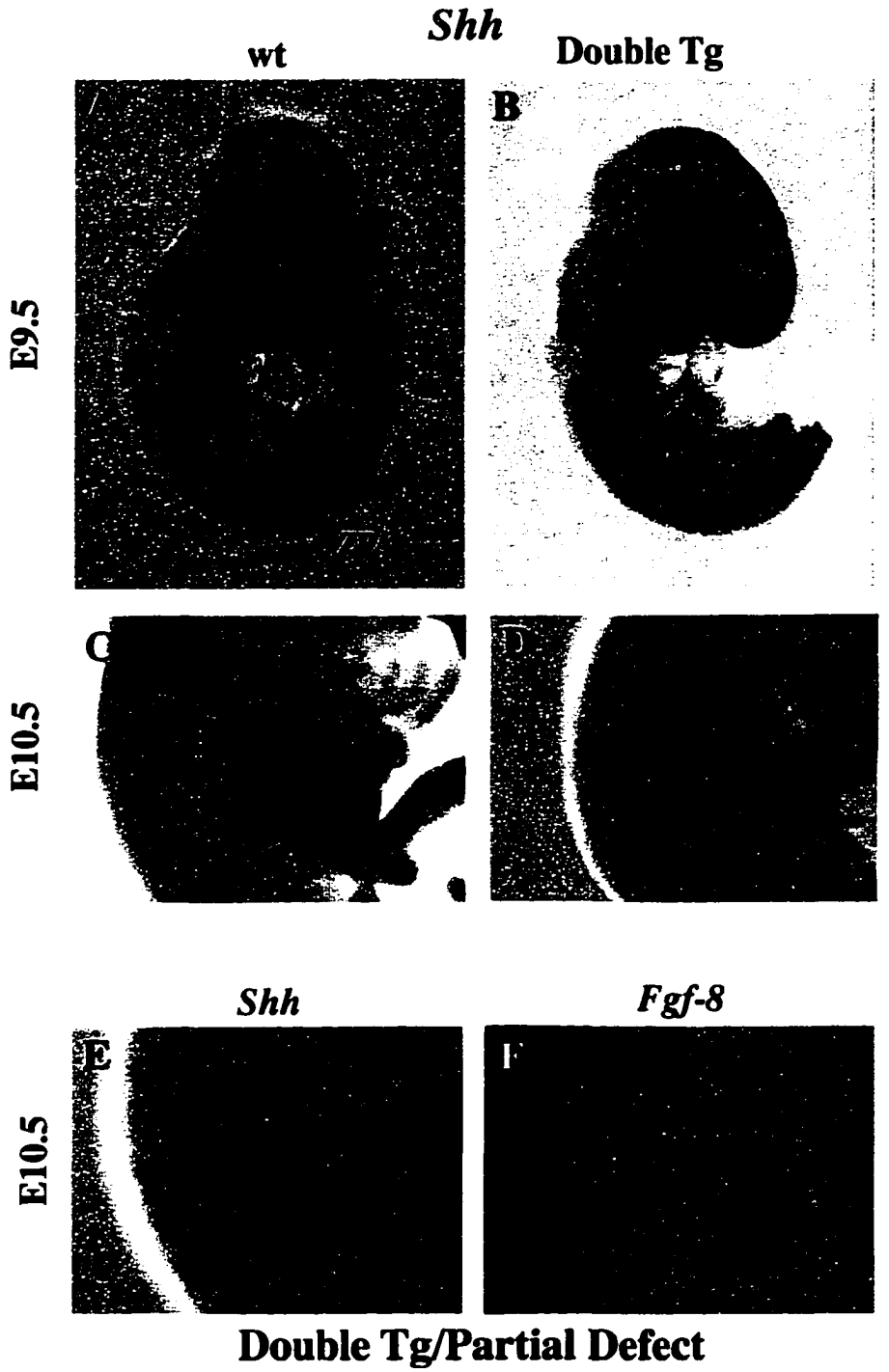

Figure 26

Figure 27. *Wnt-7a* expression in the double transgenic and wild type embryos at E9.5. Wild type sections (A and B) and double transgenic sections (C and D) at bright field (A and C) and dark field (B and D). Arrowheads, indicating signal at the dorsal limb bud ectoderm.

Normal *Wnt-7a* Expression in the Dorsal Limb Bud Ectoderm

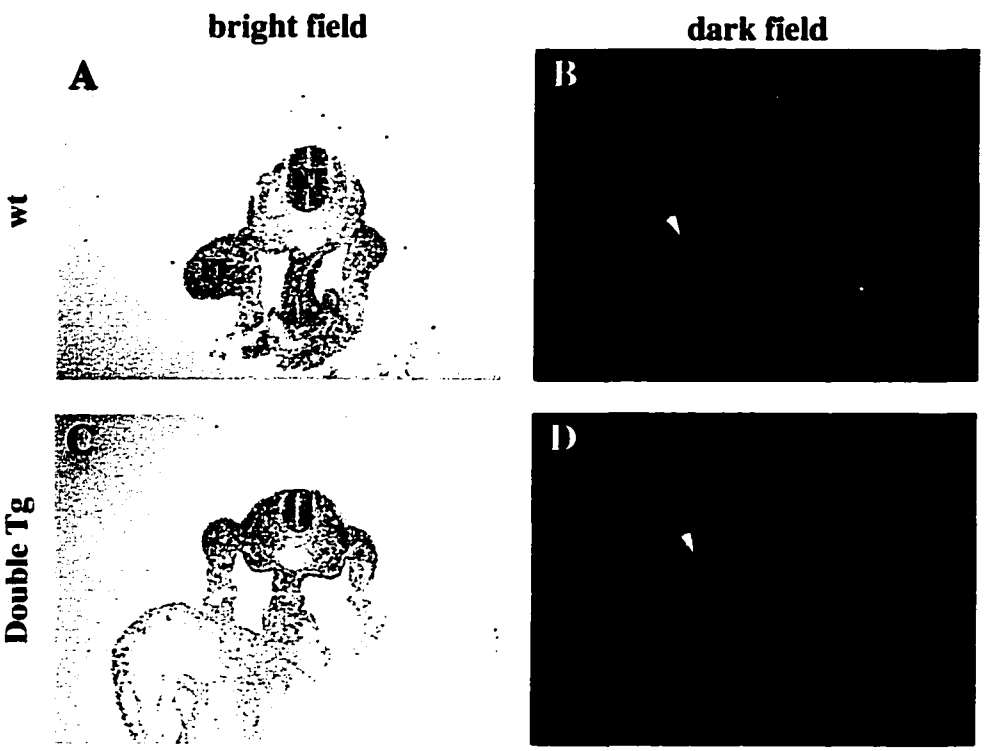

Figure 27

Discussion

On the bases of the results presented, I propose a model of limb bud initiation. The putative limb induction signals produced by the floor plate and the notochord, and possibly by the node at earlier stages, induces or maintains the expression of *Fgf-10* in the paraxial, intermediate, and lateral plate mesoderm. The expression of *Fgf-10* acts as a relay signal to induce expression of *Fgf-8* in the surface ectoderm. Unidentified, independent factors induce expression of *Shh* in the ZPA and *Wnt-7a* in the dorsal limb bud ectoderm. At later stages, interactions among *Fgf-8, Shh,* and *Wnt-7a* signaling pathways regulate the limb outgrowth and patterning which is independent of the early limb inductive activity.

In double transgenic embryos, floor plate and notochord cells undergo apoptosis as a consequence of Cre-mediated site-specific recombination. Cell death was elevated as early as E8.5 in the notochord and floor plate, but was also observed in the intermediate mesoderm, probably due to the absence of surviving signals from the floor plate and the notochord as discussed in Section III. Surprisingly, forelimb development was abnormal in double transgenic embryos. This defect was apparent by E9.5 at the stage of limb initiation. Therefore, these data suggest that the initiation rather than limb outgrowth and patterning are defective in double transgenic embryos.

Figure 28. Model of signals controlling the limb development. Early stage, notochord secrete limb initiation signal to induce expression of *Fgf-10* at the paraxial mesoderm, intermediate mesoderm, and lateral plate mesoderm. Expression of *Fgf-10* induces *Fgf-8* expression at the prospective limb ectoderm. Later stage. Interaction among dorsal signal *Wnt-7a,* posterior signal *Shh*, and distal AER signal *Fgf-8* controls the outgrowth and patterning of the limb bud. (modified from Michaud et al., 1997).

Signals Controlling the Limb Development

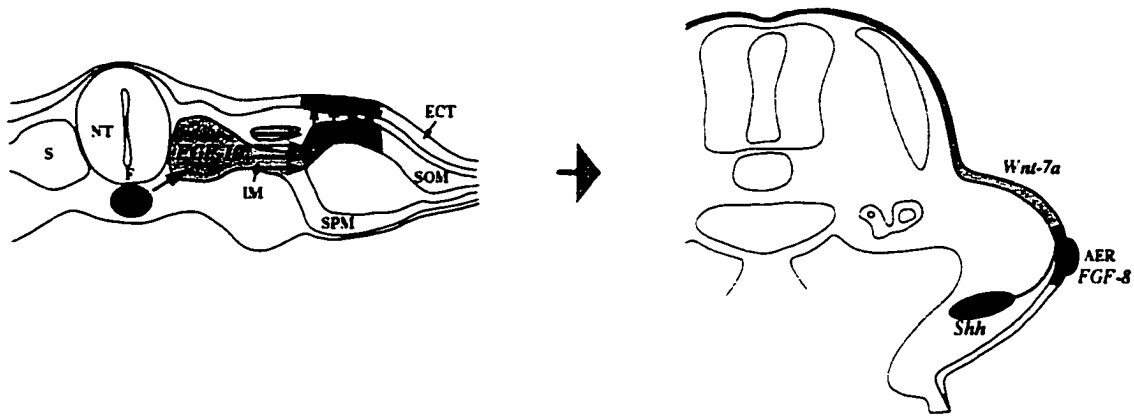

Initiation **Outgrowth and Patterning**

Figure 28

Fgf-8 is normally expressed in the limb field ectoderm prior to limb bud formation. This expression persists and defines the AER at E10.5. In addition, *Fgf-8* is transiently expressed in the intermediate mesoderm at forelimb and hindlimb levels prior to limb bud outgrowth. In double transgenic embryos, on the other hand, *Fgf-8* expression is diminished in the surface ectoderm, but is maintained in the intermediate mesoderm. These results are incompatible with the notion that *Fgf-8* expression in the intermediate mesoderm acts as an endogenous limb inducing signal. Consistent with our results, Ros et al. (1997) used membranes to block formation of the mesonephros rostral to the limb field, and showed that cells in the intermediate mesoderm underwent apoptosis and that *Fgf-8* expression was undetectable. Nevertheless, normal limb bud formation and development was observed. Our results also suggest there are different mechanisms to initiate *Fgf-8* expression in the intermediate mesoderm and surface ectoderm. Complementary to our findings that *Fgf-8* expression in the intermediate mesoderm is normal while its expression at the surface ectoderm is reduced, Ros et al. (1997) found expression in the intermediate mesoderm is diminished while the expression at the surface ectoderm is maintained.

Recent research indicates that Fgf-10 serves as an bonafide endogenous inducer of limb bud formation. Fgf-10 is expressed in the prospective limb mesoderm and precedes Fgf-8 expression in the nascent apical ectoderm. Ectopic application of Fgf-10 induces Fgf-8 expression in the adjacent ectoderm resulting in additional limb formation. Therefore, Fgf-10 is likely to be upstream of Fgf-8. In double transgenic embryos, we did not detect Fgf-10 expression in the forelimb mesoderm although expression in the hindlimb mesoderm was intact. These results support the notion that Fgf-10 is the endogenous limb induction signal. However, factors that are responsible for inducing and maintain Fgf-10 expression in the limb mesoderm are presently undefined. Data presented in the present study suggest that unidentified signals emanating from the axial region induce Fgf-10, which serves as a relay to induce Fgf-8 expression in the limb ectoderm region.

4. Discussion

The Cre/loxP site-specific recombination system has been used as a novel tool in murine molecular genetics to manipulate the genome, including conditional inactivation or activation of gene expression. This system is also used to generate specific chromosome deletions, inversions and duplications. The study presented in this thesis provides evidence to use Cre/loxP system to genetically ablate specific tissues during mouse development. During the course of this study, we discovered that ablation of the floor plate and notochord using the Cre/loxP system leads to the failure of forelimb initiation, this in turn provided the first genetic evidence to support the hypothesis that the endogenous limb inducing signal is located at the axial structures, the node, notochord or the floor plate.

The Cre-mediated recombination in transgenic mice leads to the deletion of the chromosome containing multiple loxP sites with inverted orientation (Lewandoski and Martin, 1997). The basic mechanism of the Cre recombination-mediated chromosome deletion is that the uneven recombination occurs in *trans* between two sister chromatids, which leads to the fragmentation of the chromosome and eventually loss of the chromosome during cell proliferation. Cells can not survive when one autosome is deleted. In our double transgenic embryos, the cell death was detected at E8.5, 12 hours after the expression of Cre due to the recombination-mediated cell ablation. However, at E12.5, there was no detectable cell death even though Cre is still expressed at this stage. This observation indicates that a small population of the floor plate cells have selectively survived after Cre recombination-mediated cell ablation. In theory, this would occur if recombination in *cis* reduces the transgene copy number to one and leaves only a single loxP site in the genome, and recombination in *trans* between two chromatids during cell proliferation is less efficient. Alternatively, the floor plate cells and motor neurons are post

mitotic at later stages (E12.5 and after). Cre-mediated recombination could not occur since there is only a single loxP site in the genome.

Although we favor the possibility that the Cre recombination-mediated chromosome deletion is the potential cause of cell death, we can not currently exclude other alternatives. These include that the recombination has activated or inactivated some unknown endogenous genes which is vital for the survival of floor plate and notochord cells; or that Enhancer III might be able to influence the expression of some unknown genes after recombination. However, we believe these possibilities less likely based on the following observations. First, cell death in the double transgenic embryos occurs in all areas of the Cre-expression domains. These indicates that cell death is a general phenomenon rather than a specific gene effect. Second, when the two independent E3loxP lines are mated with the CMV-Cre mice, the double transgenic embryos are lethal. This indirectly supports the idea that cell death is due to a general mechanism related directly to the Cre-mediated recombination and not the promoter used to drive expression of either loxP-containing or Cre-expression transgenes. Lastly, the observation of the same phenotypes occurring in the two independent E3loxP transgenic lines suggests that the phenotypes can not be easily explained by some rare transgene integration into a locus which is important for spinal cord and limb development.

Analysis of eight different E3loxP lines after Cre-mediated recombination demonstrates that there is no detectable activation of downstream gene expression. Therefore, it suggests that the Cre/loxP RAGE system needs to be further refined in the transgenic studies. For example, one could generate transgenic mice with single copy insertions. This can be accomplished by using ES cells instead of pronuclear injection technology to produce transgenic mice in which the transgene is usually present in a single

copy. It will also be informative to examine this system in stable transfected cultural cells before generating the transgenic mice.

The present study also provides novel evidence to support the notion that the floor plate is required for motor neuron differentiation and commissural axon guidance. In the double transgenic embryo, the floor plate and notochord is ablated between E8.5 and E11.5. The ablation of the floor plate throughout the neuraxis is accompanied by the fusion of two ventral motor columns in the thoracic region of the spinal cord, as defined by several morphological and molecular criteria. Commissural axons took abnormal pathways as they reach the ventral midline of the spinal cord at the level of thoracic region. The molecular and morphological defects of the floor plate and motor neuron formation is similar to the defects observed in the *T* and *Sd* mutants. However the defects occur in the caudal region in these mutants, whereas the defects occur only in the rostral region in our double transgenic embryos. The rostral specificity of the defects in the double transgenic embryos might reflect the expression pattern of Enhancer III which is active at the rostral region initially and then turns on at the caudal region during development.

The forelimb defects in the double transgenic embryo provide novel genetic evidence to support the hypothesis that the endogenous limb inducing signal is produced in the axial structures. Classical foil barrier studies using chick embryos has indicated that the putative limb inducing signals is present in axial structures at the critical period during early embryogenesis and that this signal is propagated through the paraxial and lateral tissues (Stephens and McNulty, 1981; Stephens et al., 1991). However, critical evidence to support this hypothesis is lacking when the formation of the axial structures is altered either physically or genetically. This is largely because the intrusive surgical procedure usually leads to early embryonic lethality. Additionally, the multiple functions of the axial structures often complicates the analysis. In the double transgenic embryos, the axial

structures undergo cell death at E8.5 which coincides with the presence of the putative limb inducing signal. Cell death is not 100 percent due to the dynamic regulation of the floor plate and notochord formation and the efficiency of Cre-mediated recombination process which is affecting in to a rang of forelimb defects spanning from complete absence to a normal limb. The reasonable explanation for the failure of limb development is that the cell death in the axial structures causes reduction of the putative limb induction signal. Alternatively, dead cells may produce some unknown factors which might influence limb development, or unknown genes essential for both the axial cell survival and the limb induction are altered after Cre-mediated recombination.

The more informative evidence to demonstrate the function of the axial structures in limb induction would be the identification of the nature of the putative limb inducing signal in the future. Based on the results of the present study, one would predict that the activity of such a putative signal should be regulated transiently at the axial structures and that this activity should be able to activate the expression of *Fgf-10* in the intermediate mesoderm. It is noteworthy that *Shh* is expressed in the right place and time, and that inactivation of *Shh* in mice causes distal truncation of the limbs (Chiang et al., 1996). This evidence therefore suggests that *Shh* might play some important role in the limb induction, in addition to limb bud patterning along the anteroposterior axis. Experiments in chick embryos have demonstrated that *Shh* induces expression of *Fgf-10* weakly (Ohuchi et al., 1997). It is therefore possible that the combination of *Shh* and other factors, including known and unknown *Fgfs*, are responsible for the induction of limb formation.

IV. Results: Part B

Cloning, Expression, and Targeting of a Pair of Murine Homeobox-Containing Genes: *Dlx5* and *Dlx6*

Introduction

The *Drosophila* homeobox-containing *distal-less* (*dll*) gene is an evolutionary conserved gene that is required for formation of the distal portion of the legs and antennae (Cohen et al., 1989). Families of *dll* homologues (*distal-less-like genes, Dlx*) have been cloned from the butterfly *precis coenia,* zebra fish, newt, *Xenopus*, mouse, and human (Akimenko et al., 1994; Beauchemin and Savard, 1992; Chen et al., 1996; Panganiban et al., 1994; Papalopulu and Kintner, 1993; Porteus et al., 1991; Simeone et al., 1994). In mammals, at least six genes (*Dlx1-Dlx6*) have been identified that are homologues of *dll.* Expression analysis has demonstrated that these genes are expressed in overlapping domains, including the developing bronchial arch, limb buds, forebrain, otic and olfactory vesicles (Chen et al., 1996; Qiu et al., 1995). However, *Dlx5* and *Dlx6* share a unique feature in being expressed in most developing skeletal structure (Chen et al., 1996). *Dlx5* and *Dlx6* have been physically mapped near to the human split hand/split foot locus on chromosome 7 and are candidate genes for ectrodactyly syndrome (Scherer and al., 1994). Presented here are the cloning and expression analyses of the mouse *Dlx5* and *Dlx6* genes. The functional analysis of these two genes using a loss-of-function approach is also addressed.

Results

1. *Cloning of the Dlx5 and Dlx6 Gene and comparison to other Dlx homeoboxes*

Using *Dlx5* and *Dlx6* loci specific probes, we isolated six independent phage clones from a mouse 129/Sv lambda genomic library spanning ~40kb of genomic sequences flanking the *Dlx5* and *Dlx6* loci. The analysis of genomic inserts indicated that the *Dlx5* and *Dlx6* homeoboxes were located 11kb apart and were transcribed towards one another (Figure 33A) as with the organization of these genes in human (Scherer and al., 1994). DNA sequencing of the homeoboxes from *Dlx5* and *Dlx6* show they have 85% and 87% identity with the *Drosophila dll* gene (Figure 29). When compared among themselves, the *Dlx* genes show 88% or greater homology with *Dlx1*, with *Dlx6* having the greatest similarity to *Dlx1*, and *Dlx5* having the greatest similarity to *Dlx2*. Both *Dlx3* and *Dlx4*, show greater similarity to one another than to the other *Dlx* genes (Figure 29). These data suggest that *Dlx1* and *Dlx6* represent paralogous genes, as do *Dlx2* and *Dlx5*. It is unclear if *Dlx3* and *Dlx4* represent paralogs of the other *Dlx* genes or of one another. Both homeodomains do show greater similarity to *Dlx2* and *Dlx5* than to *Dlx1* and *Dlx6* (Figure 29).

Amino Acid Alignment of *Drosophila* and Murine *distal-less/Dlx* Homeodomains

```
                  10        20        30        40        50        60
Dll   M RK P R T I YS S LQ LQ Q LN RR F QR TQ YL AL P E RA E LA A SL GL TQ TQ VK I W FQ N RR S K Y KK M M K  100%

Dlx1  I - - - - - - - - - - - - A - - - - -Q- - - - - - - - - - - - - - - - - - - - - - - - -K- - - F- - L - -  90%  100%
Dlx2  V - - - - - - - - - F- - AA -Q- - - -K- - - - - - - - - - - - - - - - - - - - - - - - - - - - F- - - W -  87%  90%
Dlx3  - - - - - - - - - - Y- - LA -Q- - - -KA- - - - - - - - - - -Q- - - - - - - - - - - - - -                  86%  90%
Dlx4  - - - - - - - - - - - - - AA -Q- - - -KA- - - - - - - - - - - - - - - - - - - - - - - -                  90%  93%
Dlx5  V - - - - - - - - - F- - AA -Q- - - -K- - - - - - - - - - - - - - - - - - - - - - - -K- - - I- - I - -  85%  88%
Dlx6  I - - - - - - - - - - - - A - - H- - -Q- - - - - - - - - - - - - - - - - - - - - - - -K- - - F- - L L -  87%  97%
```

Figure 29. Amino acid alignment of Drosophila and murine *dll/Dlx* homeodomains. The amino acid sequence of the *Drosophila dll* homeodomain is shown at the top. The amino acid sequence of the murine *Dlx* homeodomains is shown below. Dashes indicate identity with the *dll* sequence. Percent homology with the *dll* homeodomain is shown at the immediate right. The percent homology relative to murine *Dlx1* is shown in the far right column.

Figure 30. Chromosome localization of the murine *Dlx5* and *Dlx6* genes to the proximal end of mouse chromosome 6. Left, chromosomal map derived from the backcross panel results. Right, a consensus linkage map of the proximal region of mouse chromosome 6 indicating the position of different marker genes. Numbers to the left of each chromosome indicate the calculated distance in map units (left) or centrimorgans (right).

Dlx5 and Dlx6 Map to the Proximal End of Mouse Chromosome 6

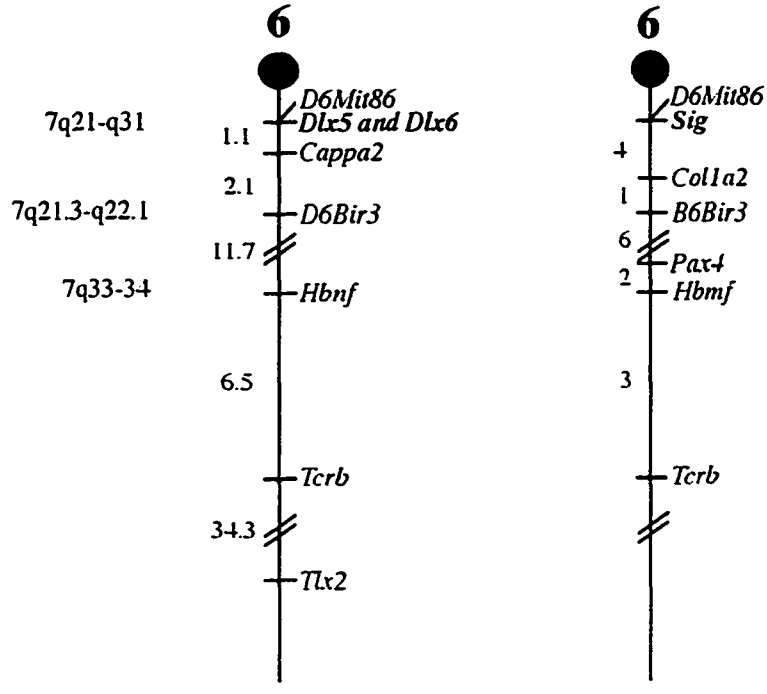

Analysis from 94 N2 progeny from the interspecific backcross (C57/6J x SPRET/Ei) x SPRET/Ei

Figure 30

2. *Chromosomal localization of Dlx5 and Dlx6*

The chromosomal location of the murine *Dlx5* and *Dlx6* genes was determined by analyzing a (C57bL/6J x SPRET/Ei) F1 female x SPRET/Ei male backcross panel. Both C57BL/6J and SPRET/Ei DNAs were digested with 22 different enzymes and analyzed by Southern blotting for a restriction fragment length polymorphism. HindIII digestion gave a 4.2kb specific C57BL/6J band and a 4.7kb specific SPRET/Ei band using a 0.8kb Bgl II-Not I probe obtained from the end of one of the genomic phage containing the *Dlx6* locus. This size difference enabled tracking the segregation of the C57BL/6J *Dlx6*-specific locus among 94 progeny present in the panel. The mapping data indicate that *Dlx5* and *Dlx6* are located in the proximal region of mouse chromosome 6 very close to the centromere (Figure 30). *Dlx5* and *Dlx6* are flanked on the distal side by the Cappα2 (capping protein alpha-two) gene and appear to be closely linked to the *sightless* gene. This region of the mouse chromosome is syntenic with human 7q21-q31 region. This is in agreement with the recent analysis of human *Dlx5* gene, which has been mapped to 7q21.3-q22.1. Interestingly, this region is a critical interval of the split hand/split foot (ectrodactyly; SHSF) human developmental malformation, which is characterized by the absence of digits and claw-like distal limb appendages. Whether this is related to alterations in either *Dlx5* and *Dlx6* remains to be determined; however, both *Dlx5* and *Dlx6* are expressed in the limb and their expression domains are consistent with a potential role in limb development.

3. *Analysis of Dlx5 and Dlx6 expression patterns during murine development*

The expression of *Dlx5* and *Dlx6* was examined in embryos between the ages of E9.5-E14.5. The expression domains of these two genes are very similar between E9.5 and E10.5 and only the expression pattern of *Dlx5* is described. At E9.5 and E10.5, *Dlx5* is expressed in the mesenchyme of the first bronchial arches (Figure 31B, 31D, and 31F). *Dlx5* is also expressed strongly in the limb ectoderm during initiation of limb bud at E9.5. This expression pattern persists and defines the formation of AER at E10.5 (Figure 31D

and 31F). There are also high level of *Dlx5* mRNA detected in the otic vesicle and olfactory plaque (Figure 31B). At E10.5, strong *Dlx5* expression is also detected in the telencephalon, primarily in the regions that later form the ganglionic eminence as well as in the region of the developing hypothalamus (Figure 31H). By E12.5 all of the previous expression domains are still positive, although more restricted in their extent of expression. At this stage, strong expression is also detected in the perichondrial region of most embryonic skeletal elements (Figure 32). This domain of expression is more pronounced for *Dlx5* than for *Dlx6* (compare Figure 32B and 32D).

Figure 31. Expression of *Dlx5* gene in E9.5 and E10.5 mouse embryos. A-D, frontal sections from an E9.5 embryo. E and F, frontal sections from an E10.5 embryo. G and H, sagittal sections from an E10.5 embryo. OE, olfactory epithelium: B, bronchial arch; OV, otic vesicle; L, limb.

Expression of *Dlx5* at E9.5 and E10.5

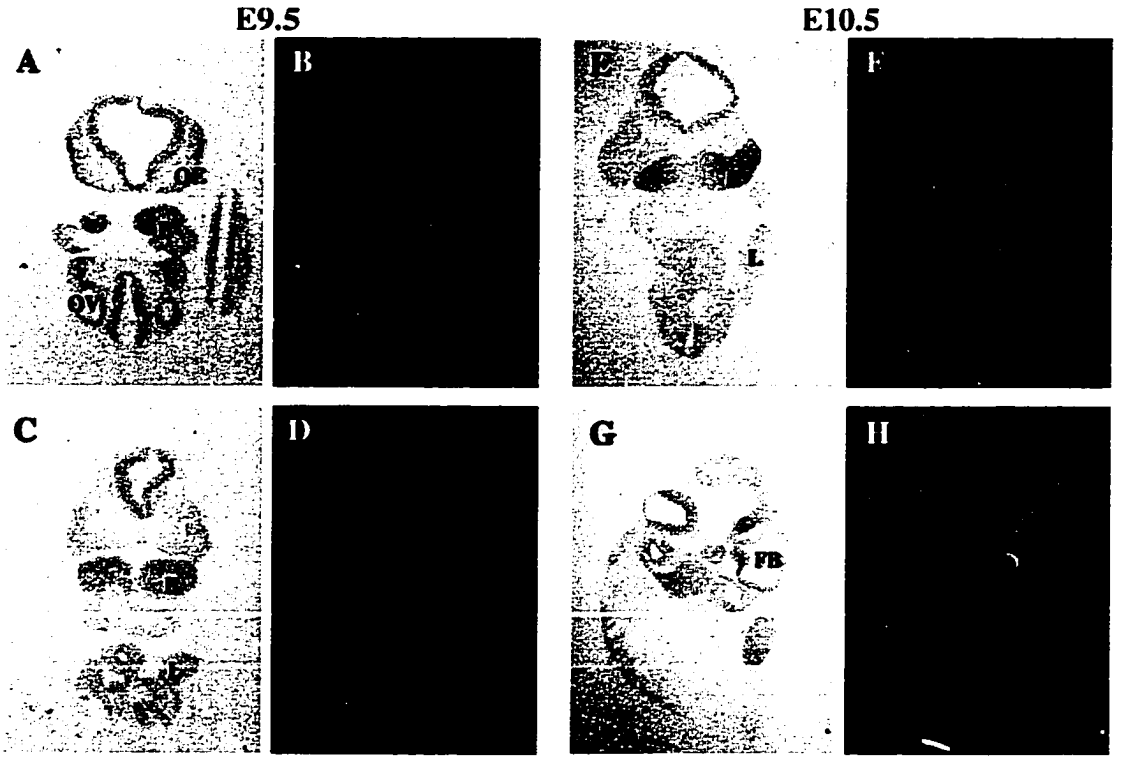

Figure 31

Figure 32. Comparison of *Dlx5* and *Dlx6* expression in E12.5 mouse embryos. Sagittal section from the E12.5 embryos. Bright field is on the left and dark field on the right. FB, forebrain; VC, vertebral column.

Comparison of *Dlx5* and *Dlx6* Expression at E12.5

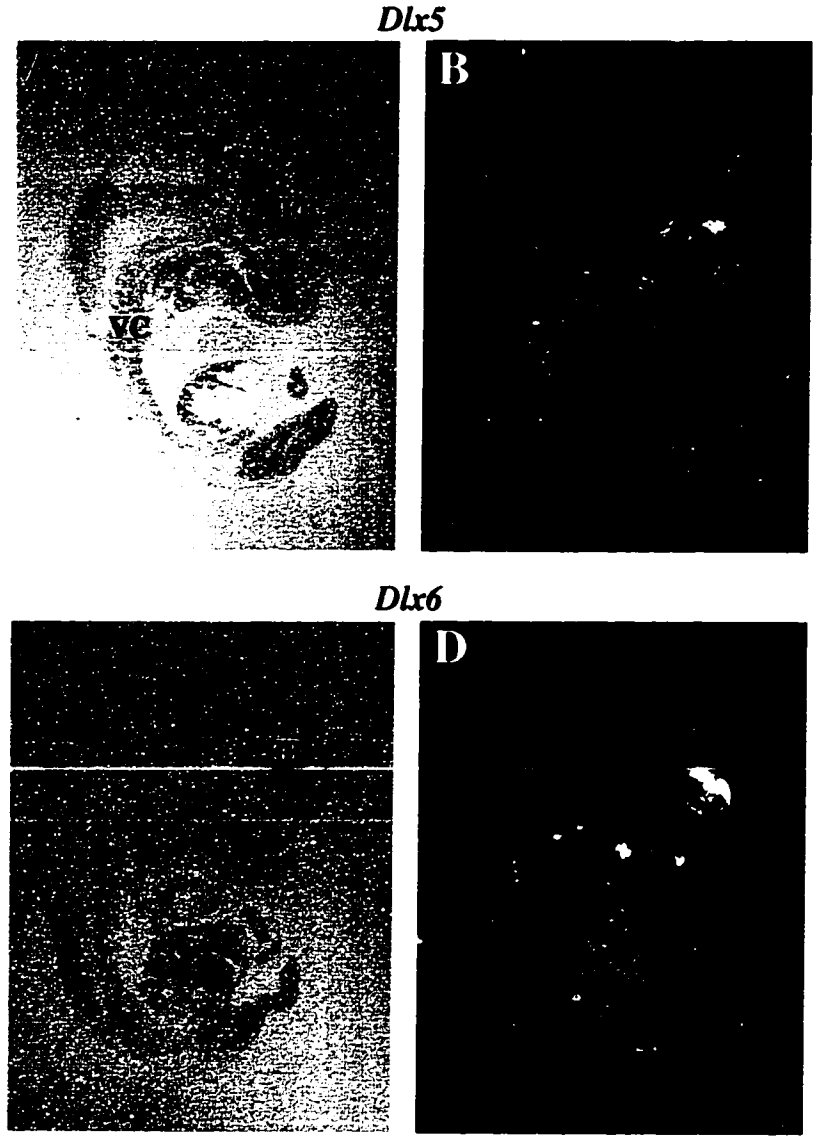

Figure 32

4. *Targeted disruption of the Dlx5 gene*

The pSL59 construct was initially used to target the *Dlx5* gene. This construct had an *IRES-lacZ* and GT1.2-*Neo* gene inserted into the *Dlx5* homeobox. The targeting construct comprised 13kb of homologous *Dlx5* genomic DNA with 1.5kb at the 5' end and 11.5kb at the 3' end. pSL59 was electroporated into $1x10^7$ D3 or R1 cells. In total, 288 ES clones, resistant to G418 selection at the concentration of 150ug/ml, were analyzed by Southern blot using diagnostic probes to differentiate homologous recombination events. However, none of these clones gave specific recombined DNA fragment on Southern blots (data not shown). Therefore, a new targeting construct, pSL81, was made with a *TK* negative selection marker subcloned at the downstream of the genomic DNA inserts in pSL59 to enhance selection for homologous recombinants (Figure 33A). The targeting construct was then electroporated into D3 or R1 cells. Unfortunately, out of 288 ES clones analyzed, (resistant to 2uM gancyclovir and 150ug/ml G418 antibiotic selection), none of them showed a homologous recombination events (data not shown). The knock out of *Dlx5* gene is not pursued further.

5. *Target Disruption of the Dlx6 Gene in ES Cells*

The construct, $pSL74^+$, was used initially to target the *Dlx6* gene. This construct has an *IRES-lacZ* and GT1.2-*Neo* coding sequences inserted into the *Dlx6* homeobox with 9kb of homologous *Dlx6* genomic DNA, 3.5kb at the 5' end and 6kb at the 3' end. Analysis of 288 ES G418 resistant clones by Southern yielded no positive ES clones (data not shown). Therefore, a new targeting construct, pSL80, was made with a *TK* negative selection marker subcloned at the downstream of genomic DNA inserts in $pSL74^+$ to enhance selection for the homologous recombinants (Figure 33A). In total, 288 gancyclovir (2uM) and G418 (150ug/ml) resistant ES clones analyzed by Southern yielded one positive clone which gave a 7.3kb recombination-specific band from an 18kb wild type band using Probe 1 after Eco RV digestion (+/-, left panel, Figure 33B). This positive ES clone was

subsequently treated with a high concentration of G418 (350ug/ml) to select for gene conversion events and generate *Dlx6* null ES cells. Analysis of 192 G418 resistant clones gave one clone with a null mutation of *Dlx6* gene (-/-, middle panel, Figure 33B).

Dlx6$^{+/-}$ ES cells were aggregated with tetraploid embryos to generate Dlx6$^{+/-}$ embryos . The expression pattern of the *lacZ* reporter gene was examined in those embryos at E10.5 and E12.5. At this stage, β-gal activity is detected at the AER, first bronchial arch, nasal epithelium, and inner ear (Figure 34). The β-gal expression pattern recapitulated the pattern of RNA *in situ* results confirms successful targeting of the *Dlx6* locus. Four chimeric mice were generated from this clone by blastocyst injection. However, coat color analysis of more than 100 offsprings from each chimeras demonstrates that ES cells are not contribute to the germ line cells in these chimeras.

Figure 33. *Dlx5* and *Dlx6* targeting construct and targeting results. A, *Dlx5* and *Dlx6* genomic structure and targeting vector used to mutate *Dlx5, Dlx6,* and *Dlx5* and *6*. Arrows indicate the direction of transcription. Probe 1 and 2 used for genotyping are indicated. B, Southern blot analysis of ES clones for *Dlx6* knockout (left panel), hyper-selection of *Dlx6* knockout clone (middle panel) using Probe 1 (Eco RV digestion), and *Dlx5* and *6* double knockout using Probe 2 (right panel, Bam HI digestion).

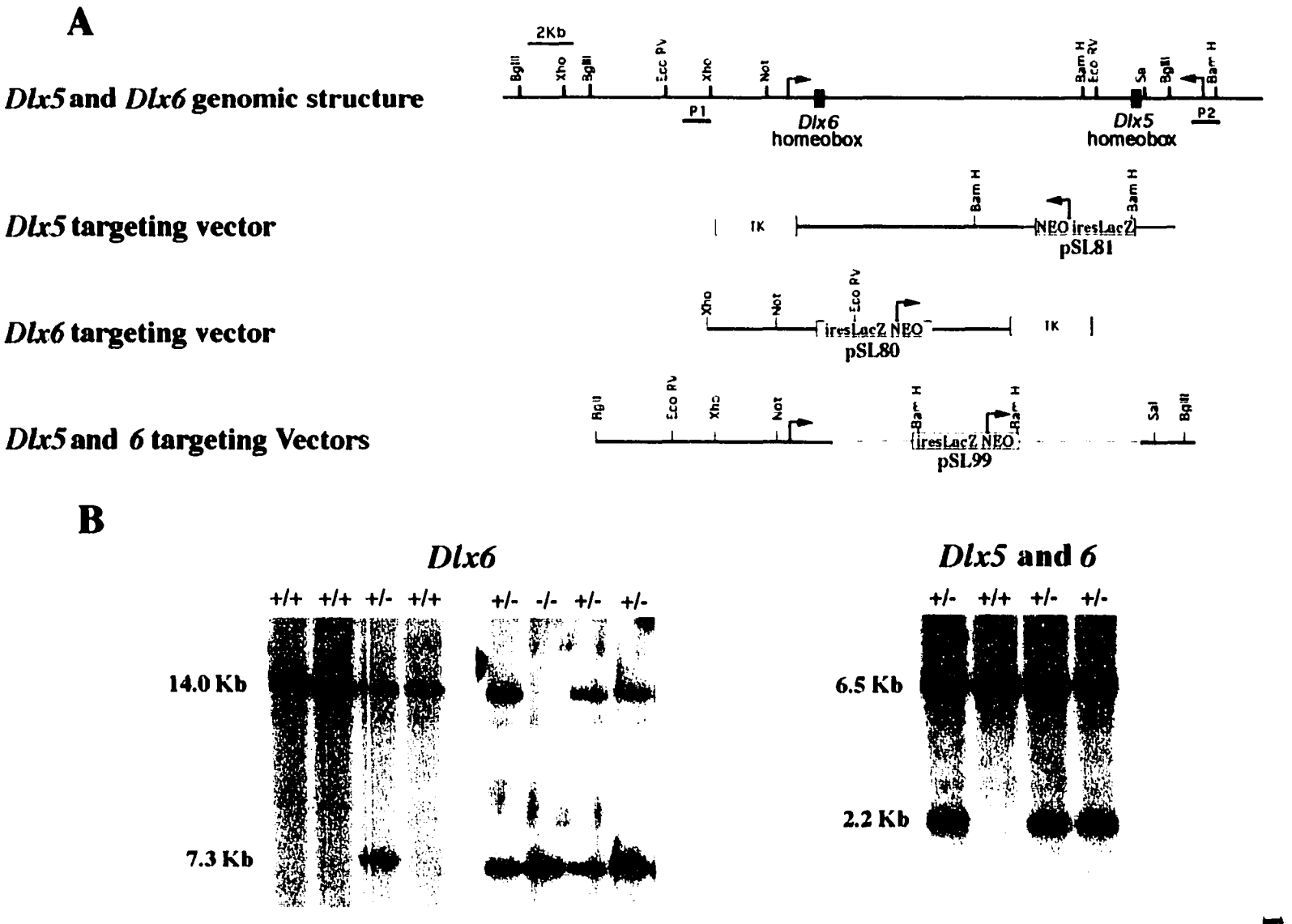

Figure 33

6. *Double Knockout of the Dlx5 and Dlx6 genes in ES cells*

Construct pSL72 was used initially to generate *Dlx5/6* double knockout. This construct has 9kb of the *Dlx6* genomic DNA at the 5' end and 1.5kb of *Dlx5* genomic DNA at the 3' end. More than 13kb of genomic sequences including both *Dlx5* and *Dlx6* homeoboxes was replaced with a cassettes containing a 1.6kb GT1.2-*Neo* and SV-40 polyadenylation signal. Analysis of 384 ES clones, resistant to G418 selection at the concentration at 150ug/ml, by Southern yielded no positive ES clones (data not shown). Therefore, a new targeting construct, pSL79, was made with a *TK* negative selection marker subcloned at the 3' end of the genomic inserts in pSL72 to enable double selection of the homologous recombinants. However, there was no positive clone obtained after analyzing 576 gancyclovir (2uM) and G418 (150ug/ml) resistant ES clones by Southern blot.

In the final attempt to target this locus, a third construct, pSL99, was generated (Figure 33A). Compared to previous double knockout constructs, pSL72 and pSL79, the new construct had more than 13kb of homologous genomic DNA from the *Dlx* loci, with 11.9kb of *Dlx6* genomic sequence at 5' end and 1.5kb *Dlx5* genomic sequence at the 3' end. An *IRES-lacZ/PGK-Neo*-polyadenylation signal cassette replaced more then 11kb of genomic sequence including both *Dlx5* and *Dlx6* homeoboxes. Apart from including 3kb more homologous sequence in this construct than in pSL72 and pSL79, the stronger PGK promoter was used to increase the level of *Neo* expression. In addition, an *IRES-lacZ* reporter gene was placed under control of the *Dlx6* promoter to monitor expression of this gene. Finally, more than 11kb of sequence downstream of the *Dlx6* gene was deleted in the targeting construct, and comparison of the expression pattern of the *lacZ* reporter with the *in situ* results would be anticipated to indicate whether important regulatory elements are located in this region.

pSL99 was electroporated into R1 ES cells and 192 G418 (150ug/ml) resistant clones were analyzed by Southern blot and obtained 4 recombination-specific clones. When the ES cell DNA was digested with Bam HI and hybridized with Probe 2, a 2.2kb recombination-specific band was present, in addition to the 6.5kb wild type band (compare +/+ and +/-, right panel, Figure 33). These 4 positive clones were expanded and confirmed by Southern blot and tetraploid embryo staining (data not shown). All four clones were injected into blastocysts to generate a total of 26 male chimeras. Agouti pups, from these chimeras mated with C57BL6 females, were screened by Southern blotting to detect the recombined allele and results demonstrate that all four ES clones has successfully transmitted the *Dlx5/6* double knockout allele through germ line.

Figure 34. β-gal staining of tetroploid embryos from *Dlx6* knock out ES clones. Left panels, low power view; right four panels, high power views.

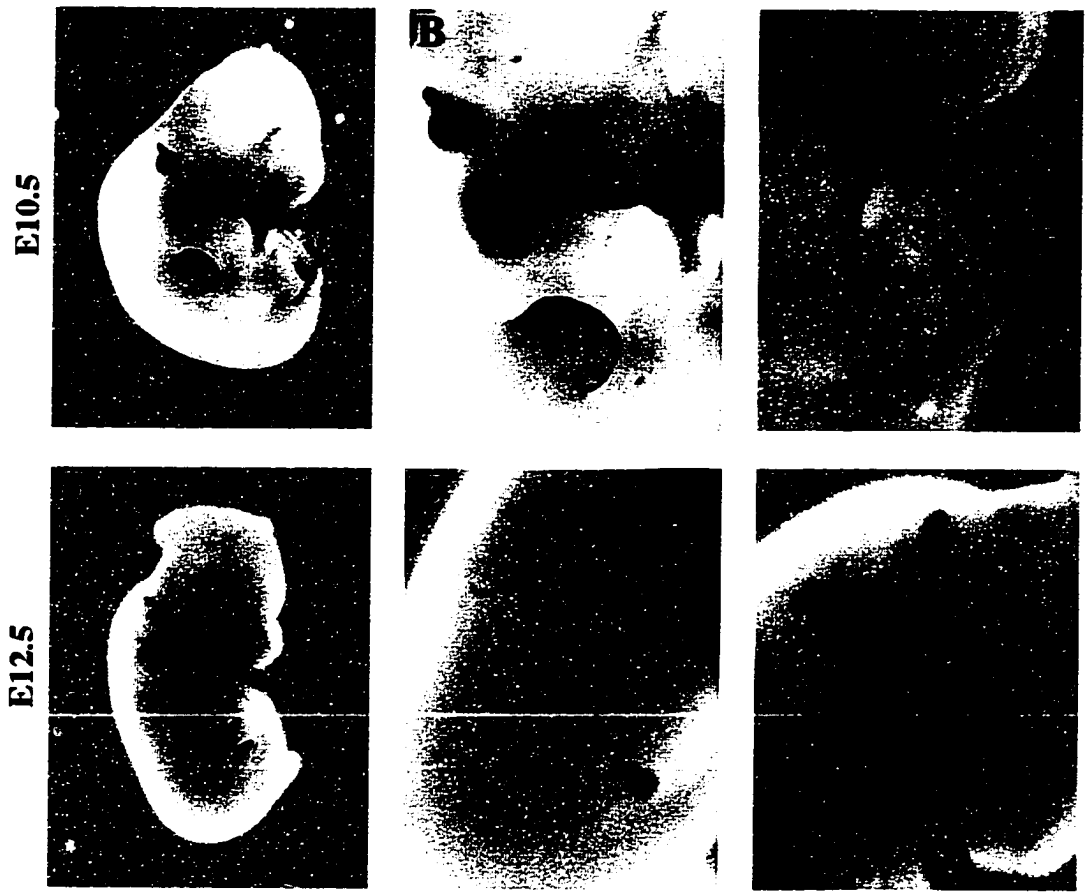

Figure 34

Discussion

In total, 2112 ES cell clones using GT1.2-*Neo* and GT1.2-*TK* selection markers were analyzed and only 1 of them had undergone homologous recombination (Table 3). Such a low targeting efficiency (0.047%) could not be explained by the size of homologous sequence present in the targeting construct, because there are at least 9.5kb homologous DNA sequences present in all the targeting constructs. Hyperselection of the *Dlx6*$^{+/-}$ ES clone demonstrated that the *Dlx6*$^{+/-}$ ES cells is very sensitive to G418 concentration. A concentration of 350ug/ml G418 killed 99% of *Dlx6*$^{+/-}$ ES cells. Replacing the GT1.2 promoter with the stronger PGK promoter, lower the G418 concentration during selection increased the targeting rate to 2.08% (4/192, Table 3). This results implies that there are putative silencers present in the *Dlx5* and *6* locus, which represses GT1.2 promoter activity in ES cells prevent antibiotic selection.

Table 3. Summary of ES Cell Analyses

Genes	Selection Markers	G418 (ug/ml)	Gancyclovir (uM)	# of ES	Positive	Rate (%)
Dlx5	GT1.2 Neo	150	N/A	288	0	
	GT1.2 Neo/GT1.2 TK	150	2	288	0	
Dlx6	GT1.2 Neo	150	N/A	288	0	0.047
	GT1.2 Neo/GT1.2 TK	150	2	288	1	
Dlx5+6	GT1.2 Neo	150	N/A	384	0	
	GT1.2 Neo/GT1.2 TK	150	2	576	0	
	PGK Neo	35	N/A	192	4	2.08
Dlx6+/-	GT1.2 Neo/GT1.2 TK	350	N/A	96	1*	2.08
			Total	2400		

* *Dlx6* null mutant

Since both *Dlx5* and *Dlx6* genes are expressed strongly in the first bronchial arch, forebrain, and AER of limb, we speculate that the mutants of this two genes in the same time will have profound defects in the formation of the craniofacial structures, forebrain and limb. Even more, since *Dlx5* and *Dlx6* are the only members in the *Dlx* family which express strongly in the perichondrial region of all developing skeletal structures, it will be very interesting to see whether there are skeletal defects in the double knockout mice.

V. Bibliography

Akimenko, M. A., Ekker, M., Wegner, J., Lin, W., and Westerfield, M. (1994). Combinatorial expression of three zebrafish genes related to *distal- less*: part of a homeobox gene code for the head. J Neurosci *14*, 3475-86.

Ang, S. L., and Rossant, J. (1994). *HNF3β* is essential for node and notochord formation in mouse development. Cell *78*, 561-574.

Argos, P., Landy, A., Abremski, K., Egan, J. B., Haggard-Ljungquist, E., Hoess, R. H., Kahn, M. L., Kalionis, B., Narayana, S. V., Pierson, L. S. d., and et al. (1986). The integrase family of site-specific recombinases: regional similarities and global diversity. EMBO J *5*, 433-40.

Ashburner, M. (1972). Ecdysone induction of puffing in polytene chromosomes of Drosophila melanogaster. Effects of inhibitors of RNA synthesis. Exp Cell Res *71*, 433-40.

Basler, K., Edlund, T., Jessell, T. M., and Yamada, T. (1993). Control of cell pattern in the neural tube: regulation of cell differentiation by *Dorsalin-1*, a novel *TGF*β family member. Cell *73*, 687-702.

Beauchemin, M., and Savard, P. (1992). Two distal-less related homeobox-containing genes expressed in regeneration blastemas of the newt. Dev Biol *154*, 55-65.

Bovolenta, P., and Dodd, J. (1991). Perturbation of neuronal differentiation and axon guidance in the spinal cord of mouse embryos lacking a floor plate: analysis of Danforth's *short tail* mutation. Development *113*, 625-639.

Brandon, E. P., Idzerda, R. L., and McKnight, G. S. (1995). Knockouts. Targeting the mouse genome: a compendium of knockouts (Part I). Curr Biol *5*, 625-34.

Brandon, E. P., Idzerda, R. L., and McKnight, G. S. (1995). Targeting the mouse genome: a compendium of knockouts (Part II). Curr Biol *5*, 758-65.

Brandon, E. P., Idzerda, R. L., and McKnight, G. S. (1995). Targeting the mouse genome: a compendium of knockouts (Part III). Curr Biol *5*, 873-81.

Braun, T., Rudnicki, M. A., Arnold, H., and Jaenisch, R. (1992). Targeted inactivation of the muscle regulatory gene *Myf*-5 results in abnormal rib development and perinatal death. Cell *71*, 369-382.

Bulfone, A., Puelles, L., Porteus, M. H., Frohman, M. A., Martin, G. R., and Rubenstein, J. L. R. (1993). Spatially restricted expression of *Dlx-1, Dlx-2 (Tes-1), Gbx2,* and *Wnt-3* in the embryonic day 12.5 mouse forebrain defines potential transverse and longitudinal segmental boundaries. The Journal of Neuroscience *13*, 3155-3172.

Capecchi, M. R. (1989). Altering the genome by homologous recombination. Science *244*, 1288-1292.

Chambon, P. (1994). The retinoid signaling pathway: molecular and genetic analysis. Seminars in Cell Biology *5*, 115-125.

Chan, D. C., Wynshaw-Boris, A., and Leder, P. (1995). Formin isoforms are differentially expressed in the mouse embryo and are required for normal expression of *Fgf*-4 and *Shh* in the limb bud. Development *121*, 3151-3162.

Chapman, G., and Rathjen, P. D. (1995). Sequence and evolutionary conservation of the murine Gbx2 homeobox gene. FEBS Lett *364*, 289-92.

Charité, J., De Graaff, W., Shen, S. B., and Deschamps, J. (1994). Ectopic expression of *Hoxb-8* causes duplication of the ZPA in the forelimb and homeotic transformation of axial structures. Cell *78*, 589-601.

Chen, X., Li, X., Wang, W., and Lufkin, T. (1996). *Dlx5* and *Dlx6*: an evolutionary conserved pair of murine homeobox genes expressed in the embryonic skeleton. Annals of the New York Academy of Sciences *785*, 38-47.

Chen, Y., and Struhl, G. (1996). Dual roles for patched in sequestering and transducing Hedgehog. Cell *87*, 553-63.

Cheng, H. J., Nakamoto, M., Bergemann, A. D., and Flanagan, J. G. (1995). Complementary gradients in expression and binding of *ELF*-1 and *Mek*-4 in development of the topographic retinotectal projection map. Cell *82*, 371-81.

Chiang, C., Ying, L. T. T., Lee, E., Young, K. E., Corden, J. L., Westphal, H., and Beachy, P. A. (1996). Cyclopia and defective axial patterning in mice lacking sonic hedgehog gene function. Nature *383*, 407-413.

Clarke, J. D. W., Holder, N., Soffe, S. R., and Storm-Mathisen, J. (1991). Neuroanatomical and functional analysis of neural tube formation in notochordless *Xenopus* embryos; laterality of the ventral spinal cord is lost. Development *112*, 499-516.

Cohen, S. M., Bröner, G., Küttner, F., Jürgens, G., and Jäckle, H. (1989). *Distal-less* encodes a homeodomain protein required for limb development in *Drosophila*. Nature *338*, 432-434.

Cohn, M. J., Izpisua-Belmonte, J. C., Abud, H., Heath, J. K., and Tickle, C. (1995). Fibroblast growth factors induce additional limb development from the flank of chick embryos. Cell *80*, 739-46.

Colamarino, S. A., and Tessier-Lavigne, M. (1995). The axonal chemoattractant *Netrin*-1 is also a chemorepellent for trochlear motor axons. Cell *81*, 621-9.

Conlon, F. L., Lyons, K. M., Takaesu, N., Barth, K. S., Kispert, A., Herrmann, B., and Robertson, E. J. (1994). A primary requirement for nodal in the formation and maintenance of the primitive streak in the mouse. Development *120*, 1919-28.

Crossley, P. H., and Martin, G. R. (1995). The mouse *Fgf*-8 gene encodes a family of polypeptides and is expressed in regions that direct outgrowth and patterning in the developing embryo. Development *121*, 439-451.

Crossley, P. H., Minowada, G., MacArthur, C. A., and Martin, G. R. (1996). Roles for *Fgf*-8 in the induction, initiation, and maintenance of chick limb development. Cell *84*, 127-36.

Davidson, D. (1995). The function and evolution of *Msx* genes: pointers and paradoxes. Trends Genet *11*, 405-411.

Davis, S., Gale, N. W., Aldrich, T. H., Maisonpierre, P. C., Lhotak, V., Pawson, T., Goldfarb, M., and Yancopoulos, G. D. (1994). Ligands for EPH-related receptor tyrosine kinases that require membrane attachment or clustering for activity. Science *266*, 816-9.

Dealy, C. N., Roth, A., Ferrari, D., Brown, A. M., and Kosher, R. A. (1993). *Wnt*-5a and *Wnt*-7a are expressed in the developing chick limb bud in a manner suggesting roles in pattern formation along the proximodistal and dorsoventral axes. Mech Dev *43*, 175-86.

Dekker, E., Vaessen, M., vandenBerg, C., Timmermans, A., Godsave, S., Holling, T., Nieuwkoop, P., van Kessel, A. G., and Durston, A. (1994). Overexpression of a cellular retinoic acid binding protein (*xCRABP*) causes anteroposterior defects in developing *Xenopus* embryos. Development *120*, 973-985.

Deutsch, U., Dressler, G. R., and Gruss, P. (1988). Pax 1, a member of a paired box homologous murine gene family, is expressed in segmented structures during development. Cell *53*, 617-25.

Dickinson, M. E., Selleck, M. A. J., Mcmahon, A. P., and Bronnerfraser, N. (1995). Dorsalization of the neural tube by the non-neural ectoderm. Development *121*, 2099-2106.

Dodd, J. (1993). Axon guidance in the mammalian spinal cord. In Cell-Cell Signaling in Vertebrate Development, E. J. Robertson, F. R. Maxfield and H. J. Vogel, eds. (San Diego: Academic Press, Inc.), pp. 81-98.

Dodd, J., and Schuchardt, A. (1995). Axon guidance: a compelling case for repelling growth cones. Cell *81*, 471-4.

Doniach, T. (1993). Planar and vertical induction of anteroposterior pattern during the development of the amphibian central nervous system. J. Neurobiol. *24*, 1256-1275.

Drescher, U., Kremoser, C., Handwerker, C., Loschinger, J., Noda, M., and Bonhoeffer, F. (1995). *In vitro* guidance of retinal ganglion cell axons by RAGS, a 25 kDa tectal protein related to ligands for Eph receptor tyrosine kinases. Cell *82*, 359-70.

Duboule, D. (1992). The vertebrate limb: a model system to study the *Hox/HOM* gene network during development and evolution. BioEssays *14*, 375-384.

Duprez, D. M., Kostakopoulou, K., Francis-West, P. H., Tickle, C., and Brickell, P. M. (1996). Activation of *Fgf*-4 and *Hox*D gene expression by *BMP*-2 expressing cells in the developing chick limb. Development *122*, 1821-8.

Echelard, Y., Epstein, D. J., St-Jacques, B., Shen, L., Mohler, J., McMahon, J. A., and McMahon, A. P. (1993). *Sonic hedgehog*, a member of a family of putative signaling molecules, is implicated in the regulation of CNS polarity. Cell *75*, 1417-1430.

Ericson, J., Rashbass, P., Schedl, A., Brenner-Morton, S., Kawakami, A., van Heyningen, V., Jessell, T. M., and Briscoe, J. (1997). *Pax*6 controls progenitor cell identity and neuronal fate in response to graded *Shh* signaling. Cell *90*, 169-80.

Ericson, J., Thor, S., Edlund, T., Jessell, T. M., and Yamada, T. (1992). Early stages of motor neuron differentiation revealed by expression of homeobox gene *Islet-1*. Science *256*, 1555-1560.

Evans, M. J., and Kaufman, M. H. (1981). Establishment in culture of pluripotential cells from mouse embryos. Nature *292*, 154-156.

Fazeli, A., Dickinson, S. L., Hermiston, M. L., Tighe, R. V., Steen, R. G., Small, C. G., Stoeckli, E. T., Keino-Masu, K., Masu, M., Rayburn, H., Simons, J., Bronson, R. T., Gordon, J. I., Tessier-Lavigne, M., and Weinberg, R. A. (1997). Phenotype of mice lacking functional *Deleted in colorectal cancer (Dcc)* gene. Nature *386*, 796-804.

Feil, R., Brocard, J., Mascrez, B., LeMeur, M., Metzger, D., and Chambon, P. (1996). Ligand-activated site-specific recombination in mice. Proc Natl Acad Sci U S A *93*, 10887-90.

Ferguson, E. L., and Anderson, K. V. (1992). Localized enhancement and repression of the activity of the *TGF*-beta family member, decapentaplegic, is necessary for dorsal-ventral pattern formation in the Drosophila embryo. Development *114*, 583-97.

Frasch, M., Chen, X., and Lufkin, T. (1995). Evolutionary-conserved enhancers direct region-specific expression of the murine *Hoxa-1* and *Hoxa-2* loci in both mice and *Drosophila*. Development *121*, 957-974.

Furth, P. A., St Onge, L., Boger, H., Gruss, P., Gossen, M., Kistner, A., Bujard, H., and Hennighausen, L. (1994). Temporal control of gene expression in transgenic mice by a tetracycline-responsive promoter. Proc Natl Acad Sci U S A *91*, 9302-6.

Goldfarb, M. (1996). Functions of fibroblast growth factors in vertebrate development. Cytokine Growth Factor Rev *7*, 311-25.

Goodman, C. S. (1994). The likeness of being: phylogenetically conserved molecular mechanisms of growth cone guidance. Cell *78*, 353-6.

Gossen, M., and Bujard, H. (1992). Tight control of gene expression in mammalian cells by tetracycline- responsive promoters. Proc Natl Acad Sci U S A *89*, 5547-51.

Gossen, M., Freundlieb, S., Bender, G., Muller, G., Hillen, W., and Bujard, H. (1995). Transcriptional activation by tetracyclines in mammalian cells. Science *268*, 1766-9.

Gossler, A., and Zachgo, J. (1993). Gene and enhancer trap screens in ES cell chimeras. In Gene Targeting, A. Joyner, ed.: Oxford: IRL Press, pp. 181-227.

Goulding, M. D., Chalepakis, G., Deutsch, U., Erselius, J. R., and Gruss, P. (1991). *Pax*-3, a novel murine DNA binding protein expressed during early neurogenesis. EMBO J. *10*, 1135-1147.

Goulding, M. D., Lumsden, A., and Gruss, P. (1993). Signals from the notochord and floor plate regulate the region-specific expression of two *Pax* genes in the developing spinal cord. Development *117*, 1001-1016.

Gu, H., Zou, Y.-R., and Rajewsky, K. (1993). Independent control of immunoglobulin switch recombination at individual switch regions evidenced through Cre/loxP-mediated gene targeting. Cell *73*, 1155-1164.

Guo, F., Gopaul, D. N., and van Duyne, G. D. (1997). Structure of Cre recombinase complexed with DNA in a site-specific recombination synapse. Nature *389*, 40-6.

Gurdon, J. B. (1992). The generation of diversity and pattern in animal development. Cell *68*, 185-99.

Hamelin, M., Zhou, Y., Su, M. W., Scott, I. M., and Culotti, J. G. (1993). Expression of the UNC-5 guidance receptor in the touch neurons of C. elegans steers their axons dorsally. Nature *364*, 327-30.

Haramis, A. G., Brown, J. M., and Zeller, R. (1995). The limb deformity mutation disrupts the *Shh/Fgf*-4 feedback loop and regulation of 5' *HoxD* genes during limb pattern formation. Development *121*, 4237-45.

Harland, R. M. (1994). Neural induction in Xenopus. Curr Opin Genet Dev *4*, 543-9.

Hatta, K. (1992). Role of the floor plate in axonal patterning in the zebrafish CNS. Neuron *9*, 629-642.

Hatta, K., Kimmel, C. B., Ho, R. K., and Walker, C. (1991). The *cyclops* mutation blocks specification of the floor plate of the zebrafish central nervous system. Nature *350*, 339-341.

Hedgecock, E. M., Culotti, J. G., and Hall, D. H. (1990). The *unc-5, unc-6,* and *unc-40* genes guide circumferential migrations of pioneer axons and mesodermal cells on the epidermis in C. elegans. Neuron *4*, 61-85.

Hemmati-Brivanlou, A., Kelly, O. G., and Melton, D. A. (1994). *Follistatin*, an antagonist of *Activin*, is expressed in the Spemann organizer and displays direct neuralizing activity. Cell *77*, 283-295.

Hemmati-Brivanlou, A., and Melton, D. A. (1994). Inhibition of *Activin* receptor signaling promotes neuralization in *Xenopus*. Cell *77*, 273-281.

Henrique, D., Adam, J., Myat, A., Chitnis, A., Lewis, J., and Ish-Horowicz, D. (1995). Expression of a Delta homologue in prospective neurons in the chick. Nature *375*, 787-90.

Herrmann, B. G. (1992). Action of the *Brachyury* gene in mouse embryogenesis. In Postimplantation development in the mouse, D. J. Chadwick and J. Marsh, eds. (Chichester: John Wiley & Sons), pp. 78-86.

Hogan, B. L. M. (1996). Bone morphogenetic proteins in development. Curr Opin Genet Develop *6*, 432-438.

Holland, P. W. (1991). Cloning and evolutionary analysis of *msh*-like homeobox genes from mouse, zebra fish and ascidian. Gene *98*, 253-257.

Ikeya, M., Lee, S. M., Jane, E. J., McMahon, A. P., and Takada, S. (1997). Wnt signalling required for expansion of neural crest and CNS progenitors. Nature *389*, 966-970.

Ishii, N., Wadsworth, W. G., Stern, B. D., Culotti, J. G., and Hedgecock, E. M. (1992). *UNC-6*, a laminin-related protein, guides cell and pioneer axon migrations in *C. elegans*. Neuron *9*, 873-81.

Jaenisch, R. (1988). Transgenic animals. Science *240*, 1468-74.

Jang, S. K., Pestova, T. V., Hellen, C. U., Witherell, G. W., and Wimmer, E. (1990). Cap-independent translation of picornavirus RNAs: structure and function of the internal ribosomal entry site. Enzyme *44*, 292-309.

Jessell, T. M., and Dodd, J. (1993). Control of neural cell identity and pattern by notochord and floor plate signals. In Cell-Cell Signaling in Vertebrate Development, E. J. Robertson, F. R. Maxfield and H. J. Vogel, eds. (San Diego: Academic Press, Inc), pp. 139-156.

Jessell, T. M., and Melton, D. A. (1992). Diffusible factors in vertebrate embryonic induction. Cell *68*, 257-270.

Jiang, R. L., and Gridley, T. (1997). Gene targeting - Things go better with Cre. Curr Biol *7*, R321-R323.

Johnson, R. L., and Tabin, C. J. (1997). Molecular models for vertebrate limb development. Cell *90*, 979-90.

Kalderon, D. (1995). Morphogenetic signalling. Responses to hedgehog. Curr Biol *5*, 580-2.

Kennedy, T. E., Serafini, T., de la Torre, J. R., and Tessier-Lavigne, M. (1994). Netrins are diffusible chemotropic factors for commissural axons in the embryonic spinal cord. Cell *78*, 425-35.

Kim, D. G., Kang, H. M., Jang, S. K., and Shin, H. S. (1992). Construction of a bifunctional mRNA in the mouse by using the internal ribosomal entry site of the encephalomyocarditis virus. Molecular and Cellular Biology *12*, 3636-3643.

Kolodkin, A. L., Matthes, D. J., and Goodman, C. S. (1993). The semaphorin genes encode a family of transmembrane and secreted growth cone guidance molecules. Cell *75*, 1389-99.

Kolodkin, A. L., Matthes, D. J., O'Connor, T. P., Patel, N. H., Admon, A., Bentley, D., and Goodman, C. S. (1992). *Fasciclin* IV: sequence, expression, and function during growth cone guidance in the grasshopper embryo. Neuron *9*, 831-45.

Krauss, S., Concordet, J.-P., and Ingham, P. W. (1993). A functionally conserved homolog of the Drosophila segment polarity gene *hh* is expressed in tissues with polarizing activity in zebrafish embryos. Cell *75*, 1431-1444.

Krumlauf, R. (1994). *Hox* genes in vertebrate development. Cell *78*, 191-201.

Kuhn, R., Schwenk, F., Aguet, M., and Rajewsky, K. (1995). Inducible gene targeting in mice. Science *269*, 1427-9.

Lakso, M., Sauer, B., Monsinger, B., Lee, E. J., Manning, R. W., Yu, S. H., Mulder, K. L., and Westphal, H. (1992). Targeted oncogene activation by site-specific recombination in transgenic mice. Proc. Natl. Acad. Sci. USA *89*, 6232-6236.

Laufer, E., Dahn, R., Orozco, O. E., Yeo, C. Y., Pisenti, J., Henrique, D., Abbott, U. K., Fallon, J. F., and Tabin, C. (1997). Expression of Radical fringe in limb-bud ectoderm regulates apical ectodermal ridge formation [published erratum appears in Nature 1997 Jul 24;388(6640):400]. Nature *386*, 366-73.

Laufer, E., Nelson, C. E., Johnson, R. L., Morgan, B. A., and Tabin, C. (1994). Sonic hedgehog and *Fgf-4* act through a signaling cascade and feedback loop to integrate growth and patterning of the developing limb bud. Cell *79*, 993-1003.

Lewandoski, M., and Martin, G. R. (1997). Cre-mediated chromosome loss in mice. Nature Genetics *17*, 223-225.

Li, X., Wang, W., and Lufkin, T. (1997). Sensitive dicistronic markers for the simultaneous analysis of multiple transgene expression in transgenic mice. BioTechniques, in press.

Liem, K. F., Jr., Tremml, G., and Jessell, T. M. (1997). A role for the roof plate and its resident *TGF*beta-related proteins in neuronal patterning in the dorsal spinal cord. Cell *91*, 127-38.

Liem, K. F., Tremml, G., Roelink, H., and Jessell, T. M. (1995). Dorsal differentiation of neural plate cells induced by *BMP*-mediated signals from epidermal ectoderm. Cell *82*, 969-979.

Loomis, C. A., Harris, E., Michaud, J., Wurst, W., Hanks, M., and Joyner, A. L. (1996). The mouse *Engrailed*-1 gene and ventral limb patterning. Nature *382*, 360-3.

Lufkin, T. (1996). Transcriptional control of *Hox* genes in the vertebrate nervous system. Curr Opin Genet Develop *6*, 575-580.

Lufkin, T., Dierich, A., LeMeur, M., Mark, M., and Chambon, P. (1991). Disruption of the *Hox-1.6* homeobox gene results in defects in a region corresponding to its rostral domain of expression. Cell *66*, 1105-1119.

Lufkin, T., Mark, M., Hart, C. P., LeMeur, M., and Chambon, P. (1992). Homeotic transformation of the occipital bones of the skull by ectopic expression of a homeobox gene. Nature *359*, 835-841.

Lumsden, A. (1995). A "LIM code" for motor neurons? Current Biology *5*, 491-495.

Luo, Y., Raible, D., and Raper, J. A. (1993). Collapsin: a protein in brain that induces the collapse and paralysis of neuronal growth cones. Cell *75*, 217-27.

Luo, Y., Shepherd, I., Li, J., Renzi, M. J., Chang, S., and Raper, J. A. (1995). A family of molecules related to *Collapsin* in the embryonic chick nervous system [published erratum appears in Neuron 1995 Nov. 15(5):following 1218]. Neuron *14*, 1131-40.

MacCabe, J. A., Errick, J., and Saunders, J. W., Jr. (1974). Ectodermal control of the dorsoventral axis in the leg bud of the chick embryo. Dev Biol *39*, 69-82.

Marti, E., Takada, R., Bumcrot, D. A., Sasaki, H., and Mcmahon, A. P. (1995). Distribution of Sonic hedgehog peptides in the developing chick and mouse embryo. Development *121*, 2537-2547.

Martin, G. R. (1981). Isolation of a pluripotent cell line from early mouse embryos cultured in medium conditioned by teratocarcinoma stem cells. Proc. Natl. Acad. Sci. U.S.A. *78*, 7634-7638.

Matsui, T., Hirai, M., Hirano, M., and Kurosawa, Y. (1993). The HOX complex neighbored by the EVX gene, as well as two other homeobox-containing genes, the GBX-class and the EN-class, are located on the same chromosomes 2 and 7 in humans. FEBS Lett *336*, 107-10.

McGinnis, W., and Krumlauf, R. (1992). Homeobox genes and axial patterning. Cell *68*, 283-302.

McHugh, T. J., Blum, K. I., Tsien, J. Z., Tonegawa, S., and Wilson, M. A. (1996). Impaired hippocampal representation of space in CA1-specific NMDAR1 knockout mice. Cell *87*, 1339-49.

McMahon, A. P. (1993). Cell signalling in induction and anterior-posterior patterning of the vertebrate central nervous system. Current Opinion in Neurobiology *3*, 4-7.

McMahon, A. P., and Bradley, A. (1990). The *Wnt*-1 (*int*-1) proto-oncogene is required for development of a large region of the mouse brain. Cell *62*, 1073-1085.

Messersmith, E. K., Leonardo, E. D., Shatz, C. J., Tessier-Lavigne, M., Goodman, C. S., and Kolodkin, A. L. (1995). Semaphorin III can function as a selective chemorepellent to pattern sensory projections in the spinal cord. Neuron *14*, 949-59.

Michaud, J. L., Lapointe, F., and LeDouarin, N. M. (1997). The dorsoventral polarity of the presumptive limb is determined by signals produced by the somites and by the lateral somatopleure. Development *124*, 1453-1463.

Moon, R. T., Brown, J. D., and Torres, M. (1997). WNTs modulate cell fate and behavior during vertebrate development. Trends Genet *13*, 157-62.

Morriss-Kay, G. M. (1992). Retinoids in normal development and teratogenesis (Oxford: Oxford University Press), pp. 299 pages.

Mountford, P. S., and Smith, A. G. (1995). Internal ribosome entry sites and dicistronic RNAs in mammalian transgenesis. Trends in Genetics *11*, 179-184.

Moury, J. D., and Jacobson, A. G. (1990). The origins of neural crest cells in the axolotl. Dev Biol *141*, 243-53.

Nagy, A., and Rossant, J. (1993). Production of completely ES cell-derived fetuses. In Gene Targeting: a practical approach, A. Joyner, ed. (Oxford: Oxford University Press), pp. 147-179.

Nagy, A., Rossant, J., Nagy, R., Abramow-Newerly, W., and Roder, J. C. (1993). Derivation of completely cell culture-derived mice from early-passage embryonic stem cells. Proc Natl Acad Sci U S A *90*, 8424-8.

Nieuwkoop, P. D. (1973). The organization center of the amphibian embryo: its origin, spatial organization, and morphogenetic action. Adv Morphog *10*, 1-39.

Niswander, L., Jeffrey, S., Martin, G. R., and Tickle, C. (1994). A positive feedback loop coordinates growth and patterning in the vertebrate limb. Nature *371*, 609-612.

No, D., Yao, T. P., and Evans, R. M. (1996). Ecdysone-inducible gene expression in mammalian cells and transgenic mice. Proc Natl Acad Sci USA *93*, 3346-3351.

Noramly, S., Pisenti, J., Abbott, U., and Morgan, B. (1996). Gene expression in the *limbless* mutant: polarized gene expression in the absence of *Shh* and an AER. Dev Biol *179*, 339-46.

Nusse, R., and Varmus, H. E. (1992). *Wnt* genes. Cell *69*, 1073-1087.

Ohuchi, H., Nakagawa, T., Yamamoto, A., Araga, A., Ohata, T., Ishimaru, Y., Yoshioka, H., Kuwana, T., Nohno, T., Yamasaki, M., Itoh, N., and Noji, S. (1997). The mesenchymal factor, *Fgf*-10, initiates and maintains the outgrowth of the chick limb bud through interaction with *Fgf*-8, an apical ectodermal factor. Development *124*, 2235-44.

Palmiter, R. D., and Brinster, R. L. (1986). Germ-line transformation of mice. Annu Rev Genet *20*, 465-99.

Panganiban, G., Nagy, L., and Carroll, S. B. (1994). The role of the *Distal-less* gene in the development and evolution of insect limbs. Curr Biol *4*, 671-5.

Panin, V. M., Papayannopoulos, V., Wilson, R., and Irvine, K. D. (1997). Fringe modulates Notch-ligand interactions. Nature *387*, 908-12.

Papalopulu, N., and Kintner, C. (1993). Xenopus *Distal-less* related homeobox genes are expressed in the developing forebrain and are induced by planar signals. Development *117*, 961-75.

Parr, B. A., and McMahon, A. P. (1995). Dorsalizing signal Wnt-7a required for normal polarity of D-V and A-P axes of mouse limb. Nature *374*, 350-353.

Parr, B. A., Shea, M. J., Vassileva, G., and McMahon, A. P. (1993). Mouse *Wnt* genes exhibit discrete domains of expression in the early embryonic CNS and limb buds. Development *119*, 247-61.

Pfaff, S. L., Mendelsohn, M., Stewart, C. L., Edlund, T., and Jessell, T. M. (1996). Requirement for LIM homeobox gene *Isl1* in motor neuron generation reveals a motor neuron-dependent step in interneuron differentiation. Cell *84*, 309-20.

Picard, D. (1994). Regulation of protein function through expression of chimeric proteins. Curr Opin Biotechnol *5*, 511-5.

Placzek, M., Tessier-Lavigne, M., Jessell, T., and Dodd, J. (1990). Orientation of commissural axons *in vitro* in response to a floor plate-derived chemoattractant. Development *110*, 19-30.

Placzek, M., Tessier-Lavigne, M., Yamada, T., Jessell, T., and Dodd, J. (1990). Mesodermal control of neural cell identity: floor plate induction by the notochord. Science *250*, 985-988.

Porteus, M. H., Bulfone, A., Ciaranello, R. D., and Rubenstein, J. L. (1991). Isolation and characterization of a novel cDNA clone encoding a homeodomain that is developmentally regulated in the ventral forebrain [published erratum appears in Neuron 1992 Jul;9(1):187]. Neuron *7*, 221-9.

Price, M., Lazzaro, D., Pohl, T., Mattei, M. G., Rüther, U., Olivio, J. C., Duboule, D., and DiLauro, R. (1992). Regional expression of the homeobox gene *Nkx-2.2* in the developing mammalian forebrain. Neuron *8*, 241-255.

Püschel, A. W., Adams. R. H., and Betz, H. (1995). Murine *Semaphorin* D/*Collapsin* is a member of a diverse gene family and creates domains inhibitory for axonal extension. Neuron *14*, 941-8.

Qiu, M., Bulfone, A., Martinez, S., Meneses, J. J., Shimamura, K., Pedersen, R. A., and Rubenstein, J. L. (1995). Null mutation of *Dlx*-2 results in abnormal morphogenesis of proximal first and second bronchial arch derivatives and abnormal differentiation in the forebrain. Genes Dev *9*, 2523-38.

Riddle, R. D., Ensini, M., Nelson, C., Tsuchida, T., Jessell, T. M., and Tabin, C. (1995). Induction of the LIM homeobox gene *Lmx*1 by *WNT7*a establishes dorsoventral pattern in the vertebrate limb. Cell *83*, 631-640.

Riddle, R. D., Johnson, R. L., Laufer, E., and Tabin, C. (1993). *Sonic hedgehog* mediates the polarizing activity of the ZPA. Cell *75*, 1401-1416.

Rodriguez-Esteban, C., Schwabe, J. W., De La Pena, J., Foys, B., Eshelman, B., and Belmonte, J. C. (1997). *Radical fringe* positions the apical ectodermal ridge at the dorsoventral boundary of the vertebrate limb. Nature *386*, 360-6.

Roelink, H., Porter, J. A., Chiang, C., Tanabe, Y., Chang, D. T., Beachy, P. A., and Jessell, T. M. (1995). Floor plate and motor neuron induction by different concentrations of the amino-terminal cleavage product of sonic hedgehog autoproteolysis. Cell *81*, 445-455.

Ros, M. A., Lopez-Martinez, A., Simandl, B. K., Rodriguez, C., Izpisua Belmonte, J. C., Dahn, R., and Fallon, J. F. (1996). The limb field mesoderm determines initial limb bud anteroposterior asymmetry and budding independent of sonic hedgehog or apical ectodermal gene expressions. Development *122*, 2319-30.

Rowe, D. A., and Fallon, J. F. (1982). The proximodistal determination of skeletal parts in the developing chick leg. J Embryol Exp Morphol *68*, 1-7.

Ruberte, E., Friederich, V., Morriss-Kay, G., and Chambon, P. (1992). Differential distribution patterns of *CRABP*I and *CRABP*II transcripts during mouse embryogenesis. Development *115*, 973-987.

Rudnicki, M. A., Braun, T., Hinuma, S., and Jaenisch, R. (1992). Inactivation of *MyoD* in mice leads to up-regulation of the myogenic HLH gene *Myf5* and results in apparently normal muscle development. Cell *71*, 383-390.

Rudnicki, M. A., Schnegelsberg, P. N., Stead, R. H., Braun, T., Arnold, H. H., and Jaenisch, R. (1993). *MyoD* or *Myf5* is required for the formation of skeletal muscle. Cell *75*, 1351-9.

Sambrook, J., Fritsch, E. F., and Maniatis, T. (1989). Molecular cloning: a laboratory manual, 2nd Edition (Cold Spring Harbor: Cold Spring Harbor Press).

Sasaki, H., and Hogan, B. L. M. (1994). *HNF3β* as a regulator of floor plate development. Cell *76*, 103-115.

Satokata, I., and Maas, R. (1994). *Msx1* deficient mice exhibit cleft palate and abnormalities of craniofacial and tooth development. Nature Genetics *6*, 348-355.

Sauer, B. (1987). Functional expression of the Cre/loxP site-specific recombination system in the yeast Saccharomyces cerevisiae. Mol Cell Biol *7*, 2087-96.

Sauer, B. (1993). Manipulation of transgenes by site-specific recombination: Use of Cre recombinase. In Guide to Techniques in Mouse Development, P. M. Wassarman and M. L. Depamphilis, eds. (San Diego: Academic Press), pp. 890-900.

Saunders, J. W., Jr, and Gasseling, M. T. (1968). Ectoderm-mesenchymal interaction in the origins of wing symmetry. In Epithelial-Mesenchymal Interactions, R. Fleischmajer and R. E. Billingham, eds. (Baltimore: Williams and Wilkins), pp. 78-97.

Scherer, S. W., and al., e. (1994). Physical mapping of the *split hand/split foot* locus on chromosome 7 and implication in syndromic ectrodactyly. Hum. Mol. Genet. *3*, 1345-1354.

Schwartzberg, P. L., Goff, S. P., and Robertson, E. J. (1989). Germ-line transmission of a c-*abl* mutation produced by targeted gene disruption in ES cells. Science *246*, 799-803.

Serafini, T., Colamarino, S. A., Leonardo, E. D., Wang, H., Beddington, R., Skarnes, W. C., and Tessier-Lavigne, M. (1996). *Netrin*-1 is required for commissural axon guidance in the developing vertebrate nervous system. Cell *87*, 1001-14.

Serafini, T., Kennedy, T. E., Galko, M. J., Mirzayan, C., Jessell, T. M., and Tessier-Lavigne, M. (1994). The Netrins define a family of axon outgrowth-promoting proteins homologous to C. elegans UNC-6. Cell *78*, 409-24.

Shockett, P., Difilippantonio, M., Hellman, N., and Schatz, D. G. (1995). A modified tetracycline-regulated system provides autoregulatory, inducible gene expression in cultured cells and transgenic mice. Proc Natl Acad Sci U S A *92*, 6522-6.

Shockett, P. E., and Schatz, D. G. (1996). Diverse strategies for tetracycline-regulated inducible gene expression. Proc Natl Acad Sci USA *93*, 5173-5176.

Simeone, A., Acampora, D., Pannese, M., D'Esposito, M., Stornaiuolo, A., Gulisano, M., Mallamaci, A., Kastury, K., Druck, T., Huebner, K., and Boncinelli, E. (1994). Cloning and characterization of two new members of the vertebrate *Dlx* family. Proc. Natl. Acad. Sci. USA *91*, 2250-2254.

Smith, J. C. (1993). Mesoderm-inducing factors in early vertebrate development. EMBO J. *12*, 4463-4470.

Sokol, S., Christian, J. L., Moon, R. T., and Melton, D. A. (1991). Injected *Wnt* RNA induces a complete body axis in *Xenopus* embryos. Cell *67*, 741-752.

Spemann, H., and Mangold, H. (1924). Über Induktion von Embryonalanlagen durch Implantation artfremder Organisatoren. Roux'Arch. Entw. Mech. *100*, 599-638.

Stark, K., Vainio, S., Vassileva, G., and McMahon, A. P. (1994). Epithelial transformation of metanephric mesenchyme in the developing kidney regulated by *Wnt*-4. Nature *372*, 679-83.

Stephens, T. D., and McNulty, T. R. (1981). Evidence for a metameric pattern in the development of the chick humerus. J Embryol Exp Morphol *61*, 191-205.

Stephens, T. D., Spall, R., Baker, W. C., Hiatt, S. R., Pugmire, D. E., Shaker, M. R., Willis, H. J., and Winger, K. P. (1991). Axial and Paraxial Influences on Limb Morphogenesis. Journal of Morphology *208*, 367-379.

Stone, D. M., Hynes, M., Armanini, M., Swanson, T. A., Gu, Q. M., Johnson, R. L., Scott, M. P., Pennica, D., Goddard, A., Phillips, H., Noll, M., Hooper, J. E., Desauvage, F., and Rosenthal, A. (1996). The tumor-suppressor gene *Patched* encodes a candidate receptor for sonic hedgehog. Nature *384*, 129-134.

Stuart, E. T., Kioussi, C., and Gruss, P. (1994). Mammalian *Pax* genes. Annu Rev Genet *28*, 219-236.

Summerbell, D. (1974). A quantitative analysis of the effect of excision of the AER from the chick limb-bud. J Embryol Exp Morphol *32*, 651-60.

Takada, S., Stark, K. L., Shea, M. J., Vassileva, G., McMahon, J. A., and McMahon, A. P. (1994). *Wnt*-3a regulates somite and tailbud formation in the mouse embryo. Genes Dev *8*, 174-89.

Tamada, A., Shirasaki, R., and Murakami, F. (1995). Floor plate chemoattracts crossed axons and chemorepels uncrossed axons in the vertebrate brain. Neuron *14*, 1083-93.

Tanabe, Y., and Jessell, T. M. (1996). Diversity and pattern in the developing spinal cord. Science *274*, 1115-1123.

Tessier-Lavigne, M. (1995). Eph receptor tyrosine kinases, axon repulsion, and the development of topographic maps. Cell *82*, 345-8.

Tessier-Lavigne, M., and Goodman, C. S. (1996). The molecular biology of axon guidance. Science *274*, 1123-33.

Tessier-Lavigne, M., Placzek, M., Lumsden, A. G., Dodd, J., and Jessell, T. M. (1988). Chemotropic guidance of developing axons in the mammalian central nervous system. Nature *336*, 775-8.

Thomas, K. R., and Capecchi, M. R. (1990). Targeted disruption of the murine int-1 proto-oncogene resulting in severe abnormalities in midbrain and cerebellar development. Nature *346*, 847-850.

Thomsen, G. H., and Melton, D. A. (1993). Processed Vg1 protein is an axial mesoderm inducer in Xenopus. Cell *74*, 433-41.

Tremblay, P., Pituello, F., and Gruss, P. (1996). Inhibition of floor plate differentiation by *Pax3*: evidence from ectopic expression in transgenic mice. Development *122*, 2555-2567.

Tsien, J. Z., Chen, D. F., Gerber, D., Tom, C., Mercer, E. H., Anderson, D. J., Mayford, M., Kandel, E. R., and Tonegawa, S. (1996). Subregion- and cell type-restricted gene knockout in mouse brain. Cell *87*, 1317-26.

Tsien, J. Z., Huerta, P. T., and Tonegawa, S. (1996). The essential role of hippocampal CA1 NMDA receptor-dependent synaptic plasticity in spatial memory. Cell *87*, 1327-38.

van der Geer, P., Hunter, T., and Lindberg, R. A. (1994). Receptor protein-tyrosine kinases and their signal transduction pathways. Annu Rev Cell Biol *10*, 251-337.

VanStraaten, H. W. M., Hekking, J. W. M., Beursgens, J. P. W. M., Terwindt-Rouwenhorst, E., and Drukker, J. (1989). Effect of notochord on proliferation and differentiation in the neural tube of the chick embryo. Development *107*, 793-803.

Vogel, A., Rodriguez, C., and Izpisua-Belmonte, J. C. (1996). Involvement of *Fgf*-8 in initiation, outgrowth and patterning of the vertebrate limb. Development *122*, 1737-50.

Vogel, A., Rodriguez, C., Warnken, W., and Izpisua Belmonte, J. C. (1995). Dorsal cell fate specified by chick *Lmx*1 during vertebrate limb development [published erratum appears in Nature 1996 Feb 29;379(6568):848]. Nature *378*, 716-20.

Wanek, N., Gardiner, D. M., Muneoka, K., and Bryant, S. V. (1991). Conversion by retinoic acid of anterior cells into ZPA cells in the chick wing bud. Nature *350*, 81-83.

Wang, W. D., Chen, X. W., Xu, H., and Lufkin, T. (1996). *Msx3:* a novel murine homologue of the *Drosophila msh* homeobox gene restricted to the dorsal embryonic central nervous system. Mechanisms of Development *58*, 203-215.

Wassarman, K., Lewandoski, M., Campbell, K., Joyner, A., Rubenstein, J., Martinez, S., and Martin, G. (1997). Specification of the anterior hindbrain and establishment of a normal mid/hindbrain organizer is dependent on Gbx2 gene function. Dev Suppl *124*, 2923-34.

Weinstein, D. C., Altaba, A. R. I., Chen, W. S., Hoodless, P., Prezioso, V. R., Jessell, T. M., and Darnell, J. E. (1994). The winged-helix transcription factor *HNF3β* is required for notochord development in the mouse embryo. Cell *78*, 575-588.

Wight, D. C., and Wagner, T. E. (1994). Transgenic mice: A decade of progress in technology and research. Mutat Res *307*, 429-440.

Wilkinson, D. G., Bailes, J. A., and McMahon, A. P. (1987). Expression of the proto-oncogene *int-1* is restricted to specific neural cells in the developing mouse embryo. Cell *50*, 79-88.

Winslow, J. W., Moran, P., Valverde, J., Shih, A., Yuan, J. Q., Wong, S. C., Tsai, S. P., Goddard, A., Henzel, W. J., Hefti, F., and et al. (1995). Cloning of AL-1, a ligand for an Eph-related tyrosine kinase receptor involved in axon bundle formation. Neuron *14*, 973-81.

Yamada, T., Pfaff, S. L., Edlund, T., and Jessell, T. M. (1993). Control of cell pattern in the neural tube: motor neuron induction by diffusible factors from notochord and floor plate. Cell *73*, 673-686.

Yamada, T., Placzek, M., Tanaka, H., Dodd, J., and Jessell, T. M. (1991). Control of cell pattern in the developing nervous system: polarizing activity of the floor plate and notochord. Cell *64*, 635-647.

Yang, Y., and Niswander, L. (1995). Interaction between the signaling molecules *WNT7a* and *SHH* during vertebrate limb development: dorsal signals regulate anteroposterior patterning. Cell *80*, 939-947.

Yao, T. P., Forman, B. M., Jiang, Z., Cherbas, L., Chen, J. D., McKeown, M., Cherbas, P., and Evans, R. M. (1993). Functional ecdysone receptor is the product of *EcR* and *ultraspiracle* genes. Nature *366*, 476-9.

Yao, T. P., Segraves, W. A., Oro, A. E., McKeown, M., and Evans, R. M. (1992). Drosophila *ultraspiracle* modulates ecdysone receptor function via heterodimer formation. Cell *71*, 63-72.

IMAGE EVALUATION TEST TARGET (QA-3)

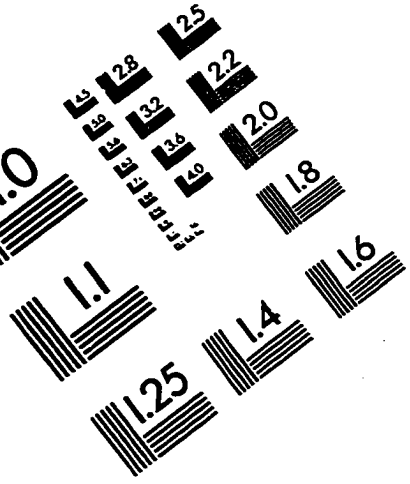

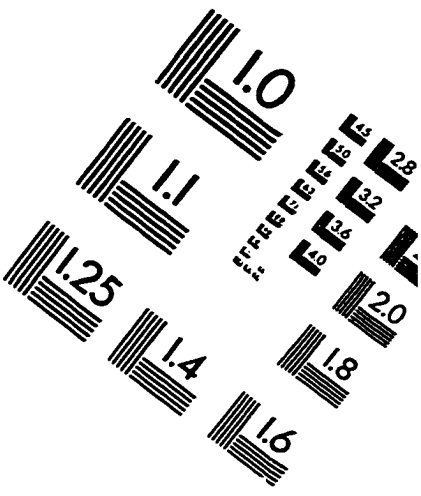

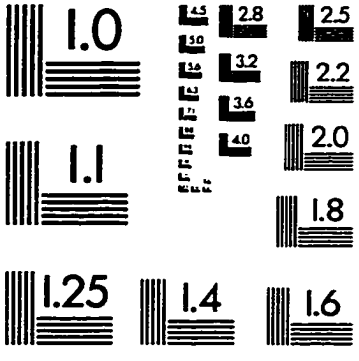

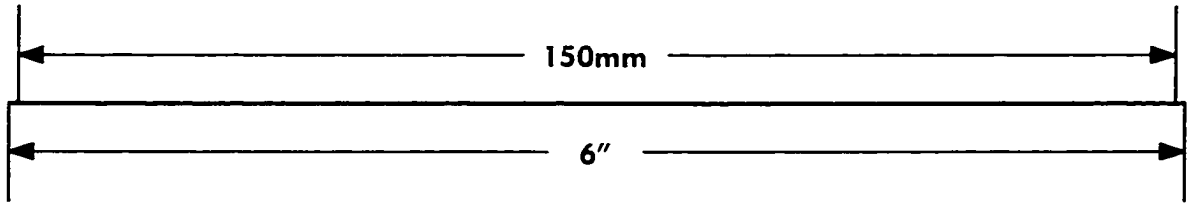

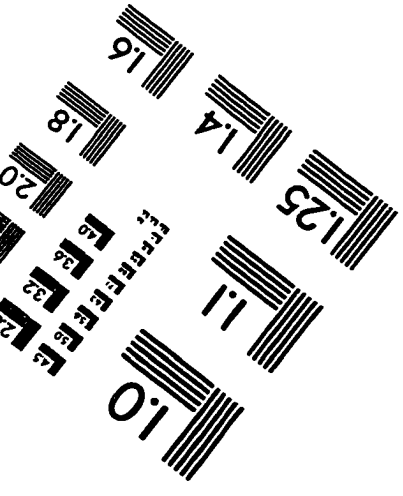

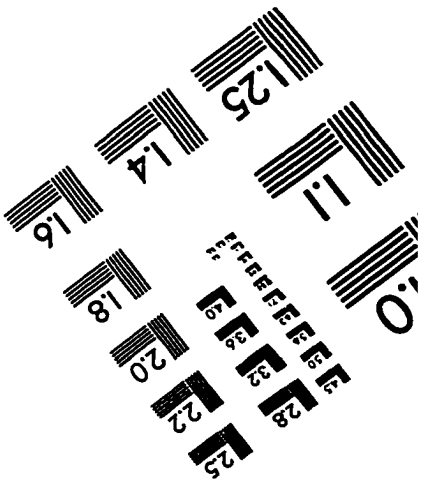

APPLIED IMAGE, Inc
1653 East Main Street
Rochester, NY 14609 USA
Phone: 716/482-0300
Fax: 716/288-5989